

การเพิ่มปริมาณการผลิตไฮโดรคาร์บอนจากแหล่งกักเก็บที่มีทั้งก๊าซธรรมชาติ
และก๊าซธรรมชาติเหลวโดยใช้การอัดคาร์บอนไดออกไซด์



นาย ภาคภูมิ ตั้งกะประเสริฐ

สถาบันวิทยบริการ จุฬาลงกรณ์มหาวิทยาลัย

วิทยานิพนธ์นี้เป็นส่วนหนึ่งของการศึกษาตามหลักสูตรปริญญาวิศวกรรมศาสตรมหาบัณฑิต

สาขาวิชาวิศวกรรมปิโตรเลียม ภาควิชาวิศวกรรมเหมืองแร่และปิโตรเลียม

คณะวิศวกรรมศาสตร์ จุฬาลงกรณ์มหาวิทยาลัย

ปีการศึกษา 2551

ลิขสิทธิ์ของจุฬาลงกรณ์มหาวิทยาลัย

ENHANCING HYDROCARBON RECOVERY FROM GAS CONDENSATE
RESERVOIR VIA CARBON DIOXIDE INJECTION



Mr. Phakphum Tangkprasert

A Thesis Submitted in Partial Fulfillment of the Requirements
for the Degree of Master of Engineering Program in Petroleum Engineering
Department of Mining and Petroleum Engineering

Faculty of Engineering
Chulalongkorn University

Academic Year 2008

Copyright of Chulalongkorn University

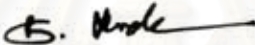
Thesis Title ENHANCING HYDROCARBON RECOVERY
FROM GAS CONDENSATE RESERVOIR VIA
CARBON DIOXIDE INJECTION

By Mr. Phakphum Tangkaprasert


Field of Study Petroleum Engineering


Thesis Advisor Assistant Professor Suwat Athichanagorn, Ph.D.


Accepted by the Faculty of Engineering, Chulalongkorn University in
Partial Fulfillment of the Requirements for the Master's Degree


..... Dean of the Faculty of Engineering
(Associate Professor Boonsom Lerdkhironwong, Dr.Ing.)

THESIS COMMITTEE


.....Chairman
(Jirawat Chewaroungroj, Ph.D.)


.....Advisor
(Assistant Professor Suwat Athichanagorn, Ph.D.)


.....Examiner
(Siree Nasakul, Ph.D.)


.....Examiner
(Thitisak, Boonpramote, Ph.D.)

ภาคภูมิ ดังคะประเสริฐ : การเพิ่มปริมาณการผลิตไฮโดรคาร์บอนจากแหล่งกักเก็บที่มีทั้ง
ก๊าซธรรมชาติและก๊าซธรรมชาติเหลวโดยใช้การอัดคาร์บอนไดออกไซด์ (ENHANCING
HYDROCARBON RECOVERY FROM GAS CONDENSATE RESERVOIR VIA
CARBON DIOXIDE INJECTION) อ. ที่ปรึกษาวิทยานิพนธ์หลัก: ผศ.ดร. สุวัฒน์ อธิชนากร
, 104 หน้า.

การเพิ่มการผลิตก๊าซธรรมชาติเหลวเป็นงานที่ท้าทาย เมื่อความดันภายในแหล่งกักเก็บ
ลดลงต่ำกว่าความดันกลั่นตัว ก๊าซธรรมชาติเหลวจะสะสมภายในแหล่งกักเก็บนำไปสู่ปัญหาการกีด
ขวางโดยก๊าซธรรมชาติเหลวขึ้น นอกจากนั้นก๊าซธรรมชาติเหลวบางส่วนยังถูกทิ้งไว้ในแหล่งกัก
เก็บ วิธีหนึ่งที่มีประสิทธิภาพในการแก้ปัญหานี้ก็คือการอัดก๊าซลงไปแหล่งกักเก็บ การอัดก๊าซ
สามารถเพิ่มผลผลิตก๊าซธรรมชาติเหลวได้โดยการทำให้ก๊าซธรรมชาติเหลวระเหยและการเพิ่ม
ความดันแหล่งกักเก็บ ก๊าซที่ใช้ในการอัดสามารถเป็นก๊าซธรรมชาติหรือก๊าซเฉื่อยขึ้นอยู่กับว่าก๊าซ
ไหนพอจะหาได้ การใช้ก๊าซคาร์บอนไดออกไซด์เป็นก๊าซในการอัดก็ยังสามารถบรรลุจุดประสงค์
ในการเก็บก๊าซคาร์บอนไดออกไซด์ไว้ในแหล่งกักเก็บ

ในงานศึกษานี้เราได้ใช้การจำลองชนิดพิจารณาองค์ประกอบเพื่อจำลองการอัดก๊าซ
คาร์บอนไดออกไซด์ในแหล่งกักเก็บสมมุติของก๊าซธรรมชาติและก๊าซธรรมชาติเหลว จากผลการ
จำลองพบว่าการอัดก๊าซคาร์บอนไดออกไซด์สามารถรักษาความดันให้อยู่สูงกว่าความดันกลั่นตัวได้
อย่างมีประสิทธิภาพ จึงป้องกันการกลั่นตัวของก๊าซธรรมชาติเหลวในแหล่งกักเก็บ เมื่อการอัดก๊าซ
คาร์บอนไดออกไซด์เริ่มขึ้นหลังจากก๊าซธรรมชาติเหลวกลั่นตัว ก๊าซคาร์บอนไดออกไซด์ยัง
สามารถทำให้ก๊าซธรรมชาติเหลวที่กลั่นตัวอยู่รอบๆ หลุมผลิตระเหยได้ ผลการจำลองยังแสดงให้เห็นว่า
อัตราการผลิตก๊าซและอัตราการอัดก๊าซคาร์บอนไดออกไซด์ไม่มีผลอย่างเด่นชัดต่อผลผลิต
ก๊าซธรรมชาติและก๊าซธรรมชาติเหลว อย่างไรก็ตามเวลาที่เริ่มอัดก๊าซคาร์บอนไดออกไซด์มีผล
อย่างชัดเจนต่อการผลิตก๊าซธรรมชาติและก๊าซธรรมชาติเหลว เพื่อให้ได้ผลผลิตก๊าซธรรมชาติเหลว
สูงสุดการอัดก๊าซคาร์บอนไดออกไซด์ควรจะเริ่มในช่วงเวลาสั้นๆหลังจากความดันกันลดลงต่ำกว่า
ความดันกลั่นตัว

ภาควิชาวิศวกรรมเหมืองแร่และปิโตรเลียม.....ลายมือชื่อนิสิต.....
สาขาวิชาวิศวกรรมปิโตรเลียม.....ลายมือชื่อ.ที่ปรึกษาวิทยานิพนธ์หลัก.....
ปีการศึกษา 2551.....

4971617921: MAJOR PETROLEUM ENGINEERING

KEYWORDS: /INJECTION/CO₂/OPTIMIZATION/GAS CONDENSATE

PHAKPHUM TANGKAPRASERT. ENHANCING HYDROCARBON RECOVERY FROM GAS CONDENSATE RESERVOIR VIA CARBON DIOXIDE INJECTION. THESIS ADVISOR: ASST. PROF. SUWAT ATHICHANAGORN, Ph.D., 104 pp.

Increasing condensate recovery in a gas condensate reservoir is a challenging task. When the reservoir pressure falls below the dew point, retrograde condensate condenses and accumulates in the pore system, causing a blockage problem. Furthermore, some of the valuable condensate will be left in the reservoir as residual oil. One of the most effective methods of solving this problem is to injecting gas into the formation. Gas injection allows enhanced condensate recovery by reservoir re-pressurization and liquid re-vaporization. The injected gas can be natural gas or other inert gases, depending on availability. The use of CO₂ as injected gas also achieves the purpose of CO₂ sequestration into geological storage.

In this study, a compositional simulator was used to simulate CO₂ injection in a hypothetical gas condensate reservoir. The simulation results show that CO₂ injection does effectively maintain reservoir pressure above the dew point pressure, preventing condensate dropout within the reservoir. When injecting CO₂ after condensate accumulates, CO₂ can still re-vaporize liquid drop-out around the wellbore. The simulation results also demonstrate that gas production and CO₂ injection rate do not have significant effect on oil and gas recovery. However, the starting time for CO₂ injection has important effects on hydrocarbon recovery. To obtain the maximum oil recovery, the injection should start shortly after the bottomhole pressure drops below the dew point pressure.

Department: Mining and Petroleum Engineering.....Student's signature: *Phakphum*
 Field of study: Petroleum Engineering.....Advisor's signature: *Suwat Athichanagorn*
 Academic Year: 2008.....

Acknowledgements

Many persons have contributed either directly or indirectly to my thesis; I wish to express my thanks to them sincerely.

Firstly and foremost, I would like to thank Asst. Prof. Suwat Athichanagorn, my thesis advisor, for giving knowledge of petroleum engineering and invaluable guidance during this study. I also would like to express my sincere gratitude for his patience and encouragement throughout this work.

Secondly, I would like to thank all faculty members in the Department of Mining and Petroleum Engineering who have offered petroleum knowledge, technical advice, and invaluable consultation. I wish to thank the thesis committee members for their comments and recommendations that make this thesis formally complete.

I would like to thank Schlumberger Overseas S.A. for providing the reservoir simulator software used in this study. I am indebted to Mr. Suphanai Jamsutee for providing some important data used in this work.

Finally, I would like to express my deeply gratitude and thank to my parents who have always been my inspiration, hope, and faith.



สถาบันวิทยบริการ
จุฬาลงกรณ์มหาวิทยาลัย

Contents

	Page
Abstract (in Thai)	iv
Abstract (in English)	v
Acknowledgement	vi
Contents	vii
List of Tables	x
List of Figures	xii
List of Abbreviations	xvi
Nomenclature	xviii
 CHAPTER	
I. INTRODUCTION	1
1.1 Outline of Methodology	2
1.2 Thesis Outline	3
 II. LITERATURE REVIEW	 4
2.1 Previous Works.....	5
 III. THEORY AND CONCEPT	 7
3.1 Review of Gas-Condensate Reservoir	7
3.1.1 Gas Condensate Phase Behavior	7
3.1.2 Regions around gas condensate wellbores.....	8
3.1.3 Non-Darcy Flow and Positive Coupling.....	10
3.2 CO ₂ Injection in Gas-Condensate Reservoir	12
3.2.1 Flooding Patterns and Sweep Efficiency	13
3.2.2 Miscible Fluid Displacement	15
3.2.3 CO ₂ Solubility in water.....	16
3.3 CO ₂ Sequestration	17
3.3.1 Sequestration Mechanism	18
3.3.1.1 Seal Trapping	18

3.3.1.2 Solubility Trapping	19
3.3.1.3 Mineralization Trapping.....	19
3.3.1.4 Phase Trapping	20
3.3.2 Safety and Risk Management.....	21
3.3.3 Verification of CO ₂ Storage.....	22
IV. SIMULATION RESERVOIR MODEL	23
4.1 Grid Section	24
4.1.1 Local Grid Refinement	25
4.2 Fluid Section.....	26
4.2.1 CO ₂ Solubility in water.....	28
4.2.2 Positive coupling	30
4.3 SCAL (Special Core Analysis) Section.....	31
4.2 Wellbore Section.....	35
V. SIMULATION RESULT AND ANALYSIS	36
5.1 Production with Natural Depletion	37
5.2 Production with CO ₂ Injection at the Beginning	43
5.3 Natural Depletion and Production with CO ₂ Injection.....	49
5.3.1 Gas Production Rate (GPR).....	49
5.3.2 Oil Production Rate (OPR)	49
5.3.3 Bottom hole pressure (BHP).....	49
5.3.4 Gas production total	50
5.3.5 Oil production total	50
5.4 Production with CO ₂ Injection at Different Starting Time.....	52
5.5 Stopping Injection before CO ₂ Concentration in Produced Gas Reaches Limit	66
5.6 Production with Gas-Recycling	76
5.6 Economic Analysis.....	81
VI. CONCLUSIONS AND RECOMMENDATIONS	84
6.1 Conclusions.....	84

	Page
6.1.1 Mechanism of CO ₂ Injection	84
6.1.2 Hydrocarbon Recovery Enhancement by CO ₂ Injection	85
6.1.3 Economic Analysis of CO ₂ Injection.....	85
6.2 Recommendations	86
References	87
Appendices.....	89
Vitae	104



สถาบันวิทยบริการ
จุฬาลงกรณ์มหาวิทยาลัย

List of Tables

	Page
Table 3.1: Areal sweep efficiency for various flooding patterns.	14
Table 3.2: Values of Coefficient in CO ₂ Solubility Correlation.	17
Table 4.1: Local Grid Refinement used in this study.	25
Table 4.2: The initial composition of the reservoir fluid	26
Table 4.3: Physical properties of each component.	27
Table 4.4: Binary interaction coefficient between components	27
Table 4.5: Oil saturation and oil relative permeability	31
Table 4.6: Water saturation and water relative permeability	32
Table 4.7: Gas saturation and gas relative permeability	33
Table 4.8: Water saturation and capillary pressure	34
Table 5.1: Economic limit for oil production rate.....	36
Table 5.2: Oil and gas total production and production life for natural depletion.	40
Table 5.3: Production time before the BHP reaches the dew point pressure and the bottomhole limit for natural depletion	40
Table 5.4: Total oil and gas production with CO ₂ injection at the beginning	46
Table 5.5: Production life for production with CO ₂ injection at the beginning.....	46
Table 5.6: Percentage of gas recovery enhancement by producing gas-condensate reservoir with CO ₂ injection.	50
Table 5.7: Percentage of oil recovery enhancement by producing gas-condensate reservoir with CO ₂ injection.....	51
Table 5.8: Total oil and gas production with maximum gas production rate of 2,000 MSCF/D and vary times prior to injection between 1 – 9 yrs.....	63
Table 5.9: Production life for production with maximum gas production rate of 2,000 MSCF/D and vary times prior to injection between 1 – 9 yrs.....	63
Table 5.10: Total oil and gas production with maximum gas production rate of 4,000 MSCF/D and vary times prior to injection between 1 – 6 yrs.....	64
Table 5.11: Production life for production with maximum gas production rate of 4,000 MSCF/D and vary times prior to injection between 1 – 6 yrs.	64

Table 5.12: Total oil and gas production and production life for starting CO ₂ injection at the beginning and stopping the injection when the produced gas has CO ₂ concentration of 5% - 35%.....	72
Table 5.13: Total oil and gas production and production life for starting CO ₂ injection 2 years afterward and stopping the injection when the produced gas has CO ₂ concentration of 5% - 35%.....	75
Table 5.14: Injected gas composition used in gas recycling scenario.....	76



สถาบันวิทยบริการ
จุฬาลงกรณ์มหาวิทยาลัย

List of Figures

	Page
Figure 3.1: Pressure-Temperature diagram of gas condensate.	8
Figure 3.2: Regions around gas condensate wellbores.	9
Figure 3.3: Flooding pattern (Five-Spot; Inverted five-spot).	14
Figure 3.4: CO ₂ geological sequestration options.	18
Figure 4.1: Top view of the reservoir model.	24
Figure 4.2: Side view of the reservoir model.	24
Figure 4.3: 3D view of the reservoir model.	25
Figure 4.4: Phase behavior of the reservoir fluid system	28
Figure 4.5: Carbon Dioxide Solubility in water	29
Figure 4.6: Formation volume factor of CO ₂ -saturated water	29
Figure 4.7: Oil relative permeability function.	341
Figure 4.8: Water relative permeability as a function of water saturation	342
Figure 4.9: Gas relative permeability as a function of gas saturation	343
Figure 4.10: Capillary pressure as a function of water saturation.	344
Figure 4.11: Casing and tubing flow model used in this study.	345
Figure 5.1: Gas production rates for natural depletion.	37
Figure 5.2: Oil production rate for natural depletion	38
Figure 5.3: Bottomhole pressure for natural depletion.	38
Figure 5.4: Oil saturation at Grid (4, 4, 2) in LGR grid representing the producer for natural depletion.	38
Figure 5.5: Total gas production for natural depletion.	41
Figure 5.6: Total oil production for natural depletion.	41
Figure 5.7: Production life for natural depletion.	42
Figure 5.8: Gas production rates for production with CO ₂ injection at the beginning	43
Figure 5.9: Oil production rates for production with CO ₂ injection at the beginning	44
Figure 5.10: Bottomhole Pressure for production with CO ₂ injection at the beginning	44

Figure 5.11: CO ₂ mole fraction in the produced gas for production with CO ₂ injection at the beginning	45
Figure 5.12: Total gas production for production with by CO ₂ injection at the beginning.....	47
Figure 5.13: Total oil production for production with by CO ₂ injection at the beginning.....	47
Figure 5.14: Production life for production with by CO ₂ injection at the beginning..	48
Figure 5.15: Gas production rates for maximum gas production rate of 2,000 MSCF/D with different times prior to injection.....	53
Figure 5.16: Gas production rates for maximum gas production rate of 4,000 MSCF/D with different times prior to injection.....	53
Figure 5.17: Oil production rate for maximum gas production rate of 2,000 MSCF/D with different times prior to injection.....	54
Figure 5.18: Oil production rate for maximum gas production rate of 4,000 MSCF/D with different times prior to injection.....	54
Figure 5.19: Bottomhole pressure for maximum gas production rate of 2,000 MSCF/D with different times prior to injection.....	55
Figure 5.20: Bottomhole pressure for maximum gas production rate of 4,000 MSCF/D with different times prior to injection.....	55
Figure 5.21: CO ₂ mole fraction for maximum gas production rate of 2,000 MSCF/D with different times prior to injection.....	56
Figure 5.22: CO ₂ mole fraction for maximum gas production rate of 4,000 MSCF/D with different times prior to injection.....	56
Figure 5.23: Oil Saturation at Grid (4, 4, 2) in the LGR for maximum gas production rate of 2,000 MSCF/D with different times prior to injection	57
Figure 5.24: Oil Saturation at Grid (4, 4, 2) in the LGR for maximum gas production rate of 2,000 MSCF/D with different times prior to injection	57
Figure 5.25: Total gas production with maximum gas production rate of 2,000 MSCF/D and vary times prior to injection between 1 – 9 yrs	60
Figure 5.26: Total gas production with maximum gas production rate of 4,000 MSCF/D and vary times prior to injection between 1 – 6 yrs	60

Figure 5.27: Total oil production with maximum gas production rate of 2,000 MSCF/D and vary times prior to injection between 1 – 9 yrs	61
Figure 5.28: Total oil production with maximum gas production rate of 4,000 MSCF/D and vary times prior to injection between 1 – 6 yrs	61
Figure 5.29: Production life with maximum gas production rate of 2,000 MSCF/D and vary times prior to injection between 1 – 9 yrs	62
Figure 5.30: Production life with maximum gas production rate of 4,000 MSCF/D and vary times prior to injection between 1 – 6 yrs	62
Figure 5.31: Gas production rates for starting CO ₂ injection at the beginning and stopping injection when the produced gas has CO ₂ concentration of 5%- 35%.....	66
Figure 5.32: Gas production rates for starting CO ₂ injection after 2 years of production and stopping injection when the produced gas has CO ₂ concentration of 5%- 35%.....	67
Figure 5.33: Oil production rates for starting CO ₂ injection at the beginning and stopping injection when the produced gas has CO ₂ concentration of 5%- 35%.....	67
Figure 5.34: Oil production rates for starting CO ₂ injection after 2 years of production and stopping injection when the produced gas has CO ₂ concentration of 5%- 35%..	68
Figure 5.35: The bottomhole pressure for starting CO ₂ injection at the beginning and stopping injection when the produced gas has CO ₂ concentration of 5%- 35%	68
Figure 5.36: The bottomhole pressure for starting CO ₂ injection after 2 years of production and stopping injection when the produced gas has CO ₂ concentration of 5%- 35%.....	69
Figure 5.37: CO ₂ mole fraction for starting CO ₂ injection at the beginning and stopping injection when the produced gas has CO ₂ concentration of 5%- 35%	69
Figure 5.38: CO ₂ mole fraction for starting CO ₂ injection after 2 years of production and stopping injection when the produced gas has CO ₂ concentration of 5%- 35% ..	70
Figure 5.39: Total gas production for starting CO ₂ injection at the beginning and stopping the injection when the produced gas has CO ₂ concentration of 5%- 35% ...	71
Figure 5.40: Total oil production for starting CO ₂ injection at the beginning and stopping the injection when the produced gas has CO ₂ concentration of 5%- 35% ...	71
Figure 5.41: Production life for starting CO ₂ injection at the beginning and stopping the injection when the produced gas has CO ₂ concentration of 5%- 35%	72

Figure 5.42: Total gas production for starting CO ₂ injection 2 years afterward and stopping the injection when the produced gas has CO ₂ concentration of 5%- 35% ...	73
Figure 5.43: Total oil production for starting CO ₂ injection 2 years afterward and stopping the injection when the produced gas has CO ₂ concentration of 5%- 35% ...	74
Figure 5.44: Production life for starting CO ₂ injection 2 years afterward and stopping the injection when the produced gas has CO ₂ concentration of 5%- 35%	74
Figure 5.45: Gas production rate for producing with gas recycling in comparison to production with CO ₂ injection	77
Figure 5.46: Oil production rate for producing with gas recycling in comparison to production with CO ₂ injection	77
Figure 5.47: Bottomhole pressure for producing with gas recycling in comparison to production with CO ₂ injection	78
Figure 5.48: Total gas production for producing with gas recycling in comparison to production with CO ₂ injection	79
Figure 5.49: Total oil production for producing with gas recycling in comparison to production with CO ₂ injection	79
Figure 5.50: Production life for producing with gas recycling in comparison to production with CO ₂ injection	80
Figure 5.51: Cash flow for selected cases.....	82
Figure 5.52: Net present value (NPV) for selected cases	82

List of Abbreviations

API	degree (American Petroleum Institute)
bbbl	barrel (bbbl/d : barrel per day)
BHP	bottom hole pressure
BTU	British thermal unit
C ₁	methane
C ₂	ethane
C ₃	propane
i-C ₄ or I-C ₄	isobutane
i-C ₅ or I-C ₅	isopentane
n-C ₄ or N-C ₄	normal butane
n-C ₅ or N-C ₅	normal pentane
C ₆	hexane
C ₇₊	alkane hydrocarbon account from heptanes forward
CDM	clean development mechanism
CDMEB	clean development mechanism executive board
CER's	certified emissions reduction credits
CO ₂	carbon dioxide
D	darcy
DNA	designated national authority
EOR	enhance oil recovery
GHG	green house gas
GPT	gas production total
GPR	gas production rate
OPT	oil production total
OPR	oil production rate
IET	international emissions trading
IRR	internal rate of return
JI	joint implementation
LGR	local grid refinement
M	¹ thousand (1,000 of petroleum unit), ² million (dollar)
MSCF/D	thousand standard cubic feet per day

NEI	non-equilibrium initialisation
NPV	net present value
PDD	project design document
PVT	pressure-volume-temperature
PSIA or psia	pounds per square inch absolute
SCAL	special core analysis
SGAS	gas saturation
SGFN	gas saturation function
SOFN	oil saturation function
STB or stb	stock-tank barrel
STB/D	stock-tank barrels per day
SWAT	water saturation
SWFN	water saturation function
TVD	true vertical depth or total vertical depth
UNFCCC	United Nations Framework Convention on Climate Change

สถาบันวิทยบริการ
จุฬาลงกรณ์มหาวิทยาลัย

Nomenclature

A	cross-section area
B	formation volume factor
b	repulsion parameter
C	salinity of brine in weight percent of solid
c_g	gas compressibility
E	sweep efficiency
k	permeability
k_r	relative permeability
k_{ri}	conventional relative permeability for capillary dominated
k_{rM}	relative permeability function in the limit of viscous dominated
k_{rg}	gas relative permeability
k_{rgI}	immiscible relative permeability
k_{rgM}	straight-line miscible relative permeability
k_{rw}	water relative permeability
k_{rog}	oil relative permeability for a system with oil, gas and connate water
k_{row}	oil relative permeability for a system with oil and water only
k_{rowg}	oil relative permeability for a system with oil and water at $S_g = 0$
K	equilibrium constant, diffusion coefficient between CO ₂ and gas condensate fluid
N_c	capillary number
p	pressure
p_c	capillary pressure
q	volumetric flow rate
R	solubility of CO ₂ in water
S	saturation
S_r	residual saturation
T	temperature
t	time period
v	velocity
x	distance

$x_{0.1}$	locations at which the CO ₂ concentration is 0.1
$x_{0.9}$	locations at which the CO ₂ concentration is 0.9
z	compressibility factor

GREEK LETTER

β	Forchheimer parameter
ε	Corey exponent
ϕ	porosity
f	capillary number dependent transition function
ρ	fluid density (mass/volume)
μ	fluid viscosity
Δ	difference operator
∇	3 dimension difference operator
α	constant in capillary number dependent transition function
σ	interfacial tension

SUPERSCRIPTS

*	end-point indicator for relative permeability
---	---

SUBSCRIPTS

A	areal
atm	at standard pressure
d	displacement
g	gas
i	vertical
sb	brine
sc	at standard condition
sw	distilled water
w	water
α	phase indicator for relative permeability and saturation

CHAPTER I

INTRODUCTION

Increasing condensate recovery is a challenging task. When the pressure falls below the dew point, retrograde condensate accumulates in the pore system. This phenomenon will create a certain quantity of liquid in the reservoir leading to a condensate blockage problem. This condensate blockage will reduce the well productivity and deliverability. Furthermore, some of the valuable condensate will be left in the reservoir as residual oil.

The pressure declining below the dew point pressure and the reduction in well productivity by condensate bank is predominantly a challenge to be avoided. One of the most effective methods of solving this problem is gas injection. Gas injection allows enhanced condensate recovery by liquid re-vaporization and reservoir re-pressurization or pressure maintenance. The injected gas can be natural gas or other inert gases, depending on gas availability of each reservoir. CO₂ is of the one alternative for the injected gas.

CO₂ is denser and more viscous than hydrocarbon lean gas and that CO₂ will generally be supercritical in deep depleted reservoirs. The large density of CO₂ relative to lean gas, predominantly CH₄, means that CO₂ will tend to migrate downward. The larger viscosity of CO₂ ensures that displacement of lean gas by CO₂ will provide a favorable mobility ratio, with fewer tendencies for the gases to finger and intermix. Furthermore, pressure diffusivity is typically three-five orders of magnitude larger than molecular diffusivity, making re-pressurization occur much faster than mixing by molecular diffusion. In addition, the uses of CO₂ as injected gas also achieve the purpose of CO₂ sequestration in to the geological storage.

In the wake of the Kyoto protocol, CO₂ emission reduction to control the level of CO₂ in the atmosphere has become an important goal. One possible solution is to sequester CO₂ in subsurface formation. Gas condensate reservoirs are becoming important targets for CO₂ sequestration. Because they have held large quantities of natural gas over geologic time scales, depleted gas condensate reservoirs offer a

proven integrity against gas escape and large available capacity for carbon sequestration.

CO₂ injection in gas condensate reservoir is a new subject that has not been studied as extensively. The purpose of this thesis is to investigate the feasibility of CO₂ injection in gas condensate reservoirs. In addition, the optimal production and injection strategy will be carried out in order to maximize hydrocarbon recovery.

1.1 Outline of Methodology

This thesis is to study the behavior of CO₂ injection in gas condensate reservoir. The most appropriate production and injection profile which is injection timing and production and injection rates will be determined. The economics analysis will be used as criteria to determine the most appropriate production and injection profile. To determine the optimal injection timing, we have to separate the production and injection strategy into three scenarios which are

- (a) Produce hydrocarbon from the reservoir with natural depletion at various production rates from one production well until oil or gas production rate drops below the economic limit.
- (b) Start producing hydrocarbon from one well together with CO₂ injection from another well until oil or gas production rate drops below the economic limit or CO₂ concentration in produce gas reaches its concentration limit.
- (c) Produce hydrocarbon from one well and then selectively perform CO₂ injection with different starting times on the other well until oil or gas production rate drops below the economic limit or CO₂ concentration in produce gas reaches its concentration limit.

In the CO₂ injection scenarios, we also study effect of stopping the injection before CO₂ concentration reaches its limit. Gas recycling scenario is also simulated in order to compare hydrocarbon recovery. In this study, the economic limits are set by oil production rate, gas production rate and CO₂ concentration limit. The 23% and

40% concentration limit are selected. The 23% limit is the common CO₂ concentration limit in Gulf of Thailand and the 40% limit is the limit used when a CO₂ removal unit is installed. Then, the economic evaluations are performed in order to investigate the feasibility of CO₂ injection project. Economic evaluations are also used to evaluate the feasibility of CO₂ removal unit installation.

1.2 Thesis Outline

This thesis paper consists of six chapters.

Chapter II outlines a list of related works/studies on CO₂ injection into gas reservoir and gas condensate reservoir to enhance hydrocarbon recovery. And, some works on CO₂ sequestration into the geological storage are also outlined.

Chapter III describes the theory of gas-condensate reservoir, the mechanism of CO₂ injection, and CO₂ sequestration.

Chapter IV describes the simulation model used in this study.

Chapter V discusses the results of reservoir simulation obtained from different values of controlled variables which are production and injection rates and time to start the injection process.

Chapter VI provides conclusion and recommendation for further study.

สถาบันวิทยบริการ
จุฬาลงกรณ์มหาวิทยาลัย

CHAPTER II

LITERATURE REVIEW

This chapter discusses some works related to CO₂ injection and the development of production of gas-condensate reservoir. Some works are significant for generating the most realistic simulation model which will be used to determine optimal production and injection strategy. Unfortunately, CO₂ injection to enhance condensate recovery has not been broadly investigated. Thus, most of the following literatures discuss related works in injecting CO₂ into gas reservoirs using a compositional reservoir simulator and lean gas injection to remove condensate bank. In addition, there are some literatures on CO₂ sequestration into geological storage.

2.1 Previous works

E. Shtepani (2006) [1] performed a special core flood test design to determine the microscale conformance of CO₂ displacement. The purpose of his study is to identify CO₂ breakthrough characteristics during liquid re-vaporization and re-pressurization process and to evaluate the recovery performance. He defined the width of dispersion zone as the distance between the locations at which CO₂ concentration is 0.1 and 0.9 mole fraction and concluded that the dispersion width is proportional to the square root of time.

He also investigated CO₂ and gas condensate phase behavior, a P - x experiment was performed on four different CO₂ and gas condensate mixtures with 20, 40, 60 and 80 mole % CO₂ additions. Each time a constant composition expansion experiment was performed, the saturation pressure and the liquid dropout was measured. He concluded that at 80 mole % CO₂ addition there was no retrograde liquid observed and the mixture was in single phase gas.

J.J. Chaback, and M.L Willium (1994) [2] investigated the phase behavior of a rich-gas-condensate reservoir fluid in admixture of CO₂. They found that admixture of CO₂ raises the mixture dewpoints instead of lowering them. Furthermore, if

retrograde liquid forms before gas injection begins, CO₂ is effective in re-vaporizing retrograde liquid.

A. Al-Hashami *et. al.* (2005) [3] investigated the process of injecting CO₂ into gas reservoirs using a compositional reservoir simulator. The effects of gas mixing, CO₂ diffusion and CO₂ solubility in formation water were investigated. CO₂ dispersion effect where the diffusion coefficient is high will cause an early CO₂ breakthrough. When the diffusion coefficient is smaller than 10⁻⁶ m²/sec, the effect of diffusion can be neglected. Thus, the mixing of CO₂ and methane is totally due to convective flow.

They also studied the effect of CO₂ solubility in formation water. When CO₂ solubility in formation water was taken into account, CO₂ breakthrough time was delayed. However, the same incremental gas recovery was achieved. Therefore, the solubility of CO₂ in formation water has some positive effect on CO₂ storage in the reservoir, which can delay CO₂ breakthrough and store more gas in the reservoir.

Yih-Bor Chang *et. al.* (1998) [4] presented correlations for computing the solubility of CO₂ in water and other properties of CO₂ saturated water. A new empirical correlation was presented for the solubility of CO₂ in formation water as a function of pressure and temperature. The calculated solubility in formation water can also be adjusted further for the effects of salinity to obtain the solubility of CO₂ in brine. Furthermore, correlations for computing the formation volume factor, compressibility, and viscosity of CO₂ saturated water were given in this study.

Sinisha A. Jikich *et. al.* (2003) [5] investigated the amount of carbon dioxide sequestered and the effect of carbon dioxide injection on gas recovery. Different injection strategies were used for a thin, shaly sandstone reservoir in Northern West Virginia. Two injection scenarios were studied: (1) simultaneous CO₂ injection and methane recovery from the beginning of the project, and (2) primary production of natural gas to the economic limit, followed by injection of carbon dioxide for secondary gas recovery.

The simulation results showed that the highest methane recovery was obtained when the reservoir was produced under primary recovery until the economic limit, followed by CO₂ injection. The maximum amount of incremental gas recovery was less than 10% of the original gas in place (OGIP). Lower recovery factors for methane

were obtained in the case when CO₂ injection was injected early. However, the early CO₂ injection accelerated methane recovery and improved CO₂ retention in the reservoir.

Curtis M. Odenburg *et. al.* (2002) [6] applied simulations to the Rio Vista Gas Field in California. The purpose of their study was to investigate the mechanism of CO₂ injections into heterogeneous depleted gas reservoirs. The results showed that significant amounts of CO₂ can be injected to produce significant quantities of additional natural gas. Mixing in the gas reservoir is limited by the large density and viscosity of CO₂ relative to CH₄. These physical property differences become larger at higher pressures.

Permeability heterogeneity accelerates breakthrough by the creation of fast flow paths. However, by injecting CO₂ at large distances from CH₄ production wells, one can take advantage of fast repressurization effects long before mass transfer allows CO₂ to contaminate produced gas even in a strongly heterogeneous system. Injecting CO₂ at relatively deeper levels in a reservoir while producing from higher levels will decrease CO₂ upconing and mixing. Mixing is inhibited by the strong density contrast that causes CO₂ to fill the reservoir from the bottom up, making an effective vertical and lateral sweep.

M. Sengul (2006) [7] illustrated framework of CO₂ sequestration and vital aspects such as site selection, reservoir characterization, modeling of storage and long term leakage monitoring techniques. He concluded that CO₂ capture and storage (CCS) offers possibilities for making further use of fossil fuels more compatible with climate change and mitigation policies. Technologies required for CO₂ capture and storage, monitoring, verification are widely available today.

He also concluded that the probability of CO₂ leakage in oil and gas reservoirs is very low. However, brine formations, which generally are not well characterized and do not have caprocks or seals will require significant effort to evaluate potential risks, and these risks must be taken seriously.

CHAPTER III

THEORY AND CONCEPT

This chapter discusses fundamental of gas condensate reservoir, its region around the wellbore, and related theories involved with the mechanism of CO₂ injection in a gas condensate reservoir. The important issues about CO₂ sequestration into geological storage are also discussed in this chapter.

3.1 Review of Gas-Condensate Reservoir

Gas-condensate reservoirs have been considered the most complex reservoir among other types of petroleum reservoirs. These reservoirs have unusual phase behaviors of reservoir fluids such as the condensing and vaporizing mechanism within the reservoirs. As the gas is produced, the reservoir pressure decreases. After it reaches the dew point pressure, it will exhibit the regions around the wellbore based on the liquid saturation and type of flow. One unique phenomenon in near wellbore region of gas condensate reservoir is positive coupling, which occurs when the flow velocity is high, and the interfacial tension between the flowing phases is low.

3.1.1 Gas Condensate Phase Behavior

The phase diagram of a gas condensate system is smaller than that of oil, and the critical point is further down the left side of the envelope. The phase diagram and pressure path of this type of reservoir is shown in Figure 3.1.

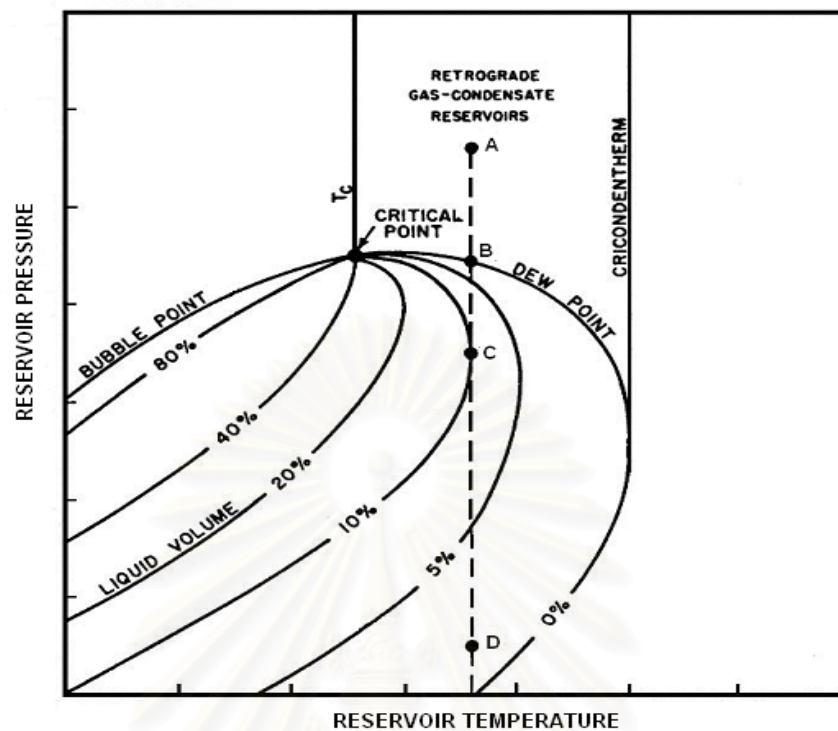


Figure 3.1: Pressure-Temperature diagram of gas condensate.

The reservoir initially contains single-phase gas (from point A to point B) where its pressure is above the dew point pressure. When the reservoir pressure declines on production phase until it reaches the dew point pressure (point B), liquid starts to drop out in the pore space. This phenomenon will leave a certain quantity of valuable liquid in the reservoir, and the liquid also causes problems such as condensate blocking. This phenomenon continues until the maximum liquid dropout pressure is reached (point C). After the pressure is lower than the maximum liquid dropout pressure (point D), liquid saturation will decrease due to the re-vaporization process, but this pressure is typically below the economic life of the field, and this re-vaporization process will not be reached.

3.1.2 Regions around Gas Condensate Wellbores

Based on the type of flow, the region around the wellbore in a gas condensate reservoir can be subdivided into three parts. For a given producing condition, one, two, or all three regions may exist. They are illustrated in Figure 3.2.

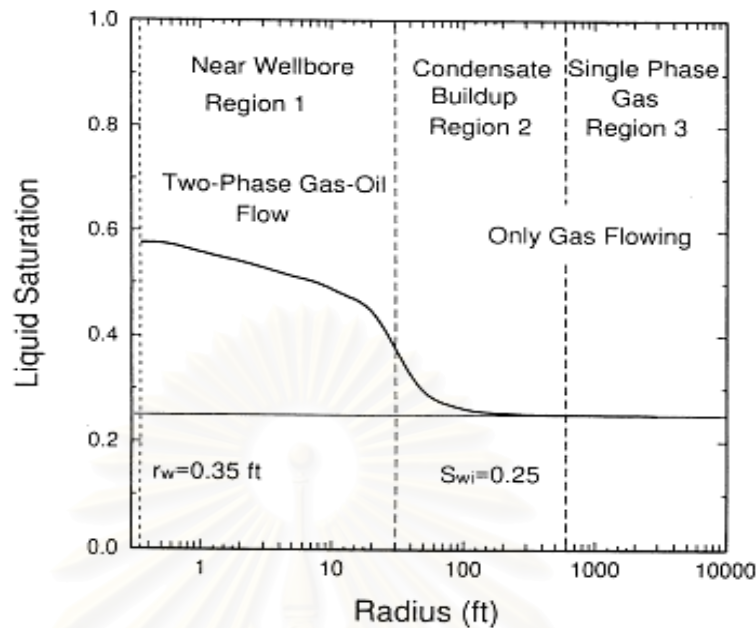


Figure 3.2: Regions around gas condensate wellbores

Region 1 is the region close to the wellbore with high condensate saturation where both gas and condensate are flowing simultaneously. Region 1 exists only when the bottomhole flowing pressure is less than the pressure at which condensate saturation is equal to the critical saturation. The condensate saturation in this region is high enough to allow the condensate movement.

The flowing composition within Region 1 is constant throughout. This means that the single-phase gas entering Region 1 has the same composition as the produced wellstream mixture. Conversely, if we know the producing wellstream, then we know the flowing composition within Region 1. Furthermore, the dew point of the producing wellstream mixture equals the reservoir pressure at the outer edge of Region 1.

Region 1 is the main source of deliverability loss in a gas-condensate well. Gas relative permeability is reduced owing to condensate buildup. The size of Region 1 increases with time. For steady-state conditions, the condensate saturation in Region 1 is determined (as a function of radius) specifically to ensure that all liquid that condenses from the single-phase gas entering Region 1 has sufficient mobility to flow through and out of Region 1 without any net accumulation.

In region 2, condensate is dropping out. This region exists when the reservoir pressure declines below the dew point pressure. However, liquid is not mobile since the condensate saturation is less than the critical saturation. Therefore, in this region only gas phase is mobile whereas the condensate is immobile.

Region 3 contains only the original reservoir gas. This is the farthest region in the reservoir where the reservoir pressure is greater than the dew point pressure. Gas velocity in this region is generally low due to the large cross sectional area available to flow.

There may also exist a region 4 near the wellbore where low interfacial tension at high gas velocity leads to decreased condensate saturation and increased gas mobility. This phenomenon was referred to as 'positive coupling'.

3.1.3 Non-Darcy Flow and Positive Coupling

In near wellbore region of gas condensate reservoirs, there are two phenomena that affect the well productivity and cannot be expressed by Darcy equation which are non-Darcy flow and positive coupling.

Non-Darcy flow is typically observed in high-rate gas wells when the flow converging to the wellbore reaches flow velocities exceeding the Reynolds number for laminar or Darcy flow, and results in turbulent flow. The effect of non-Darcy flow can be treated using the Forchheimer equation with an empirical correlation. Forchheimer [8] proposed the following quadratic equation to express the relationship between pressure drop and velocity in a porous medium:

$$\frac{dp}{dx} = \left(\frac{\mu}{kk_r A} \right) q + \beta \rho \left(\frac{q}{A} \right)^2 \quad (3.1)$$

where:

- q is the volumetric flow rate
- k is the rock permeability
- k_r is the relative permeability
- A is the area through which flow occurs
- μ is the fluid viscosity

ρ is the fluid density
 β is the Forchheimer parameter
 $\frac{dp}{dx}$ is the pressure gradient normal to the area

Another phenomenon, which is known as positive coupling, occurs when the flow velocity is high and the interfacial tension between the flowing phases is low. Then, capillary forces may no longer dominate the distribution of the phases on a pore scale. As a consequence, macroscopic flow properties become dependent on the ratio of viscous to capillary forces on a pore scale, denoted by the capillary number N_c .

$$N_c = \frac{k|\nabla P|}{\phi\sigma} \quad (3.2)$$

where:

σ is interfacial tension
 ϕ is porosity

Relative permeability to both phases is enhanced by large viscous forces, and the curves tend to straighten. Two causes for this enhancement are a decrease in tortuosity of the flow paths and a reduction of non-conductive saturation. The tortuosity will decrease because viscous forces may allow a short-cut at particular spots where, under capillary dominated flow conditions, one of the phases is blocking a shorter way for the other phase. At the same time, high viscous forces will reduce the non-conductive part of the fluid saturation by mobilizing the residual oil.

We can include effect of positive coupling to relative permeability by making it depend on capillary number. The correlations can be divided into two classes which are:

- a) **Corey relative permeability functions.** A way to include the capillary number that uses part of the general knowledge on relative permeability, is to represent the relative permeability functions by a Corey function, whose coefficients depend on the capillary number:

$$k_{r\alpha}(S_\alpha, N_C) = k_{r\alpha}^*(N_C) \left(\frac{S_\alpha - S_{r\alpha}(N_C)}{1 - S_{r\alpha}(N_C)} \right)^{\varepsilon_\alpha(N_C)} \quad (3.3)$$

where k_r^* is the end-point relative permeability, S_r is the residual saturation, and ε is the Corey exponent that fixes the curvature of the relative permeability function.

b) Interpolate between immiscible (low capillary number) and miscible (high capillary number) relative permeability functions. Relative permeability curves at near-critical conditions have often been represented by a weighted linear function of immiscible and miscible relative permeability curves, where the weighting factor is a function of the capillary number:

$$k_{r\alpha}(S_\alpha, N_C) = f_\alpha(N_C)k_{rai}(S_\alpha) + \{1 - f_\alpha(N_C)\}k_{raM}(S_\alpha) \quad (3.4)$$

Here α is a phase indicator (condensate, gas), k_{ri} is the conventional relative permeability for capillary dominated (immiscible) flow, and k_{rM} is the relative permeability function in the limit of viscous dominated (miscible) flow. This approach is particularly suitable for fitting large sets of measured data on relative permeability at varying capillary numbers. The N_C -dependence is more explicit than in the case of interpolating Corey coefficients, so that convergence causes fewer problems.

3.2 CO₂ Injection in Gas-Condensate Reservoir

Re-pressurization or pressure maintenance is one of the most common methods to enhance gas and condensate recovery. By pressurizing the reservoir so that the reservoir pressure is above the dew point pressure, condensate blockage can be prevented.

For CO₂ injection into gas condensate fields, high viscosity of CO₂ provides a favorable mobility ratio for the displacement of methane, leading to fewer tendencies

of the gases to finger and intermix. Furthermore, pressure diffusivity is typically 3 to 5 orders of magnitude larger than molecular diffusivity, making re-pressurization occur much faster than mixing by molecular diffusion.

Re-vaporization will remove the condensate blockage by changing the phase behavior of the reservoir fluid. The admixture of CO₂ to gas condensate fluid will reduce the percent liquid and improve productivity and condensate recovery.

3.2.1 Flooding Patterns and Sweep Efficiency

Production wells and injection wells are typically arranged in a certain pattern for an EOR project. The most common patterns are,

- (a) Two-spot
- (b) Three-spot
- (c) Regular four-spot and skewed four-spot
- (d) Normal five-spot and inverted five-spot
- (e) Normal seven-spot and inverted seven-spot
- (f) Normal nine-spot and inverted nine-spot
- (g) Direct line drive
- (h) Staggered line drive

Different areal sweep efficiencies at breakthrough have been reported for a variety of flooding patterns. The most popular pattern for studying is the five-spot pattern. There is satisfactory agreement among most investigators that the five-spot flooding pattern gives the highest sweep efficiency. The areal sweep efficiency at breakthrough was determined by various experimental techniques. The percentage of such areal sweep efficiency performance was calculated for a mobility ratio of unity. Table 3.1 presents the percentage of areal sweep efficiency at breakthrough calculated at unity mobility ratio for different flooding patterns.

Table 3.1: Areal sweep efficiency for various flooding patterns [9].

Flooding Pattern	Mobility Ratio	Areal sweep efficiency at breakthrough (%)
Isolated two-spot	1.0	52.5 – 53.8
Isolated three-spot	1.0	78.5
Skewed four-spot	1.0	55.0
Normal five-spot	1.0	105.0
Inverted five-spot	1.0	80.0
Normal seven-spot	1.0	74.0-82.0
Inverted seven-spot	1.0	82.2

The overall efficiency at breakthrough is defined as

$$E = E_A \times E_i \times E_d \quad (3.5)$$

where E_A is areal sweep efficiency, E_i is invasion or vertical sweep efficiency, and E_d is displacement efficiency.

In this study, injection-production well arrangement is selected by considering the highest areal sweep efficiency. Normal and inverted five-spot flooding patterns have been studied and reported to have the highest sweep efficiency at breakthrough. Figure 3.3 shows the schematic of five-spot flooding pattern. In five-spot flooding pattern, the injection well is located at the center of a square defined by four production wells.

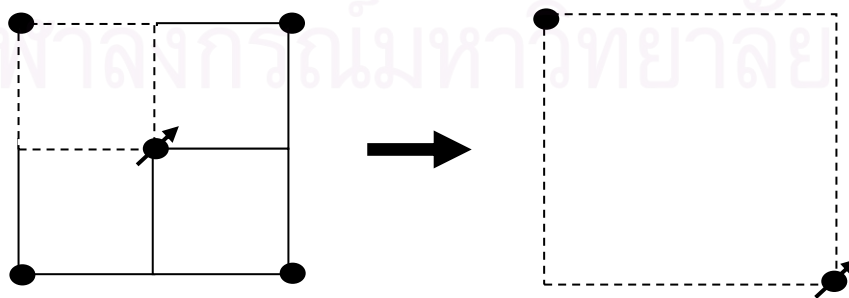


Figure 3.3: Flooding pattern (Five-Spot; Inverted five-spot)

3.2.2 Miscible Fluid Displacement

A miscibility fluid displacement would be defined as a displacement process where no phase boundary or interface exists between the displaced and displacing fluids. In this process, the displacing fluid is miscible, or will mix in all proportions with the displaced fluid. According to the definition described above, the main miscible fluid displacement processes are as follows:

- (1) High pressure dry gas miscible displacement.
- (2) Enriched gas miscible displacement.
- (3) Miscible slug flooding, where the leading edge of the slug is miscible with the displaced fluid.
- (4) Aqueous and oleic miscible slug flooding (such as several of the alcohols).
- (5) Carbon dioxide, flue or inert gas displacements.

For CO₂ injection into gas condensate fields, the important issues involve the effect of miscible mixing of the gases by dispersion, as a contribution of convection and molecular diffusion. We can define the width of dispersion zone as the distance between the locations at which the CO₂ concentration is 0.1 and 0.9 mole fraction. The width of dispersion zone as defined above can be calculated from Equation 3.9. This equation was obtained from lab experiment by E. Shtepani. From the equation, we can see that the dispersion width is proportional to \sqrt{t} .

$$x_{0.1} - x_{0.9} = 3.625\sqrt{Kt} \quad (3.9)$$

where

- $x_{0.1}$ is the locations at which the CO₂ concentration is 0.1
- $x_{0.9}$ is the locations at which the CO₂ concentration is 0.9
- K is the diffusion coefficient between CO₂ and gas condensate fluid
- t is time after CO₂ injection begin

3.2.3 CO₂ Solubility in water

In most of the published models, all hydrocarbon components exist in the oil and gas phases but are not allowed to dissolve in the aqueous phase. Usually, this assumption is adequate because the hydrocarbon solubility in water is low over the range of temperature and pressure for gas injection. But, the solubility of CO₂ in water is much higher than that of hydrocarbon components and is a factor that cannot be neglected in the simulation process. When CO₂ dissolution was taken into account, CO₂ breakthrough time was delayed comparing with the case without considering CO₂ solubility in water. This increases the benefit of process since CO₂ can be storage in the connate water.

The solubility of CO₂ in water can be calculated using a correlation developed by Chang *et al*⁵. The correlations are given below

$$R_{sw} = a \cdot p \cdot \left[1 - b \cdot \sin \left(\frac{\pi}{2} \cdot \frac{c \cdot p}{c \cdot p + 1} \right) \right] \quad \text{if } p < p^o \quad (3.7)$$

$$R_{sw} = R_{sw}^0 + m \cdot (p - p^o) \quad \text{if } p \geq p^o \quad (3.8)$$

where a , b , c , m , R_{sw}^0 , and p^o are given below:

$$a = \sum_{i=0}^4 a_i \cdot 10^{-3i} \cdot T^i, \quad (3.9)$$

$$b = \sum_{i=0}^4 b_i \cdot 10^{-3i} \cdot T^i, \quad (3.10)$$

$$c = \sum_{i=0}^4 c_i \cdot 10^{-3i} \cdot T^i \quad (3.11)$$

$$R_{sw}^0 = a \cdot p^o \cdot (1 - b^3), \quad (3.12)$$

$$p^o = \frac{2}{\pi} \frac{\sin^{-1}(b^2)}{c \cdot [1 - 2/\pi \sin^{-1}(b^2)]}, \quad (3.13)$$

$$m = a \left\{ 1 - b \left[\sin \left(\frac{\pi}{2} \cdot \frac{c \cdot p^o}{c \cdot p^o + 1} \right) + \frac{\pi}{2} \cdot \frac{c \cdot p^o}{(c \cdot p^o + 1)^2} \cos \left(\frac{\pi}{2} \cdot \frac{c \cdot p^o}{c \cdot p^o + 1} \right) \right] \right\} \quad (3.14)$$

R_{sw} is CO₂ solubility in scf of CO₂ per STB of water, T is temperature (°F), p is pressure (psia), and the coefficients are shown in Table 3.2.

Table 3.2: Values of Coefficient in Eqs 3.8 to 3.10

	$i = 0$	$i = 1$	$i = 2$	$i = 3$	$i = 4$
a_i	1.163	-16.630	111.073	-376.859	524.889
b_i	0.965	-0.272	00.0923	-0.1008	0.0998
c_i	1.280	-10.757	53.696	-222.395	462.672

The calculated solubility in distilled water can be adjusted further for the effects of salinity to obtain the solubility of CO₂ in brine:

$$\log\left(\frac{R_{sb}}{R_{sw}}\right) = -0.028 \cdot C \cdot T^{-0.12} \quad (3.14)$$

where R_{sb} is CO₂ solubility in scf of CO₂ per STB of brine, C is the salinity of brine in weight percent of solid, and T is temperature (°F).

The formation volume factor of CO₂-saturated water (or brine) is calculated with

$$B_w = \frac{\rho_{w,sc} + 0.02066 \cdot R_{sb}}{\rho_{w,atm} + 0.0058 \cdot R_{sb}} \quad (3.15)$$

where B_w is water formation volume factor in reservoir barrel per STB of water (rb/STB), $\rho_{w,sc}$ is water density at standard temperature and pressure in lb/ft³, and $\rho_{w,atm}$ is water density at reservoir temperature and 14.7 psia in lb/ft³.

3.3 CO₂ Sequestration

Because the injected CO₂ is stored inside the reservoir, the fundamental of CO₂ sequestration is discussed in this section. The options of CO₂ sequestration into the geological storage are illustrated in Figure 3.5.

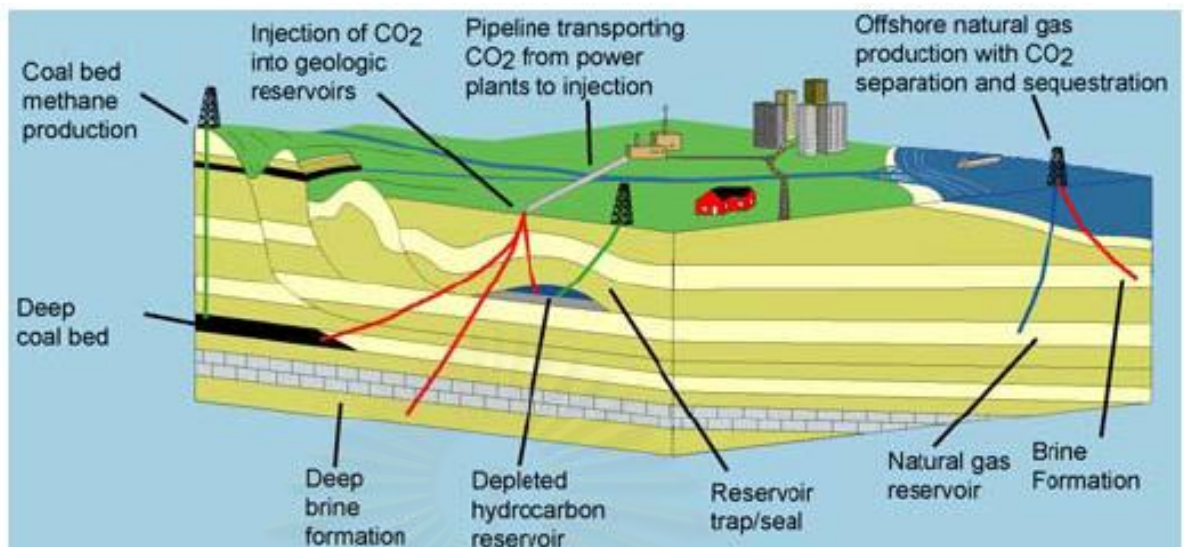


Figure 3.4: CO₂ geological sequestration options.

3.3.1 Sequestration Mechanism

As the concept of geologic sequestration developed, it was recognized that CO₂ can be sequestered in geologic formations by four principal mechanisms:

3.3.1.1 Seal Trapping

CO₂ can be trapped as a gas or supercritical fluid under a low-permeability caprock, similar to the way that natural gas is trapped in gas reservoirs or that gas is stored in aquifer gas storage. This process is commonly referred to as hydrodynamic trapping. In the short term, this process is likely to be the most important mechanism for sequestration. It is rapid and the biggest contributor to storage process. However, mobility of CO₂ requires monitoring and verification.

To make a full use of storage capacity, CO₂ should be stored in its dense or supercritical phase, above the critical pressure of 1,071 psia and critical temperature of 88 °F. Since CO₂ under these pressure and temperature conditions will still be less dense than formation water, it will naturally rise to the top of the reservoir, and a trap is needed to ensure that it does not reach the surface. In oil and gas reservoirs and

aquifers which are analogous to hydrocarbon fields, CO₂ is immobilized by geologic traps.

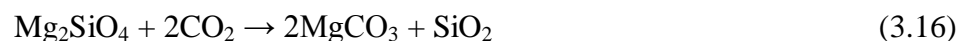
3.3.1.2 Solubility Trapping

Solubility trapping involves the dissolution of CO₂ into the reservoir fluids; CO₂ can dissolve into the fluid phase (water and oil). In oil reservoirs, this lowers the viscosity and swells the oil, which provides the basis for one of the more common enhanced oil recovery (EOR) techniques. The relative importance of solubility trapping depends on a large number of factors, such as the sweep efficiency of CO₂ injection, and the effects of formation heterogeneity. It offers rapid process but limited volume. Mobility is less but still may require monitoring and verification.

3.3.1.3 Mineralization Trapping

Mineral trapping involves the reaction of CO₂ with minerals present in the host formation to form stable, solid compounds, e.g. carbonates. CO₂ can react, either directly or indirectly, with the minerals and organic matter in the geologic formations to become part of the solid mineral matrix. Formation of carbonate minerals such as calcite or siderite and adsorption onto coal are examples of mineral trapping. In this very slow process, sequestered CO₂ become immobile.

Aquifers associated with igneous rocks such as basalt are good candidates for sequestering CO₂, presumed that the geological and hydrogeological conditions are suitable for high pressure CO₂ injections. When high pressure CO₂ is injected into deep aquifers, it will acidify the groundwater. This acid may be neutralized by reactions with the surrounding igneous rocks.



Under high CO₂ pressure, these reactions may be driven to the right to form carbonates. Solubility and mineral trapping mechanisms are particularly important in the case of an aquifer with no lateral seals. As the CO₂ moves through the reservoir along the flow path, it comes into contact with uncarbonated formation water and reactive minerals. A proportion of the CO₂ dissolves in the formation water and some of this dissolved CO₂ becomes permanently fixed by reactions with minerals in the host rock. If the flow path is long enough, the CO₂ might all dissolve or become fixed by mineral reactions before it reaches the basin margin, essentially becoming permanently trapped in the reservoir.

3.3.1.4 Phase Trapping

This process occurs when relative permeability to CO₂ is zero. It is a rapid process, but requires more reservoirs. Abandoned, un-economic coal seams are another potential storage site. CO₂ diffuses through the pore structure of coal and is physically adsorbed to it. This process is similar to the way in which activated carbon removes impurities from air or water. CO₂ can also be used to enhance the recovery of coal bed methane. In some cases, this can be very cost-effective or even cost-free, as the additional methane removal can offset the cost of the CO₂ storage operations.

The relative important of these mechanisms depends on the type of formation used for sequestration. For example, in brine formations, solubility trapping is most important, at least in the short term. By comparison, in coal formations, much of the CO₂ adsorbs to the solid phase.

The basic principle associated with all in situ methods of storing CO₂ is that it is stored in a geological structure which contains it and prevents short-term or medium term release to the atmosphere. The structure must consist of a permeable layer, to allow ingress of CO₂ and an impermeable or low permeable layer to prevent escape of CO₂ to the atmosphere. In this study, the seal trapping is considered as the main mechanism for gas condensate reservoir.

3.3.2 Safety and Risk Management

Safe and secure storage of CO₂ is a key requirement of this technology. The petroleum industry has injected millions of tones of CO₂ into oil reservoirs and aquifers over the past few decades in the successful operation of EOR, CO₂ storage, and acid gas disposal projects. For such operations, safety has been achieved by risk management systems that make use of information from site characterization, operational monitoring, scientific understanding, and engineering experience. Full consideration of the risks of geological storage is required to form the basis for engineering, management, and regulatory systems to achieve acceptable and safe operation. Elements of the risk management are:

Risk Assessment

- Safety assessment methodology
- Risk assessment framework: features, events, processes
- Public perception involvement

Monitoring

- Influence of injection on properties of reservoir & cap rocks
- Geophysical techniques for monitoring CO₂ movement
- Long term sealing integrity of wells
- Integrated simulation

Long Term Monitoring

- Natural CO₂ analogs
- Fracture mechanics approach to seal evaluation
- Time lapsed seismic and electromagnetic surveys
- Integrated surface and subsurface sensors
- Mechanical integrity assessment

3.3.3 Verification of CO₂ Storage

If CO₂ storage were to be used as a basis for emissions trading or to meet national commitments on emissions reduction, it would be necessary to verify the quantities of CO₂ stored. Verification is also a significant challenge for other carbon storage options, such as forestry and enhanced storage in soils.

For CO₂ capture, the flows of gas would be measured as a normal part of the chemical engineering of the process; technology already exists to do this and additional costs would be small. Capture of flue gases can be measured with great accuracy and at low cost.

Also, with transport of CO₂, pipelines already carry CO₂ on a commercial scale, with large quantities of CO₂ monitored accurately in real time using equipment that is available now at low cost. Similar measurements would be used to monitor CO₂ injected into geological reservoirs.

Major oil and gas companies and their contractors have the technology to track gas flows in underground reservoirs using seismic, well logging, and reservoir simulation tools. These technologies are being successfully applied in EOR projects.

Logging technology would be most easily applied in reservoirs where there are also production wells (e.g. oil production). The application to seismic technology for tracking stored CO₂ in underground reservoirs is showing promise, but further development of the technique is required. Tracking will need to be accurate over much longer periods of time for CO₂ storage compared to EOR, where slow leakage is not a major concern.

CHAPTER IV

SIMULATION RESERVOIR MODEL

In order to determine optimal production and injection strategy of CO₂ injection to enhance gas and condensate recovery, reservoir simulator is used as a tool to predict gas and condensate production under different strategies. As a result, the best strategy can be obtained.

We used composition simulator (ECLIPSE: E300) to simulate CO₂ injection in gas condensate reservoir. The compositional simulation provides more accurate calculation of liquid dropout in the porous media by using flash calculation. We can categorize the reservoir simulation model in to 4 main sections which are

- 1. Grid section.** In this section the geometry of the reservoir and its permeability and porosity are specified.
- 2. Fluid section.** The reservoir and injected fluid composition are specified in this section. The physical properties of each component and the EOS used in flash calculation are also specified. Initial reservoir condition is also included in this section.
- 3. SCAL section.** In special core analysis or SCAL section, the 3-phase relative permeabilities are specified.
- 4. Wellbore section.** The wellbore model is constructed and will be used to calculate the vertical performance.

This chapter describes each section in details and how properties in each section were gathered. The detail of the simulation input is shown in Appendix A

4.1 Grid Section

The reservoir model is constructed by amount of established volume elements namely 'grid blocks' that represent the geological reservoir construction. Cartesian grid model, which is commonly used to simulate the full field simulation model, will

be used. The reservoir model is assumed to be homogenous. The top of reservoir is located at a depth of 8,000 ft, with dimensions of 2,250 ft x 2,250 ft and a thickness of 120 ft. The number of block is 15 x 15 x 3. The porosity of the reservoir is assumed as 16.5%, the horizontal permeability is 10.85 mD, and vertical permeability is 1.27 mD. Figures 4.1, 4.2, and 4.3 illustrate the model used in this study in the top view, side view and 3D view, respectively.

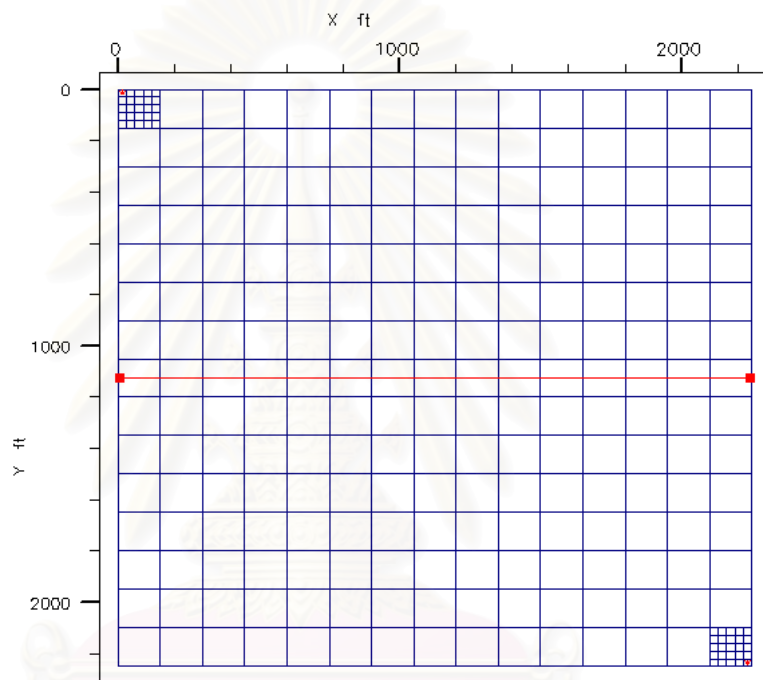


Figure 4.1: Top view of the reservoir model

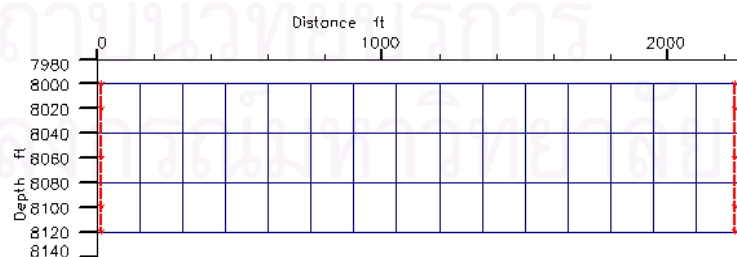


Figure 4.2: Side view of the reservoir model

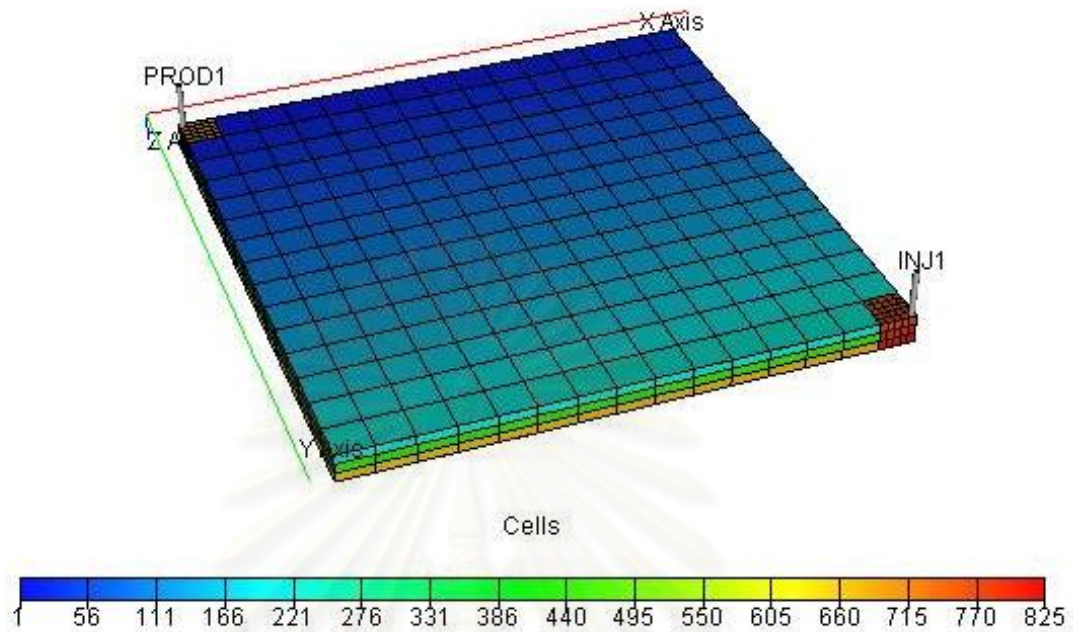


Figure 4.3: 3D view of the reservoir model

4.1.1 Local Grid Refinement

Local Grid Refinement (LGR) provides additional grids in selected grids. This is required for accurate calculation of liquid dropout around the wellbore. In Eclipse, we need to specify LGR name, coordinate, and the number of refined cells. The detail of LGR used in this study are shown in Table 4.1.

Table 4.1: Local Grid Refinement used in this study

LGR Name	LGR Coordinate			Number of refined cells		
	I	J	K	X	Y	Z
Producer	1	1	1-3	5	5	3
Injector	15	15	1-3	5	5	3

4.2 Fluid Section

The initial fluid composition was specified in Non-Equilibrium Initialization (NEI) section. The NEI is used to generate consistent oil and gas compositions for each cell. The initial composition of the reservoir fluid for the study is specified and tabulated in Table 4.2, and the injected fluid is assumed to be pure CO₂.

Table 4.2: The initial composition of the reservoir fluid

Component	Mole Fraction
Methane	0.59991
Ethane	0.084326
Propane	0.063988
Isobutane	0.034127
Normal butane	0.038989
Isopentane	0.014286
Normal pentane	0.013988
Hexane	0.072718
Hepthane plus	0.065366
Carbon dioxide	0.012302

The initial composition of the reservoir fluid is obtained from one sample in the Gulf of Thailand. The initial water saturation is 0.11 and the initial gas saturation is 0.89. The initial water/gas saturation used in this study is an average value from one gas field. In this model, the gas in place is equal to 90,124,961 RCF, which can be separated to be 14,882 MMSCF of gas and 1,851 MSTB of oil at surface.

To calculate the reservoir fluid properties at different reservoir pressures, the Peng Robinson Equation of State will be used. The physical properties of each component were acquired from Engineering Data Book, GPSA1987, as shown in Table 3.2.

In this study, the reservoir temperature is assumed to be constant at 293 °F and the initial reservoir pressure is 3,000 psi. With this reservoir pressure, temperature and fluid composition, the phase behavior of this reservoir fluid system is predicted as illustrated in Figure 4.4.

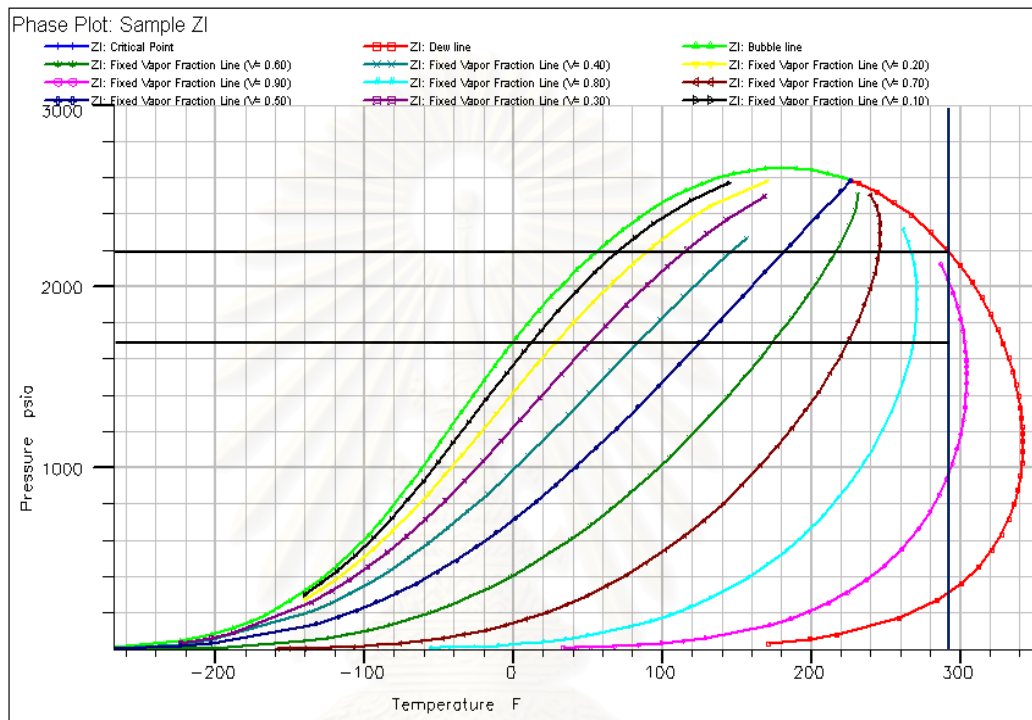


Figure 4.4: Phase behavior of the reservoir fluid system

This phase behavior was calculated by PVTi program. The dew point pressure is 2,200 psi and the maximum liquid dropout of 12% will occur when the reservoir pressure drops to 1,650 psi.

4.2.1 CO₂ Solubility in Water

To simulate CO₂ injection in a gas condensate reservoir, CO₂ solubility in water is one of the importance that cannot be ignored. The solubility of CO₂ in water can be calculated using a correlation developed by Chang *et al.* [5] The formation volume factor of CO₂-saturated water (or brine) is also calculated and used in the model. Three percent by weight of NaCl was used in the correlation. This value of

salinity is commonly seen in the Gulf of Thailand. The solubility of CO₂ in water and the formation volume factor of CO₂-saturated water is shown in Figures 4.6 and 4.7, respectively.

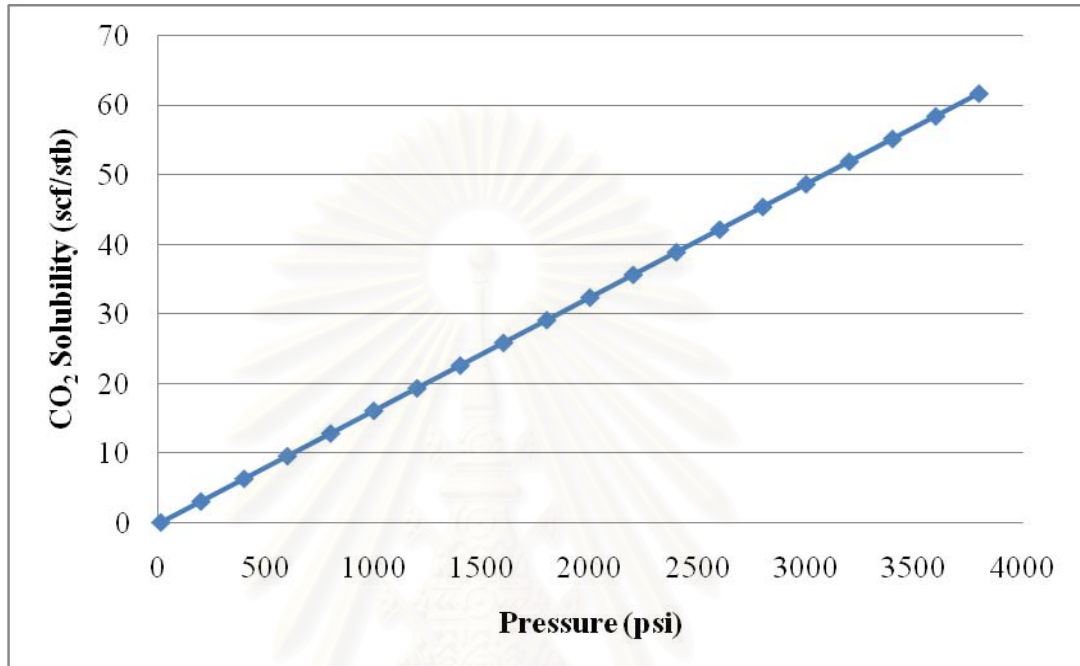


Figure 4.5: Carbon Dioxide solubility in water

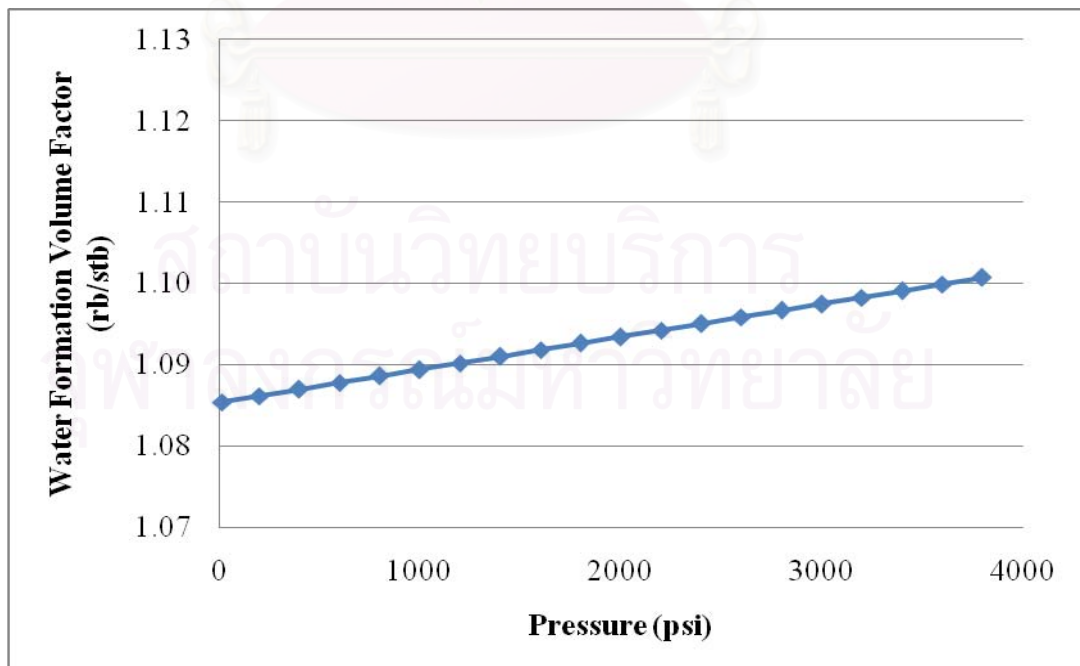


Figure 4.6: Formation volume factor of CO₂-saturated water

4.2.2 Positive coupling

In this study, the interpolation between immiscible and miscible relative permeability functions is used to capture the positive coupling phenomenon. A capillary number modified gas relative permeability is given by

$$k_{rg} = f_I k_{rgI} + (1 - f_I) k_{rgM} \quad (4.1)$$

where k_{rg} is the capillary number modified gas relative permeability,

k_{rgM} is the straight-line miscible relative permeability,

k_{rgI} is the immiscible relative permeability, and

f_I is the capillary number dependent transition function,

The capillary number dependent transition function depends on the gas capillary number, N_{cg} , and is given by:

$$f_I = \frac{1}{(\alpha \cdot N_{cg})^n + 1} \quad (4.2)$$

where $\alpha = \alpha^0 / \overline{k_{rg}}$, with $\overline{k_{rg}} = \frac{k_{rgM} + k_{rgI}}{2}$, and α^0 is a constant depending only on rock properties and is obtained from Equation 4.3.

$$\alpha^0 = \frac{\alpha_c^0}{\sqrt{K \cdot \phi}} \quad (4.3)$$

where K is the rock permeability, and

ϕ is the porosity

And, the capillary number is given by

$$N_{cg} = \frac{v_g \mu_g}{\sigma} \quad (4.4)$$

where v_g is gas velocity,

μ_g is gas viscosity, and

σ is an interfacial tension,

This model depends on two parameters: the exponent n in equation 4.2 and the α_c^0 coefficient in Equation 4.3. These parameters are typically defaulted to 0.65 and 10^4 , respectively. These default values are used in this study.

4.3 SCAL (Special Core Analysis) Section

The oil saturation and oil relative permeabilities are tabulated in Table 4.5 and shown in Figure 4.7. Two types of relative permeability, K_{row} and K_{rowg} , are used. K_{row} is the oil relative permeability for a system with oil and water only, and K_{rowg} is the oil relative permeability for a system with oil, water, and gas.

Table 4.5: Oil saturation and oil relative permeabilities

S_o	K_{row}	K_{rowg}
0	0	0
0.2	0	0
0.32	0.00463	0.015625
0.44	0.037037	0.125
0.56	0.125	0.421875
0.68	0.296296	1
0.95	1	1

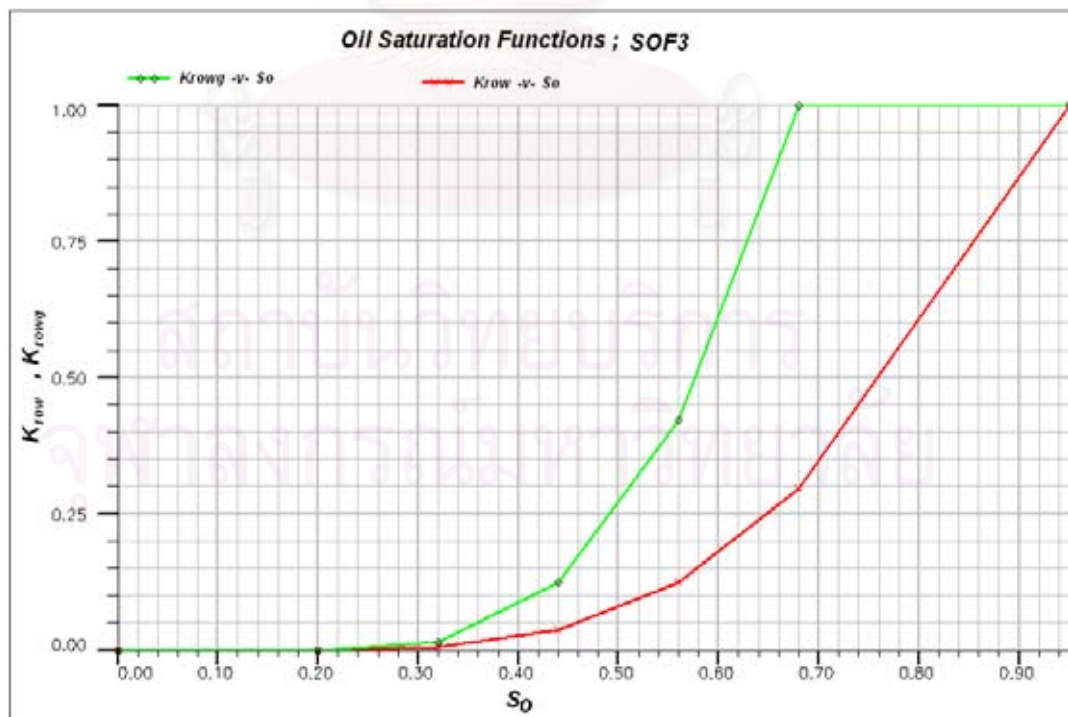


Figure 4.7: Oil relative permeability function.

The water saturation and water relative permeability are tabulated in Table 4.6 and shown in Figure 4.8.

Table 4.6: Water saturation and water relative permeability

S_w	K_{rw}
0.11	0
0.157	0
0.216	0
0.313	0.02
0.44	0.06
0.56	0.10
0.68	0.15
0.80	0.30
0.90	0.65

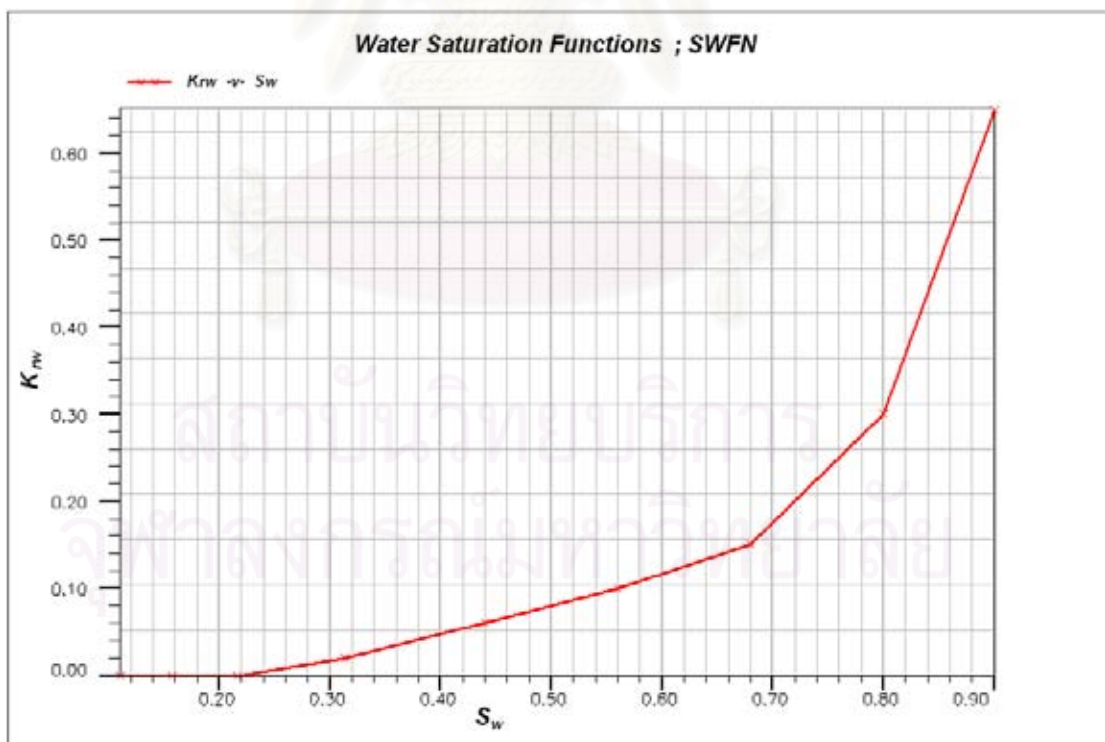


Figure 4.8: Water relative permeability as a function of water saturation.

The gas saturation and gas relative permeability are tabulated in Table 4.7 and shown in Figure 4.9.

Table 4.7: Gas saturation and relative gas permeability

Sg	Krg
0	0
0.1	0
0.2	0
0.3	0.2
0.4	0.4
0.6	0.85
0.7	0.90
0.8	0.92
0.9	0.95
0.95	0.95

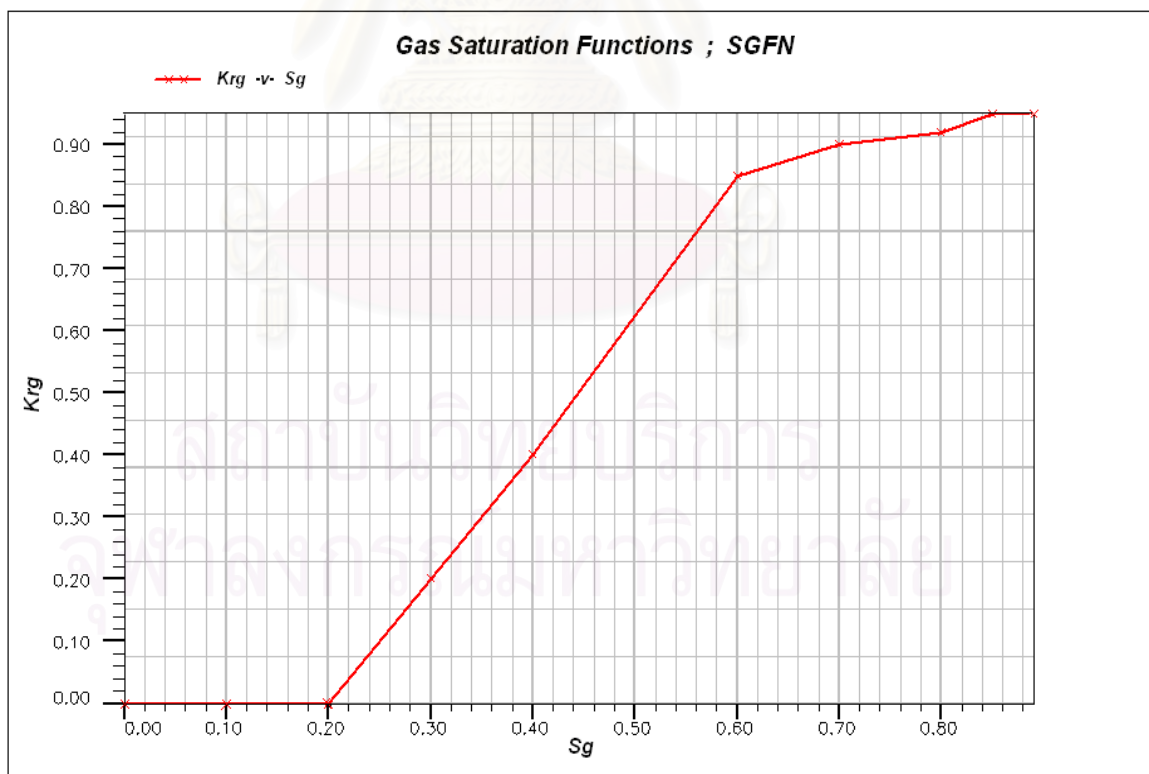


Figure 4.9: Gas relative permeability as a function of gas saturation.

The water saturation and capillary pressure is tabulated in Table 4.8, and their relation curve is shown in Figure 4.10.

Table 4.8: Water saturation and capillary pressure

Sw	Pc (psia)
0.11	250
0.157	53
0.216	13
0.313	1
0.44	0
0.56	0
0.68	0
0.80	0
0.90	0

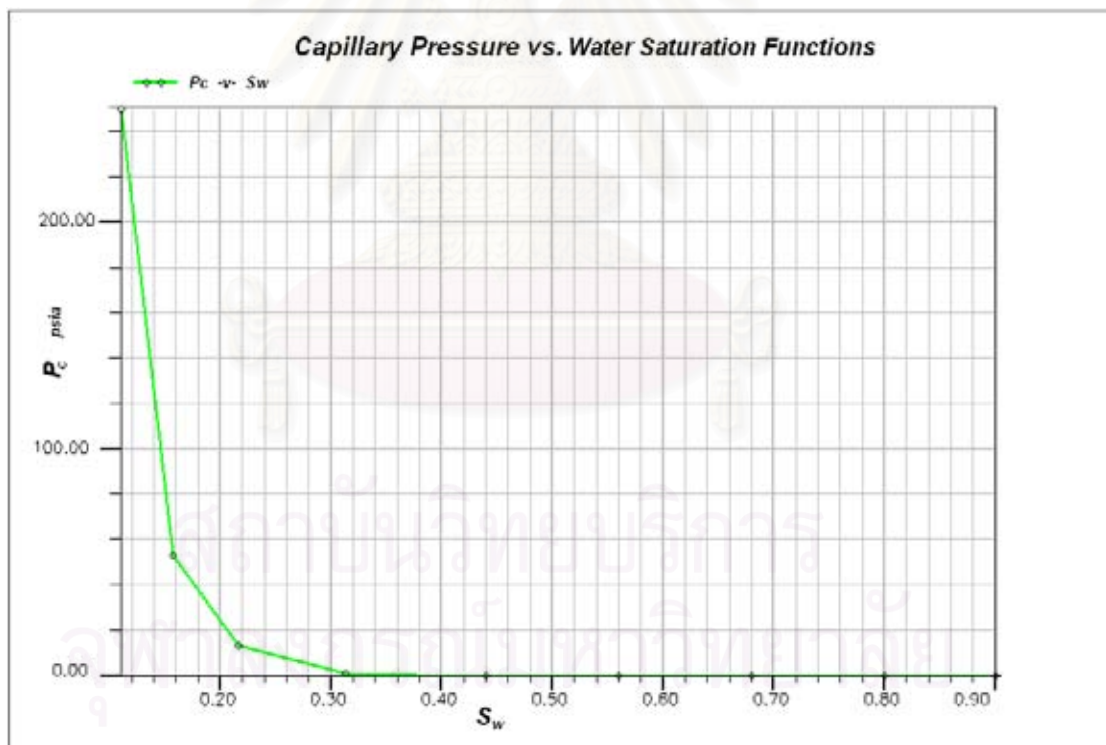


Figure 4.10: Capillary pressure as a function of water saturation.

Gas-condensate reservoir properties in this compositional simulation were obtained from average values of special core analysis data of samples collected from one of the gas fields in the Gulf of Thailand.

4.4 Wellbore Section

The production and injection wells in this study have the same wellbore diameter of 3-1/2 inches with an inside diameter of 2.992 inches. The perforation interval is from the top to the bottom of the reservoir. The schematic of wellbore configuration is shown in Figure 4.11.

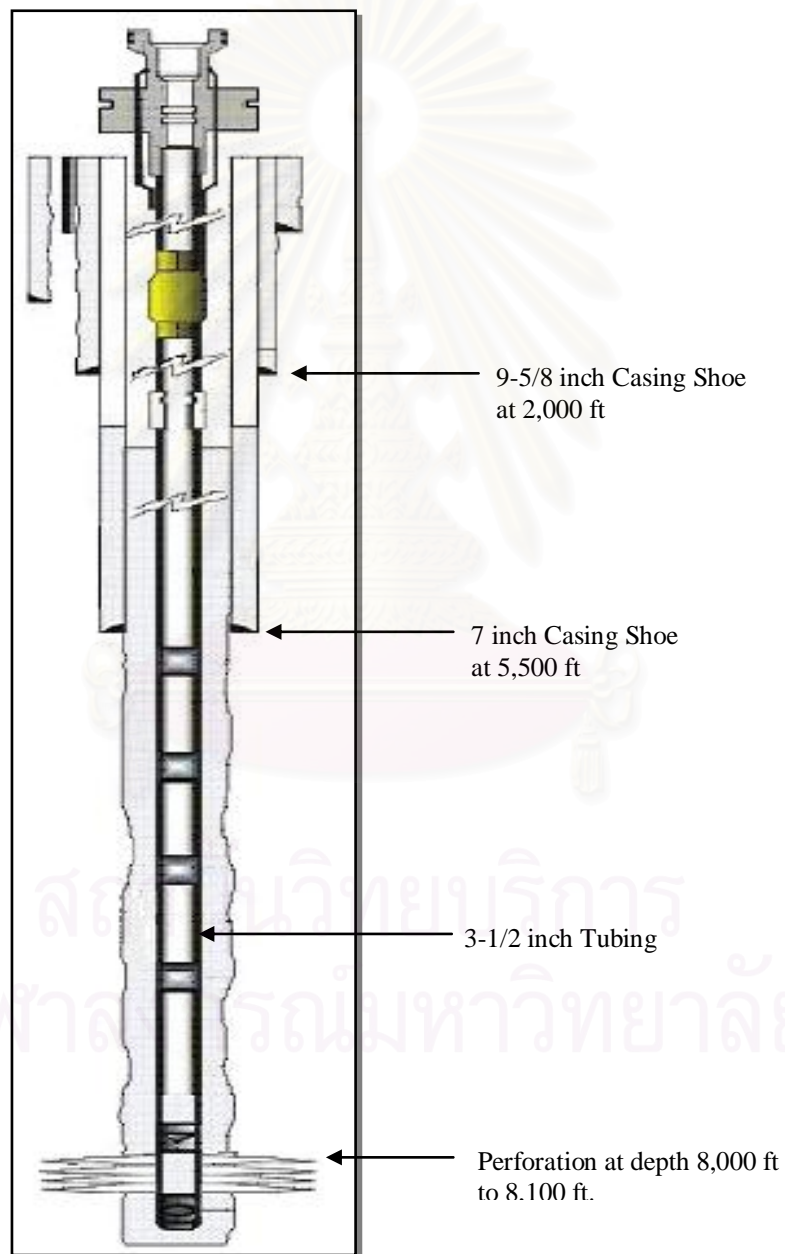


Figure 4.11: Casing and tubing flow model used in this study.

CHAPTER V

SIMULATION RESULT AND ANALYSIS

In this chapter, productions of gas-condensate reservoir simulated under different production and injection scenarios are reported. The results are discussed in term of CO₂ injection mechanism and the effect of different production and injection scenarios. Three main scenarios which are natural depletion, CO₂ injection at the beginning and timely CO₂ injection were simulated. In the CO₂ injection, we also studied the effect of stop ping the injection before CO₂ concentration reaches the limit. Gas recycling scenario was also simulated in order to compare its mechanism and hydrocarbon recovery with CO₂ injection scenario. Then, the economic evaluations were performed in order to investigate the feasibility of CO₂ injection project. Economic evaluations were also used to evaluate the feasibility of CO₂ removal unit installation.

The bottomhole pressure target of 1,800 psia was used for production well. The economic limits were defined at minimum gas rate of 100 MSCF/D and minimum oil production rate was varied. The economic limit for minimum oil production rate is 3 STB/D for production by natural depletion, and varies with gas production rates for CO₂ injection scenario. The economic limits for oil production rate are shown in Table 5.1.

Table 5.1: Economic limit for oil production rate

Gas production rate (MSCF/D)	Minimum oil rate (STB/D)
1,000	4.03
2,000	5.06
3,000	6.1
4,000	7.13
5,000	8.16
6,000	9.19
7,000	10.22
8,000	11.25
9,000	12.29
10,000	13.32

5.1 Production with Natural Depletion

In this scenario, we simulated the production of gas-condensate reservoir by natural depletion method. The maximum gas production rate was used as the control variable. The maximum gas production rate was varied in the range of 1,000 MSCF/D to 10,000 MSCF/D in a step of 1,000 MSCF/D increment, in order to observe effect of production rate limit to depletion mechanism, production life and cumulative production of oil and gas.

For each varied rate, the gas production rate is kept constant as long as the reservoir pressure can sustain such rate with a bottomhole pressure limit of 1,800 psia. After the bottomhole pressure reaches the limit, it is kept constant. Then, the gas production rate starts to decline. Simulation will stop when the gas or oil production rate reach economic limit. Gas production rate (GPR) and oil production rate (OPR) are shown in Figures 5.1 and 5.2, respectively.

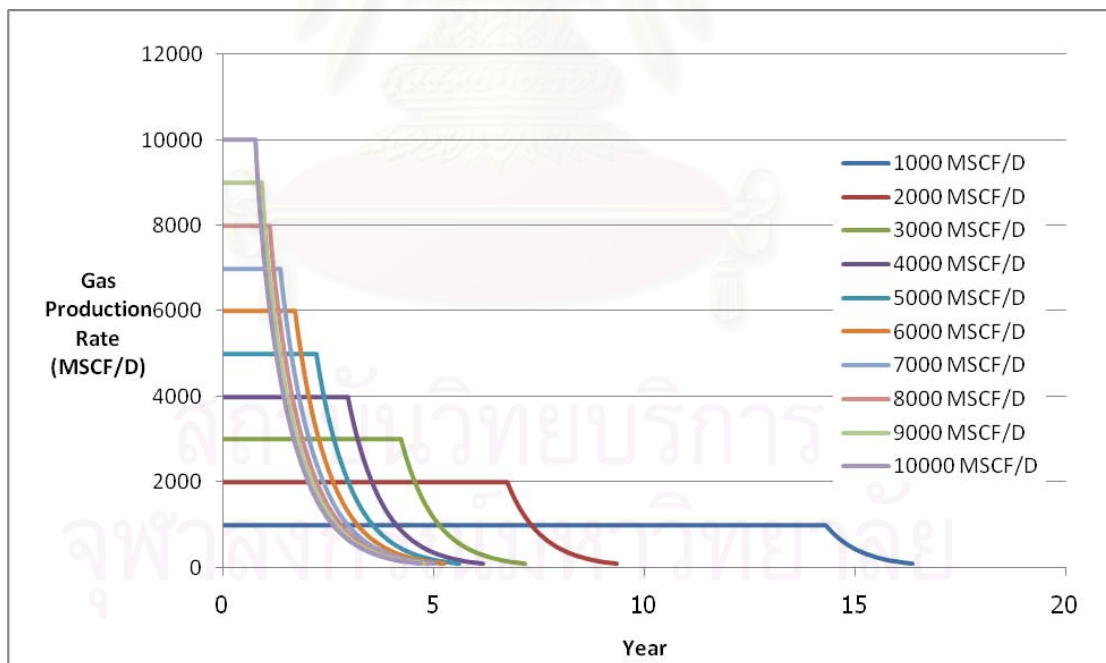


Figure 5.1: Gas production rates for natural depletion.

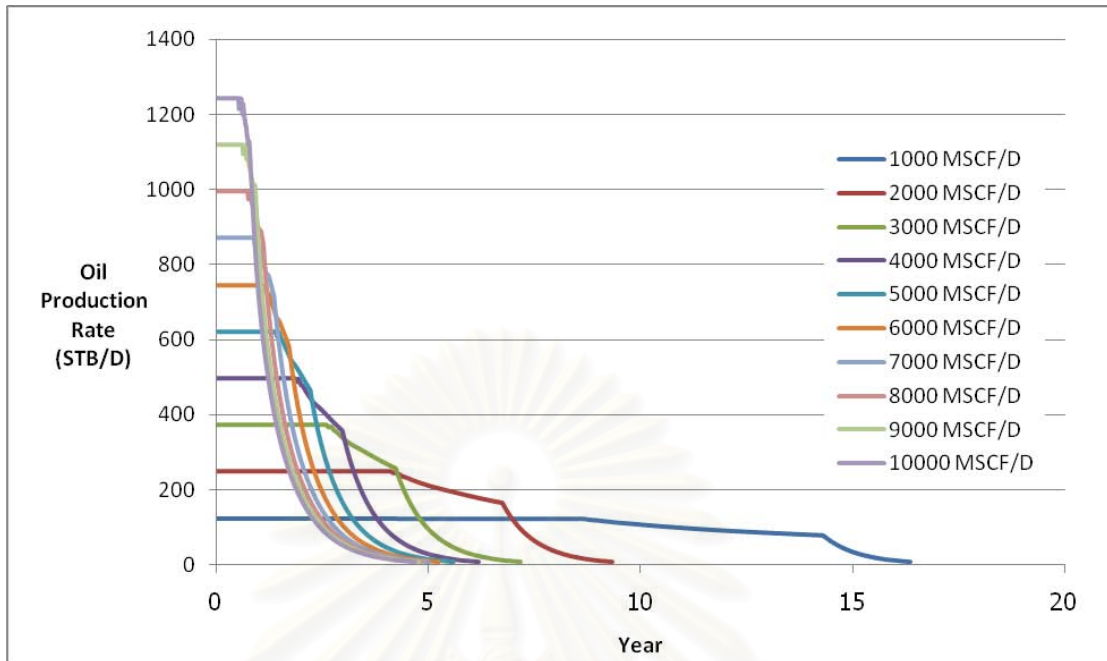


Figure 5.2: Oil production rate for natural depletion.

The bottomhole pressure of the production well and oil saturation at the producer are shown in Figures 5.3 and 5.4, respectively.

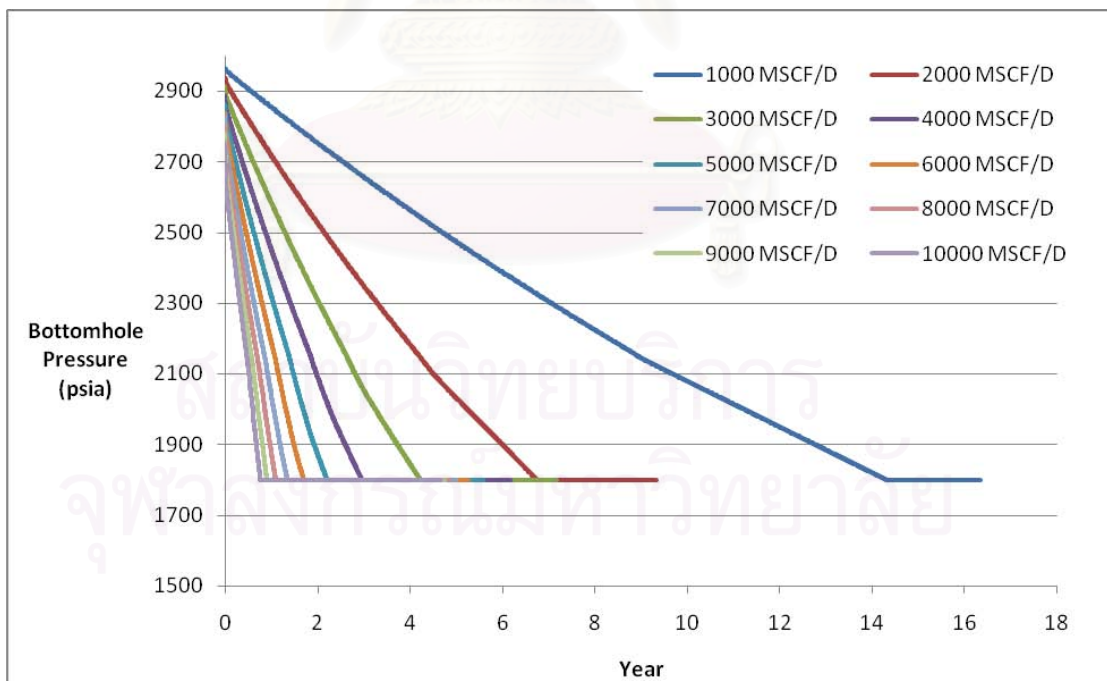


Figure 5.3: Bottomhole pressure for natural depletion.

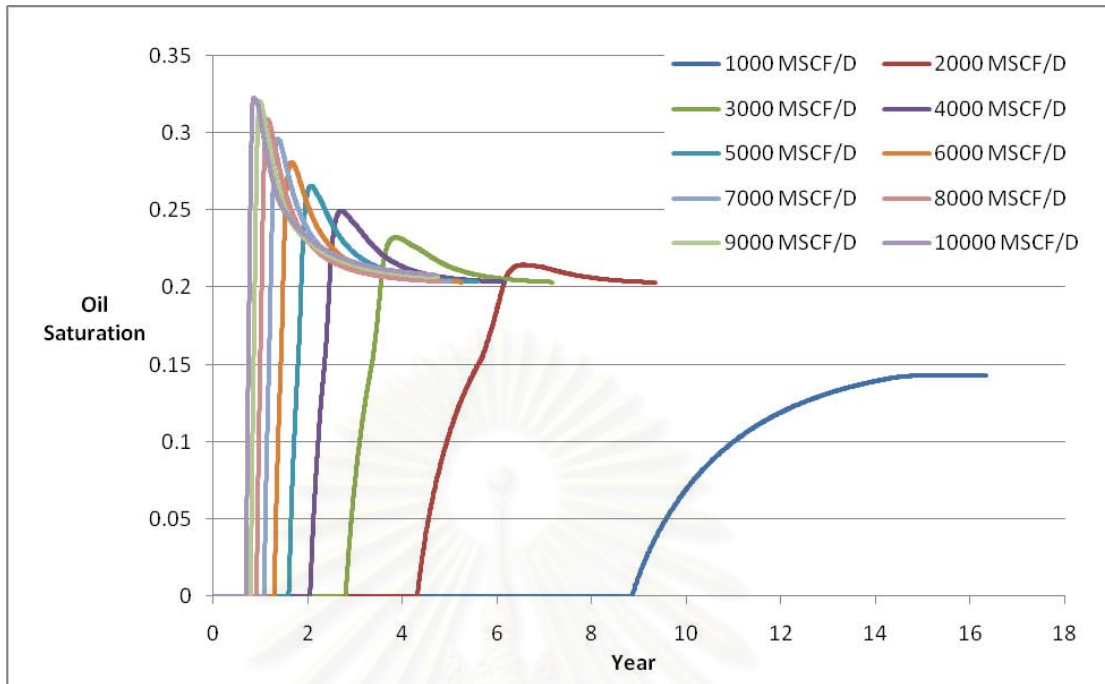


Figure 5.4: Oil saturation at Grid (4, 4, 2) in LGR grid representing the producer for natural depletion.

From Figures 5.1 to 5.4, mechanism of producing gas-condensate reservoir with natural depletion can be summarized as follows:

- a) At early times, gas and oil production rates are constant while the bottomhole pressure declines. After the bottomhole pressure drops below the dew point pressure, the oil production rate declines and liquid starts to condense in the pore space. The oil saturation around the wellbore increases as oil accumulates around the wellbore. Then, the saturation drops and becomes constant at the critical oil saturation. The value of the highest oil saturation depends on the maximum gas production rate. The higher the gas flowrate, the higher the oil saturation. Since a higher rate incurs a lower wellbore pressure, more liquid condense out of the gas phase. Then, the gas production rate drops, and the bottomhole pressure becomes constant at the limit of 1,800 psia. Finally, the simulation stops because the gas production rate drops below 100 MSCF/D.

Table 5.2 illustrates the cumulative production of gas and oil and the production life. Table 5.3 illustrates the production time before the BHP drops to the dew point pressure and limit of 1,800 psia.

Table 5.2: Oil and gas total production and production life for natural depletion.

Production Rate	Production Life (Years)	Gas Recovery (MSCF)	Oil Recovery (STB)
1000 MSCF/D	16.34	5,493,985	615,480
2000 MSCF/D	9.33	5,494,779	611,625
3000 MSCF/D	7.17	5,496,940	608,481
4000 MSCF/D	6.16	5,498,391	605,683
5000 MSCF/D	5.58	5,498,980	603,180
6000 MSCF/D	5.25	5,499,947	601,128
7000 MSCF/D	5.00	5,499,933	599,454
8000 MSCF/D	4.84	5,500,374	598,254
9000 MSCF/D	4.75	5,501,873	597,716
10000 MSCF/D	4.67	5,502,221	597,536

Table 5.3: Production time before the BHP reaches the dew point pressure and the bottomhole limit for natural depletion.

Production Rate	Producing time before reaching the dew point (Years)	Producing time before reaching BHP limit (Years)
1000 MSCF/D	8.59	14.29
2000 MSCF/D	4.08	6.74
3000 MSCF/D	2.58	4.22
4000 MSCF/D	1.84	2.96
5000 MSCF/D	1.38	2.20
6000 MSCF/D	1.09	1.71
7000 MSCF/D	0.88	1.35
8000 MSCF/D	0.72	1.10
9000 MSCF/D	0.60	0.91
10000 MSCF/D	0.50	0.76

The total oil and gas production and the production life as a function of maximum gas production rate are shown in Figures 5.5, 5.6 and 5.7 respectively.

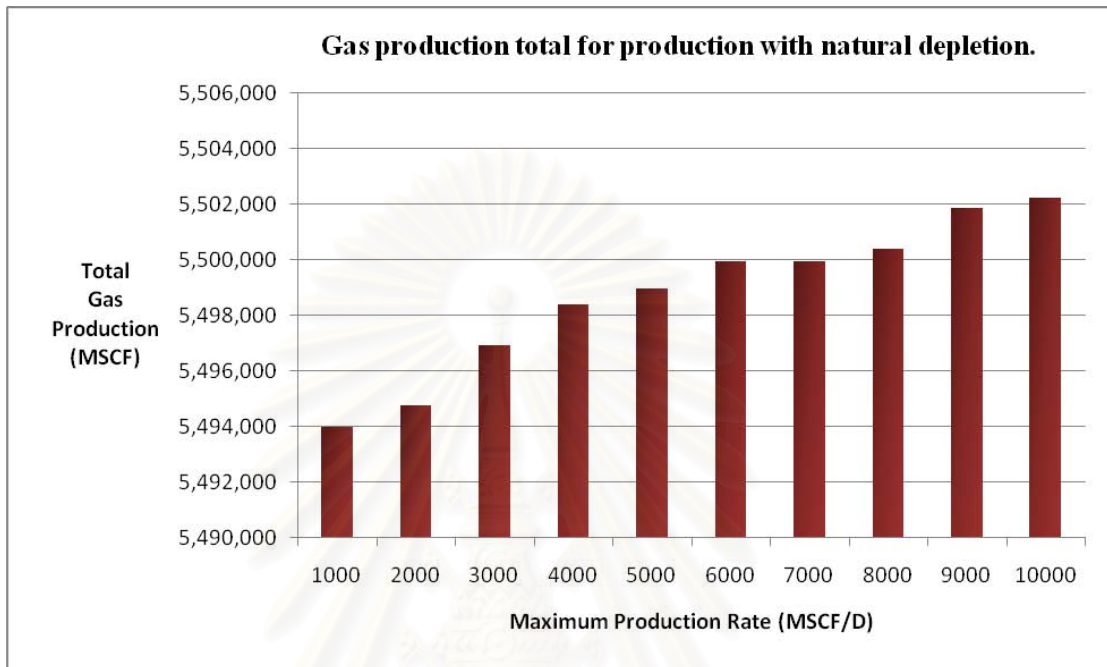


Figure 5.5: Total gas production for natural depletion.

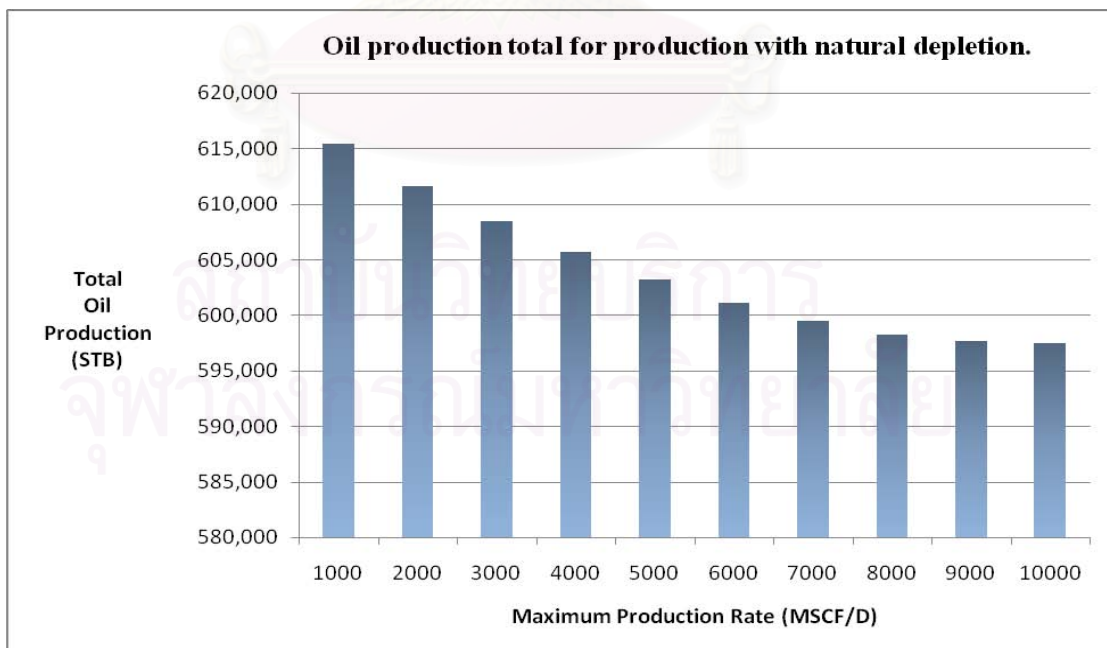


Figure 5.6: Total oil production for natural depletion.

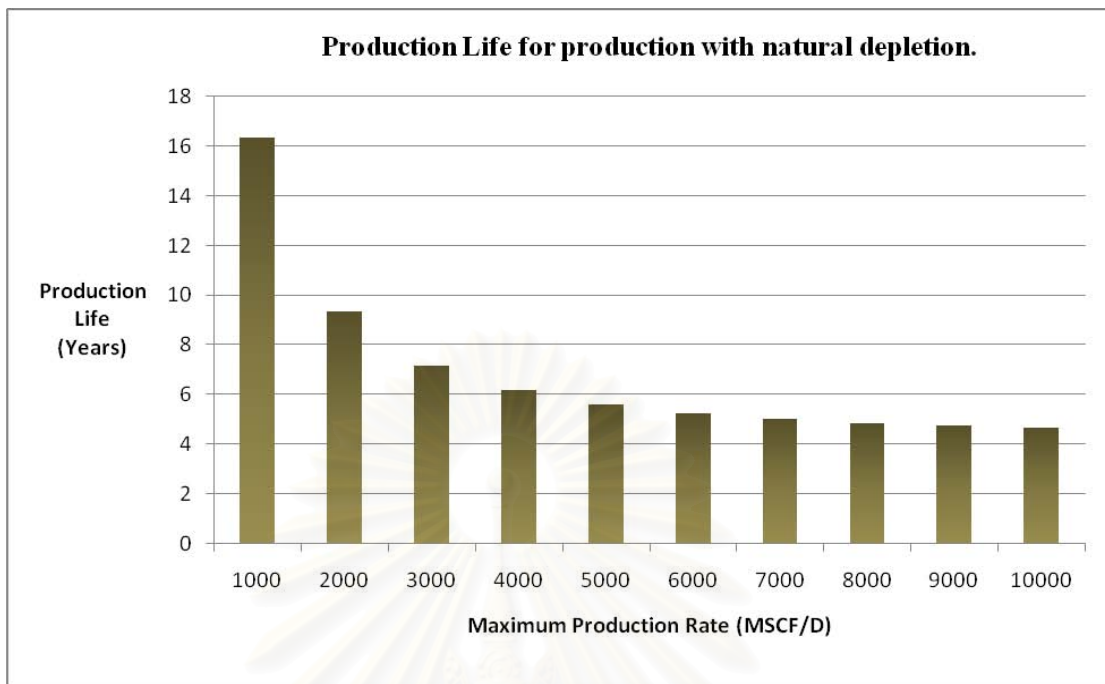


Figure 5.7: Production life for natural depletion.

From Figures 5.5 to 5.7, performance of producing gas-condensate reservoir with natural depletion can be summarized as follows:

- a) The maximum gas production rate does not have a significant effect on gas and oil recovery. There is only 0.14% difference in the gas recovery and 2.96% difference in condensate recovery between the highest and the lowest rates. By increasing the maximum gas rate, higher amount of gas can be recovered but lower condensate recovery. The total production volume of oil and gas fall in a narrow range of 597,536 – 615,480 STB and 5,494 – 5,502 MMSCF, as tabulated in Table 5.2.
- b) Increasing the maximum gas production rate accelerates production and also shortens the production life.

In this scenario, we can see that production with natural depletion does not effectively recover oil and gas from the reservoir. At early times, the bottomhole pressure declines very quickly until reaches the BHP limit. Then, gas production rate declines until reaches the economic limit. As a result, only 37% of gas and 32.5% of condensate can be recovered.

5.2 Production with CO₂ Injection at the Beginning

In this scenario, the gas-condensate reservoir is produced together with CO₂ injection at the beginning in order to maintain the reservoir pressure above the dew point pressure. The injection rate is set to be equal to the production rate in each production profile. Different cases with the values varying from 1,000 MSCF/D to 10,000 MSCF/D in a step of 1,000 MSCF/D increment. In this simulation model, the production well is placed at coordinate (1, 1) in LGR grid representing the producer (located at coordinate (1, 1) in the global grid), and injection well is placed at coordinate (5, 5) in LGR grid representing the injector (located at coordinate (15, 15) in the global grid) in order to simulate a quarter five-spot pattern. The simulation stops if the gas or oil production rate drops below the economic limit. In this scenario, the economic limits were set by oil production rate, gas production rate and CO₂ concentration limit. The 23% and 40% concentration limits were used. The 23% limit is commonly used in the Gulf of Thailand, and the 40% limit is used when a CO₂ removal unit is installed. The gas production rate and oil production rate are shown in Figures 5.8 and 5.9, respectively.

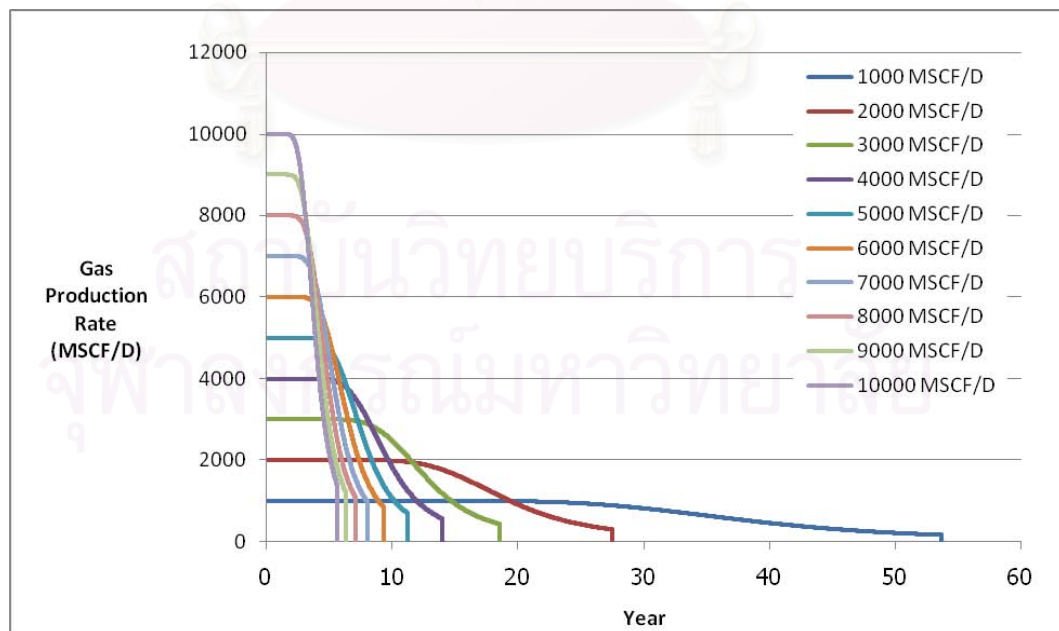


Figure 5.8: Gas production rates for production with CO₂ injection at the beginning.

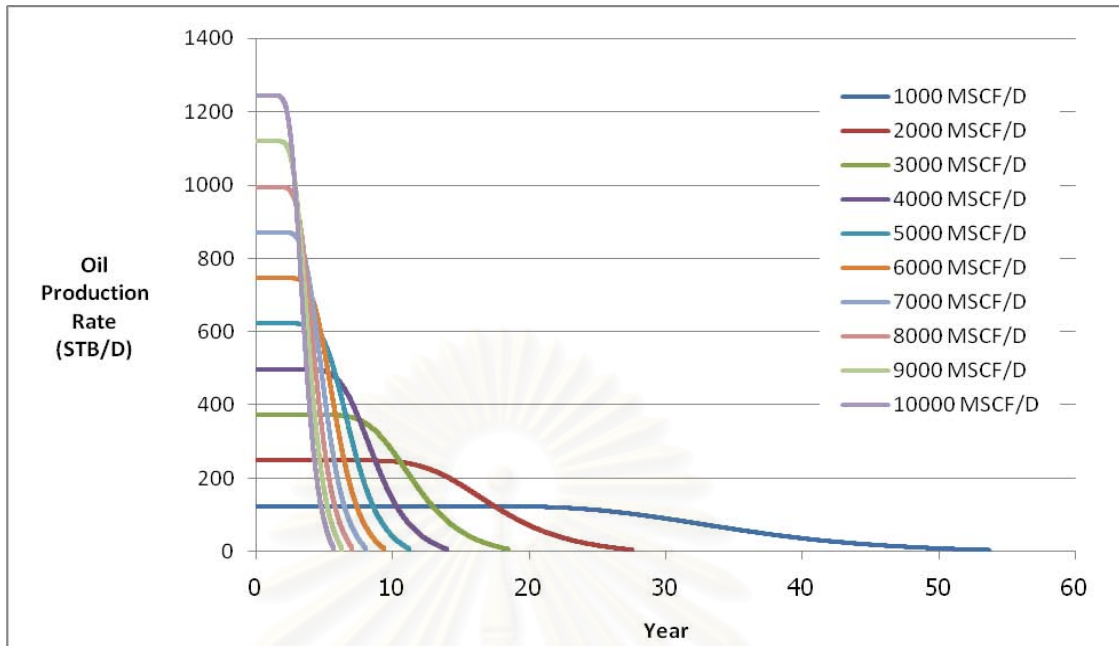


Figure 5.9: Oil production rates for production with CO₂ injection at the beginning.

The bottomhole pressure of the production well and CO₂ mole fraction in produced gas are shown in Figures 5.10 and 5.11, respectively.

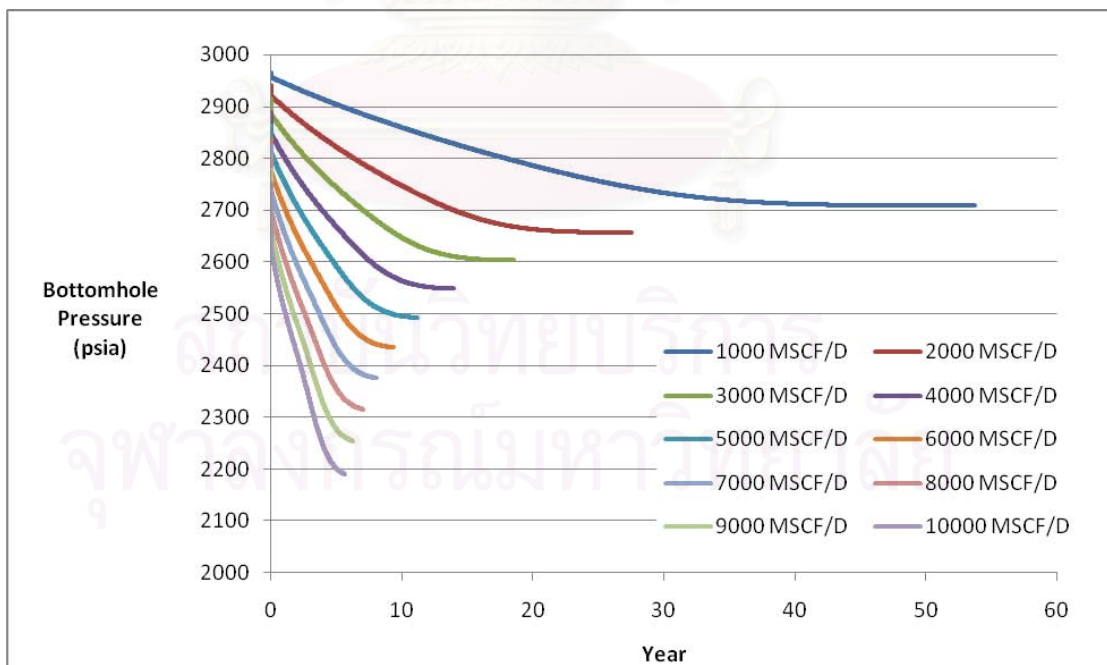


Figure 5.10: Bottomhole Pressure for production with CO₂ injection at the beginning.

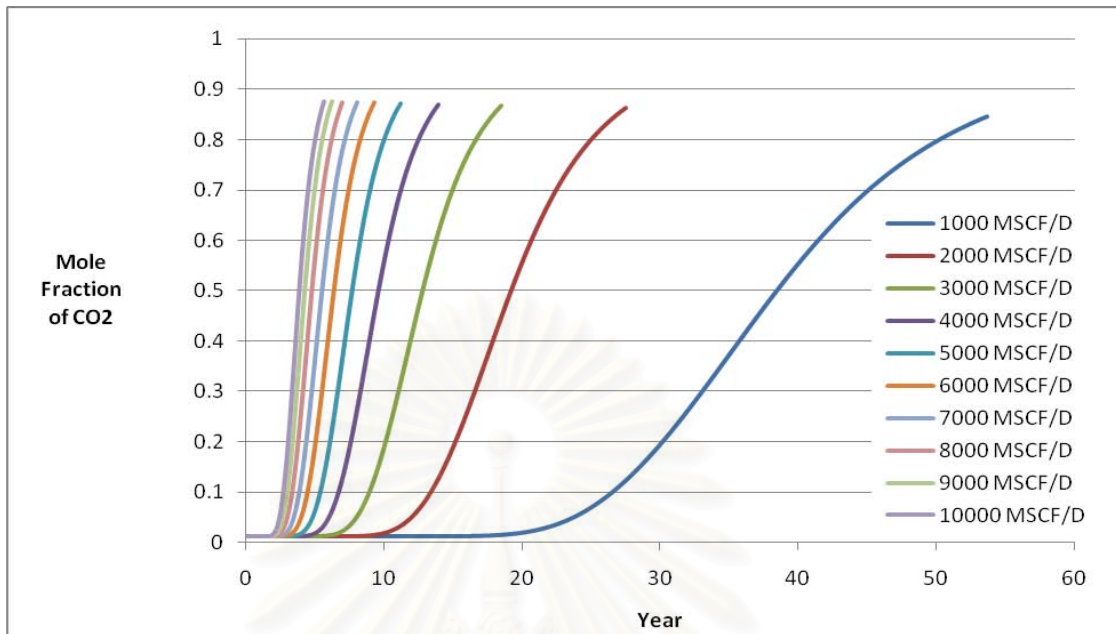


Figure 5.11: CO₂ mole fraction in the produced gas for production with CO₂ injection at the beginning.

From Figures 5.10 to 5.11, mechanism of producing gas-condensate reservoir with CO₂ injection at the beginning can be summarized as follows:

- a) At early times, the gas production rate is constant and the bottomhole pressure declines. After CO₂ breakthrough, the oil and gas production rate declines. CO₂ concentration in the produced gas increase very quickly especially in the case of high gas rate. The simulation stops when the oil production rate is lower than the economic limit.
- b) By increasing the maximum gas production rate, the gas production is accelerated. The mechanism of hydrocarbon recovery is not affected by changing the rate. In Figure 5.10, the bottomhole pressure of the producer is lower when the maximum gas production rate is higher. Since, higher rate requires higher drawdown pressure. And, CO₂ concentration increases faster when the maximum gas production rate is higher as shown in Figure 5.11 because CO₂ flow faster.

Table 5.4 illustrates the gas and oil recovery, and Table 5.5 illustrates production life.

Table 5.4: Total oil and gas production with CO₂ injection at the beginning.

Case	Gas Recovery (MMSCF)			Oil Recovery (MSTB)		
	No Limit	23% CO ₂ limit	40% CO ₂ limit	No Limit	23% CO ₂ limit	40% CO ₂ limit
1000 MSCF/D	14,447	10,999	12,183	1,620	1,346	1,466
2000 MSCF/D	14,528	11,053	12,209	1,624	1,353	1,470
3000 MSCF/D	14,555	11,065	12,215	1,624	1,354	1,471
4000 MSCF/D	14,570	11,070	12,216	1,625	1,355	1,471
5000 MSCF/D	14,579	11,074	12,217	1,625	1,356	1,471
6000 MSCF/D	14,584	11,074	12,222	1,625	1,356	1,472
7000 MSCF/D	14,591	11,077	12,221	1,625	1,356	1,472
8000 MSCF/D	14,592	11,078	12,224	1,625	1,356	1,472
9000 MSCF/D	14,595	11,080	12,224	1,625	1,356	1,472
10000 MSCF/D	14,596	11,083	12,224	1,625	1,357	1,472

Table 5.5: Production life for production with CO₂ injection at the beginning.

Case	Production Life (Years)		
	NoLimit	23% CO ₂ limit	40% CO ₂ limit
1000 MSCF/D	53.70	31.06	35.71
2000 MSCF/D	27.52	15.60	17.87
3000 MSCF/D	18.51	10.41	11.91
4000 MSCF/D	14.01	7.81	8.93
5000 MSCF/D	11.26	6.25	7.15
6000 MSCF/D	9.42	5.21	5.96
7000 MSCF/D	8.09	4.47	5.11
8000 MSCF/D	7.09	3.91	4.47
9000 MSCF/D	6.33	3.47	3.97
10000 MSCF/D	5.67	3.13	3.57

The total oil and gas production and production life as a function of maximum gas production rate are shown in Figures 5.12, 5.13 and 5.14 respectively.

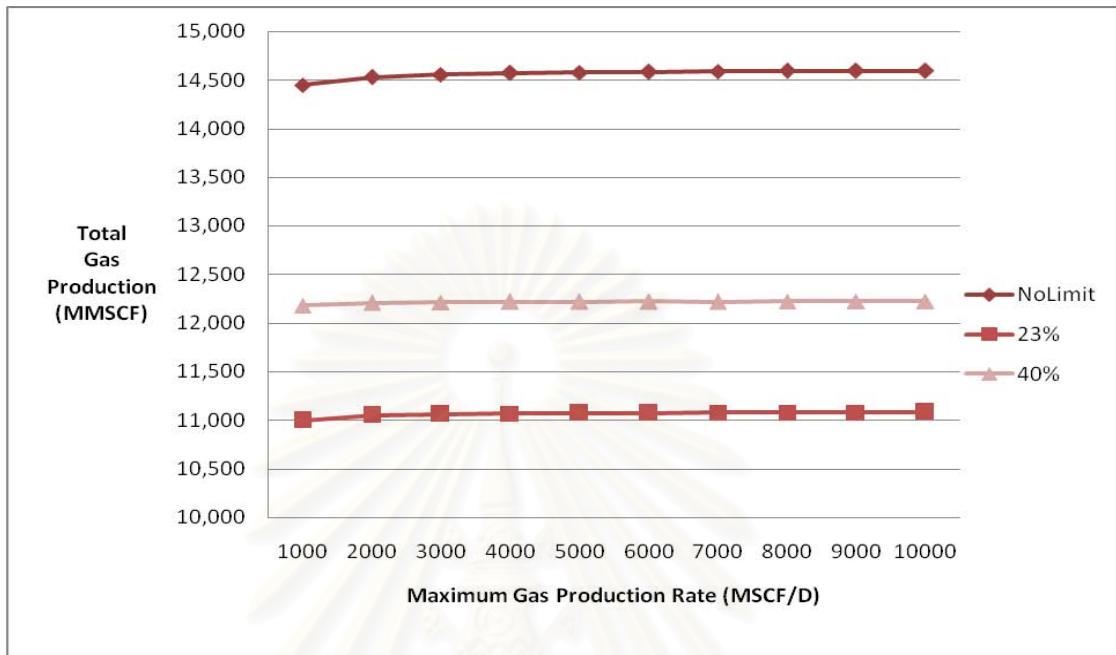


Figure 5.12: Total gas production for production with by CO₂ injection at the beginning.

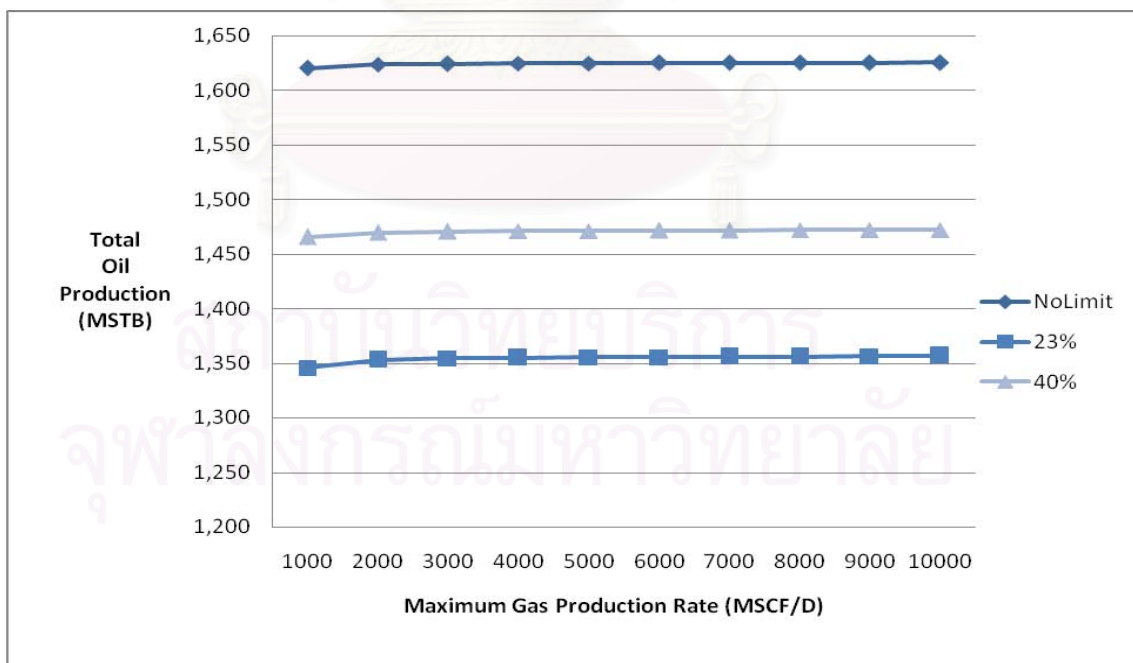


Figure 5.13: Total oil production for production with by CO₂ injection at the beginning.

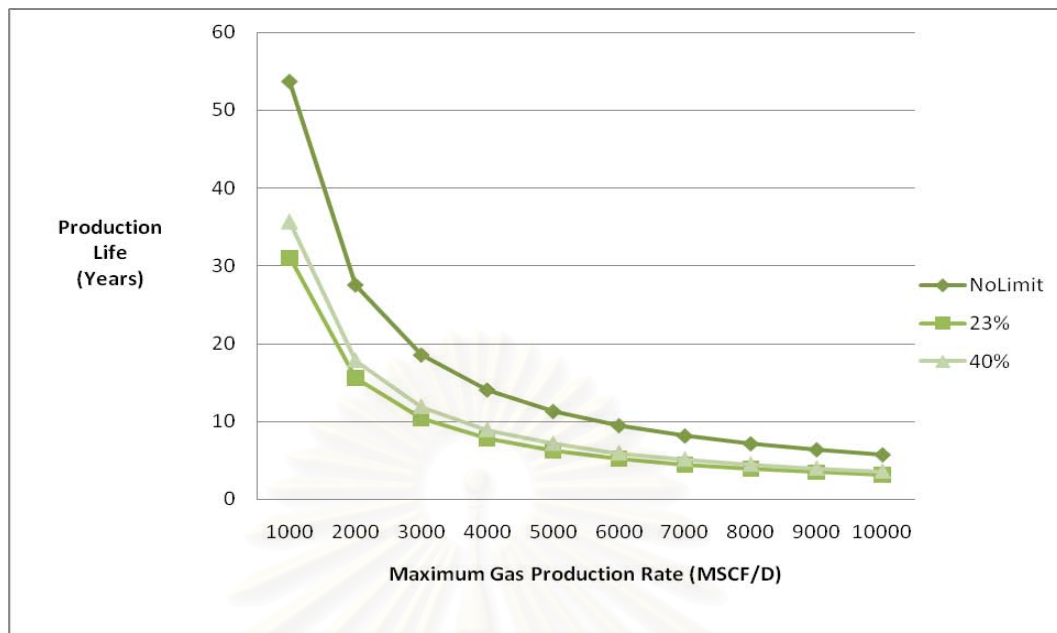


Figure 5.14: Production life for production with by CO₂ injection at the beginning.

From Figures 5.12 to 5.14, performance of producing gas-condensate reservoir with CO₂ injection at the beginning can be summarized as follows:

- In the case of no CO₂ concentration limit, increasing the maximum gas rate increases gas and oil total production. And, in the case of 23% and 40% CO₂ concentration limit, the maximum gas rate does not have significant effect on gas and condensate recovery.
- Compared between with and without CO₂ concentration limit, gas and oil total production for 23% limit case are around 24.4% and 16.6% less than those for no CO₂ limit case, respectively. For 40% limit case, the gas and oil total production are around 16.2% and 9.45% less than those for no CO₂ limit case, respectively. By installing a CO₂ removal unit, 9.4% more gas and 7.9% more oil are recovered.

In this scenario, we can see that CO₂ injection does effectively maintain the reservoir pressure above the dew point pressure, preventing condensate dropout in the reservoir. The simulation results also demonstrate that gas production and CO₂ injection rate do not have significant effect on oil and gas recovery. And installing a CO₂ removal unit does significantly increase oil and gas recovery.

5.3 Natural Depletion and Production with CO₂ Injection

In this section, comparisons between the simulation results between natural depletion case and production with CO₂ injection at the beginning case are reported. The oil and gas production rates, bottomhole pressure, oil and gas total productions and production life are discussed.

5.3.1 Gas Production Rate

As shown in Figures 5.1 and 5.8, the gas production rate in natural depletion case drops when the bottomhole pressure reaches the limit of 1,800 psia. In the case of CO₂ injection, the hydrocarbon gas production rate drops because of the increase in CO₂ concentration in the produced gas. Between natural depletion and CO₂ injection cases, the times before the gas production rate starts to decline in CO₂ injection are generally more than two times longer than those for natural depletion cases.

5.3.2 Oil Production Rate

In natural depletion cases, the oil production rate declines when the bottomhole pressure drops below the dew point pressure. Then, oil production rate drops again when bottomhole pressure reaches the limit of 1,800 psia. In the case of CO₂ injection, the oil production rate remains constant and declines when CO₂ breaks through at the producer. The oil production rates of both cases are shown in Figures 5.2 and 5.9.

5.3.3 Bottom Hole Pressure

As mentioned earlier, the main objective of CO₂ injection is to maintain the reservoir pressure above the dew point pressure. But, the bottomhole pressure of the CO₂ injection case declines, as shown in Figure 5.10 as a result of reservoir injection and production rate difference. However, CO₂ injection does effectively maintain the reservoir pressure and the simulation always stops before the reservoir pressure drops below the dew point pressure.

5.3.4 Total Gas Production

The increase in gas recovery when producing gas-condensate reservoir with CO₂ injection is shown in Table 5.6. From the table, the variation of gas rate does not have much effect on increase in gas recovery. There are around 101.4% improving in gas recovery and 122.2% improving in oil recovery.

Table 5.6: Percentage of gas recovery enhancement by producing gas-condensate reservoir with CO₂ injection.

Case	Percentage of Gas Recovery Enhancement (%)		
	No Limit	23% CO ₂ limit	40% CO ₂ limit
1000 MSCF/D	163.00%	100.20%	121.70%
2000 MSCF/D	164.40%	101.20%	122.20%
3000 MSCF/D	164.80%	101.30%	122.20%
4000 MSCF/D	165.00%	101.30%	122.20%
5000 MSCF/D	165.10%	101.40%	122.20%
6000 MSCF/D	165.20%	101.30%	122.20%
7000 MSCF/D	165.30%	101.40%	122.20%
8000 MSCF/D	165.30%	101.40%	122.20%
9000 MSCF/D	165.30%	101.40%	122.20%
10000 MSCF/D	165.30%	101.40%	122.20%

5.3.5 Total oil production

The increase in oil recovery when producing gas-condensate reservoir with CO₂ injection is shown in Table 5.7. From the table, the oil recovery for each CO₂ concentration limit increases when the maximum production rate increases. There are around 125% improving in gas recovery and 144% improving in oil recovery.

Table 5.7: Percentage of oil recovery enhancement by producing gas-condensate reservoir with CO₂ injection

Case	Percentage of Condensate Recovery Enhancement (%)		
	No Limit	23% CO ₂ limit	40% CO ₂ limit
1000 MSCF/D	163.20%	118.70%	138.10%
2000 MSCF/D	165.40%	121.20%	140.30%
3000 MSCF/D	166.90%	122.60%	141.70%
4000 MSCF/D	168.20%	123.70%	142.90%
5000 MSCF/D	169.40%	124.70%	143.90%
6000 MSCF/D	170.30%	125.50%	144.80%
7000 MSCF/D	171.10%	126.20%	145.50%
8000 MSCF/D	171.70%	126.70%	146.10%
9000 MSCF/D	171.90%	126.90%	146.30%
10000 MSCF/D	172.00%	127.10%	146.40%

5.4 Production with CO₂ Injection at Different Starting Time

In this scenario, CO₂ injection begins at different starting times in order to study the effect of the delay in injection. Injection rate is set to be equal to the production rate for each profile. In this simulation model, the production well is placed at coordinate (1, 1) in LGR grid representing the producer (located at coordinate (1, 1) in the global grid), and injection well is placed at coordinate (5, 5) in LGR grid representing the injector (located at coordinate (15, 15) in the global grid) in order to simulate a quarter five-spot pattern. Time prior to injection was varied from 1 to 10 years in a step of 1 year increment. The simulation will stop if gas or oil production rate drops below the economic limit.

In this scenario, the economic limits were set by oil production rate as shown in Table 5.1, gas production rate of 100 MSCF/D and CO₂ concentration limit. The 23% and 40% concentration limit were selected. The 23% limit is commonly used in Gulf of Thailand and the 40% limit is used when a CO₂ removal unit is installed. Results of the cases which the maximum production rate equal to 2,000 and 4,000 MSCF/D are shown in this chapter.

Gas Production Rate

Gas production rates for maximum gas production rate of 2,000 and 4,000, MSCF/D are shown in Figures 5.15 and 5.16, respectively.

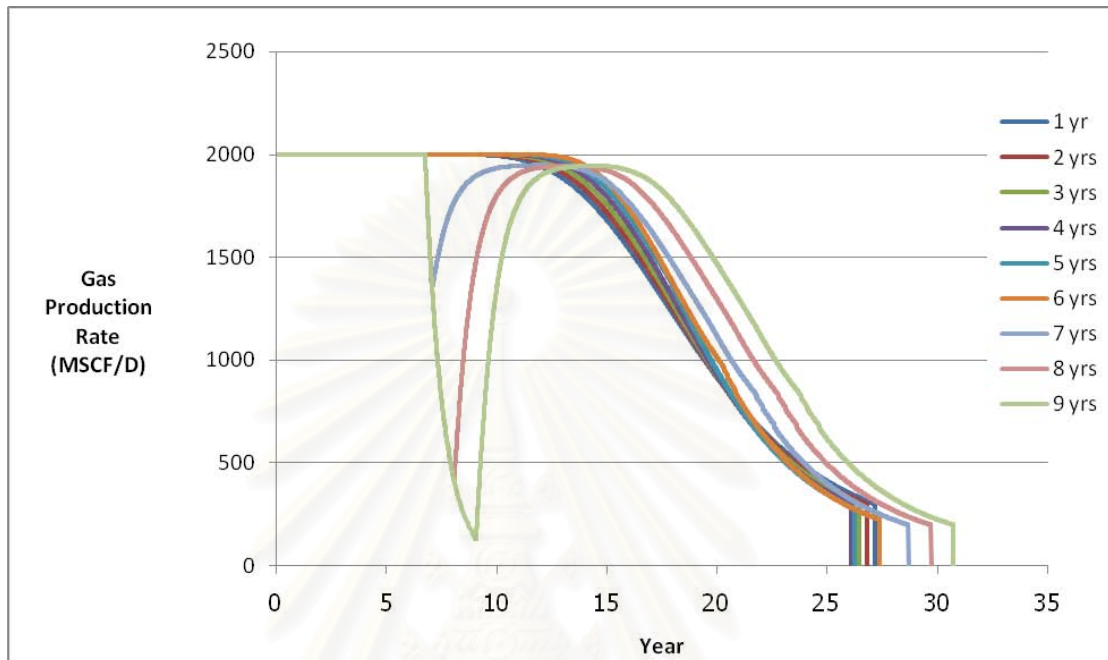


Figure 5.15: Gas production rates for maximum gas production rate of 2,000 MSCF/D with different times prior to injection.

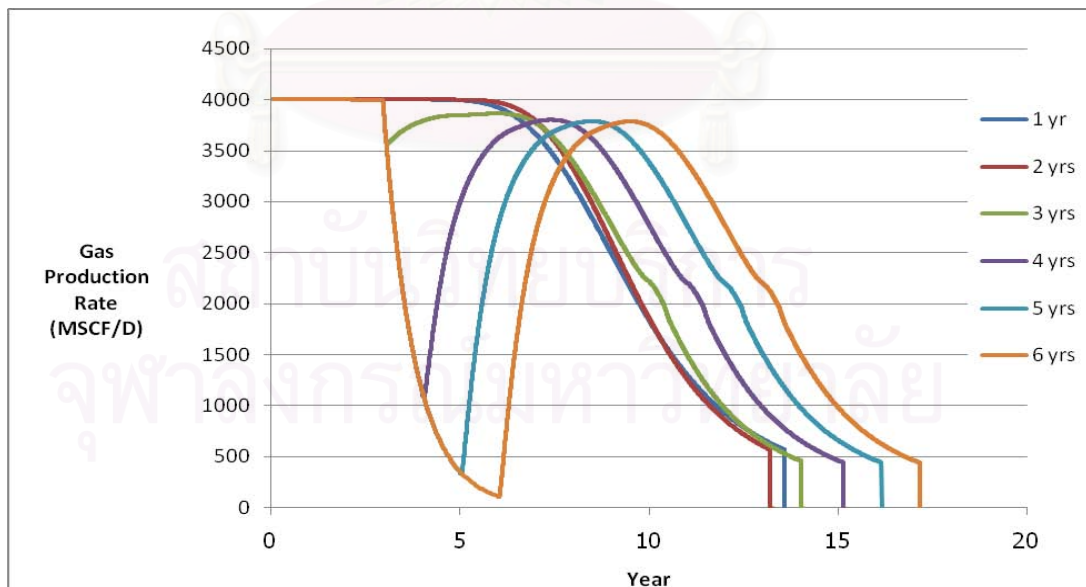


Figure 5.16: Gas production rates for maximum gas production rate of 4,000 MSCF/D with different times prior to injection.

Oil Production Rate

Oil production rates for maximum gas production rate of 2,000 and 4,000 MSCF/D are shown in Figures 5.17 and 5.18, respectively.

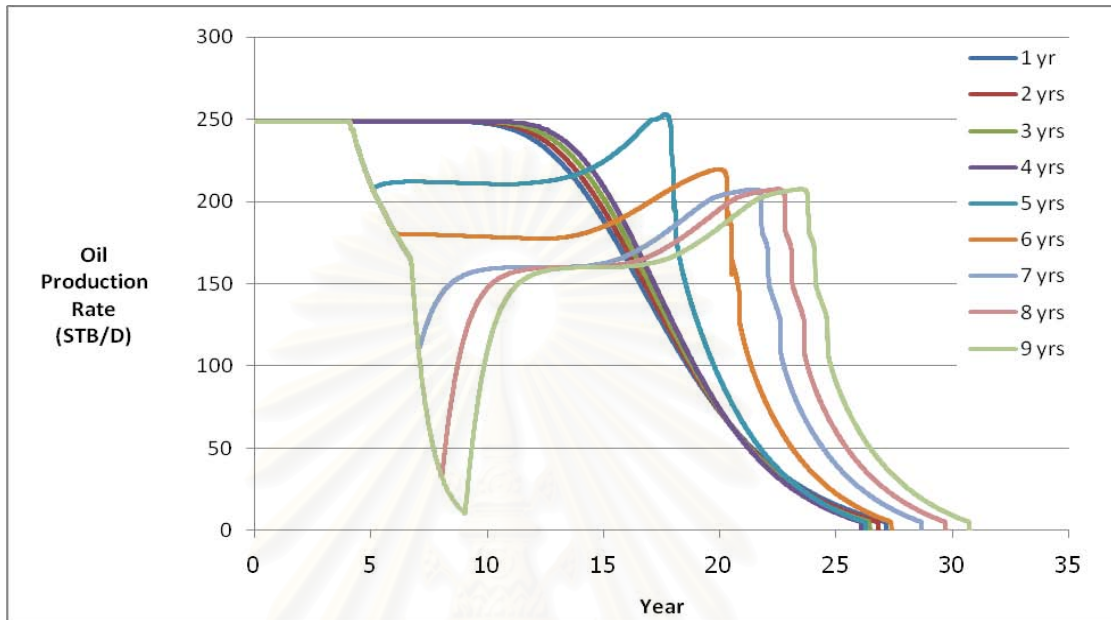


Figure 5.17: Oil production rate for maximum gas production rate of 2,000 MSCF/D with different times prior to injection.

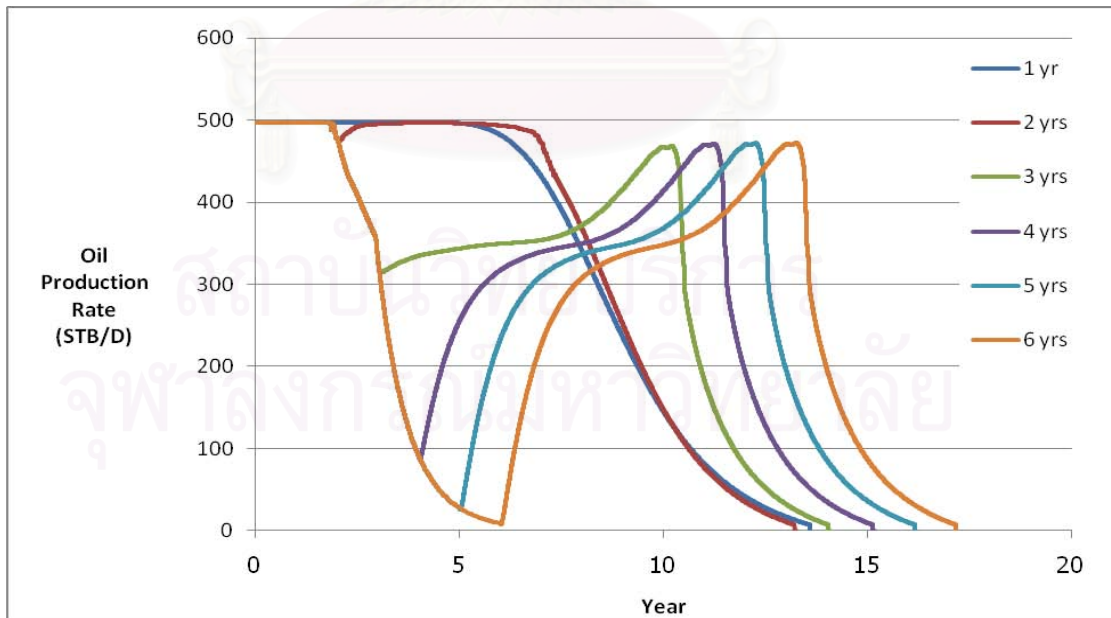


Figure 5.18: Oil production rates for maximum gas production rate of 4,000 MSCF/D with different times prior to injection.

Bottomhole Pressure

The bottomhole pressures of the production well for maximum gas production rate of 2,000 and 4,000 MSCF/D are shown in Figures 5.19 and 5.20, respectively.

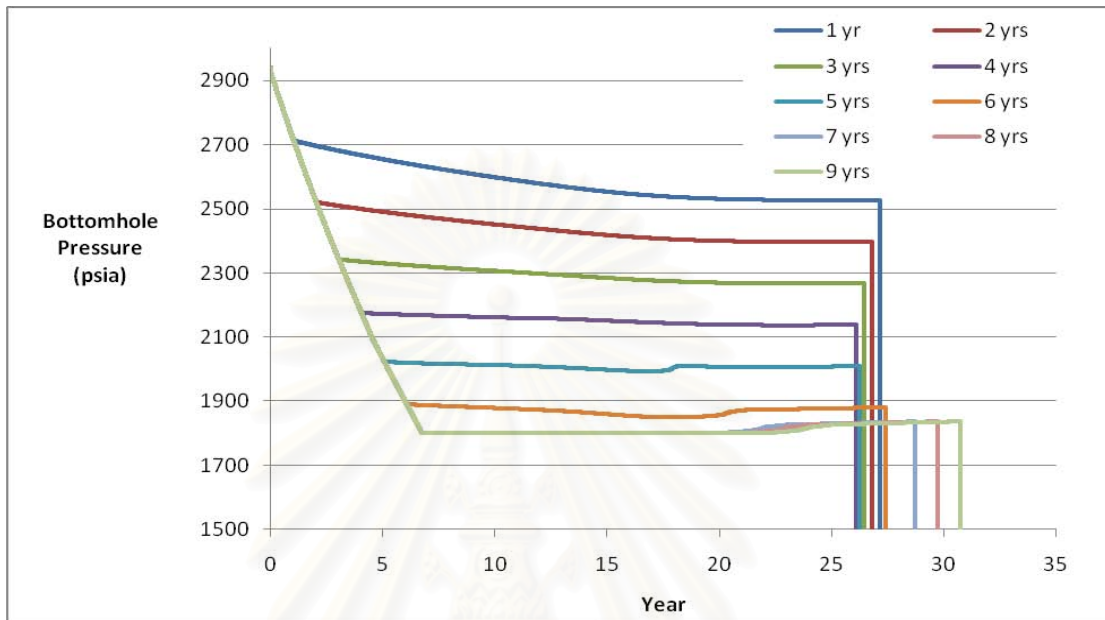


Figure 5.19: Bottomhole pressure for maximum gas production rate of 2,000 MSCF/D with different times prior to injection.

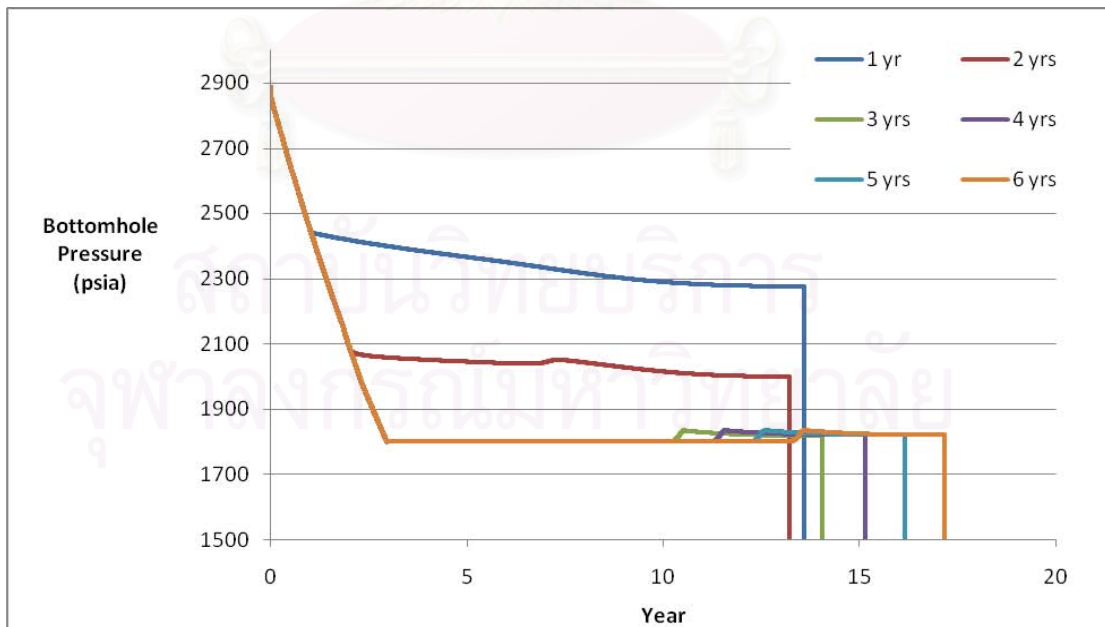


Figure 5.20: Bottomhole pressure for maximum gas production rate of 4,000 MSCF/D with different times prior to injection.

Mole Fraction of CO₂

CO₂ mole fraction in the produced gas for maximum gas production rate of 2,000 and 4,000 MSCF/D are shown in Figures 5.21 and 5.22, respectively.

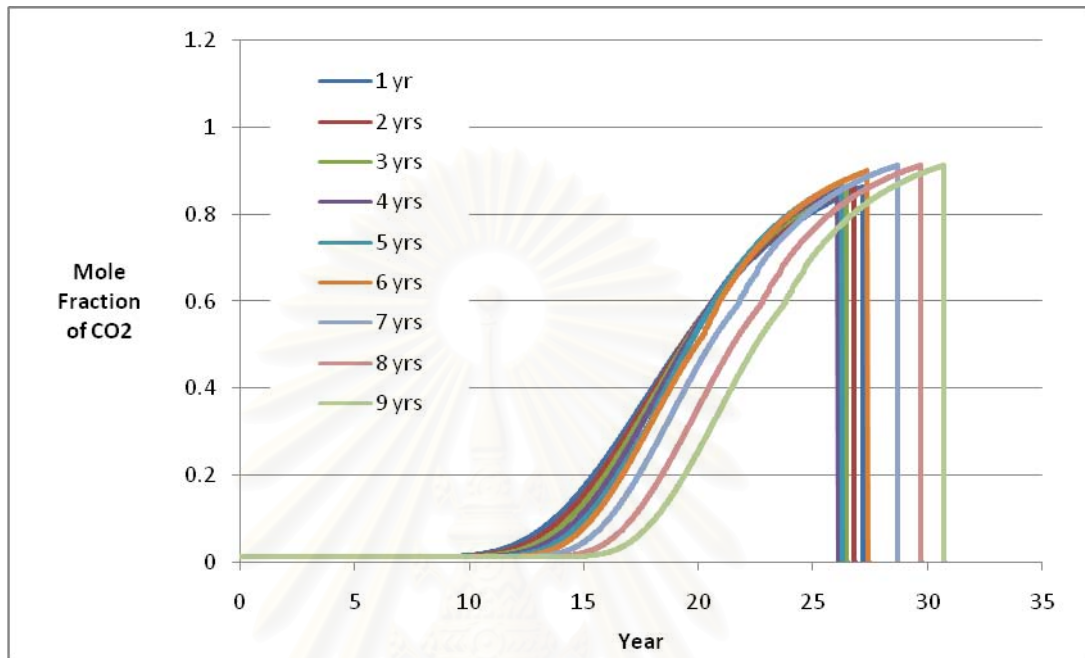


Figure 5.21: CO₂ mole fraction for maximum gas production rate of 2,000 MSCF/D with different times prior to injection.

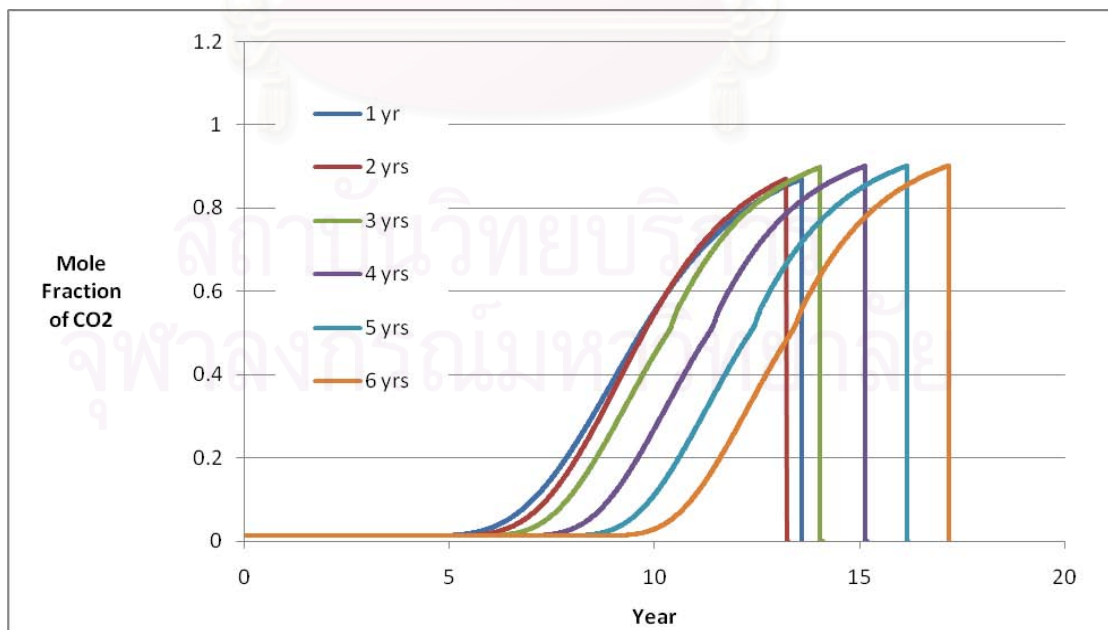


Figure 5.22: CO₂ mole fraction for maximum gas production rate of 4,000 MSCF/D with different times prior to injection.

Oil Saturation around the wellbore

The oil saturation at Grid (4, 4, 2) in the LGR grid which in the producer for maximum gas production rate of 2,000 and 4,000 MSCF/D are shown in Figures 5.23 and 5.24, respectively.

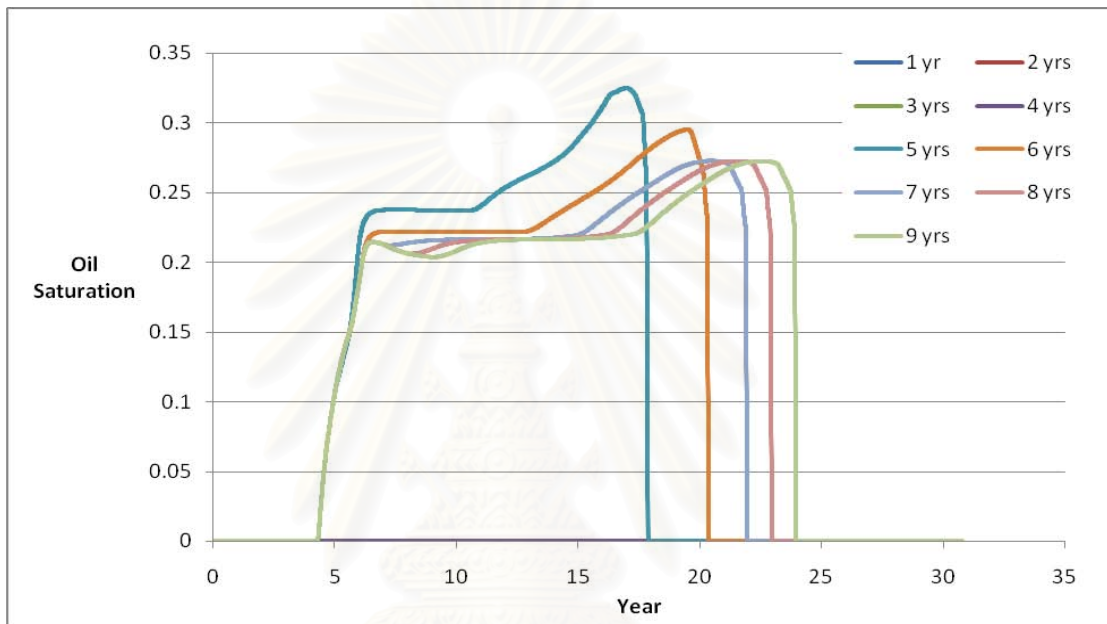


Figure 5.23: Oil Saturation at Grid (4, 4, 2) in the LGR for maximum gas production rate of 2,000 MSCF/D with different times prior to injection.

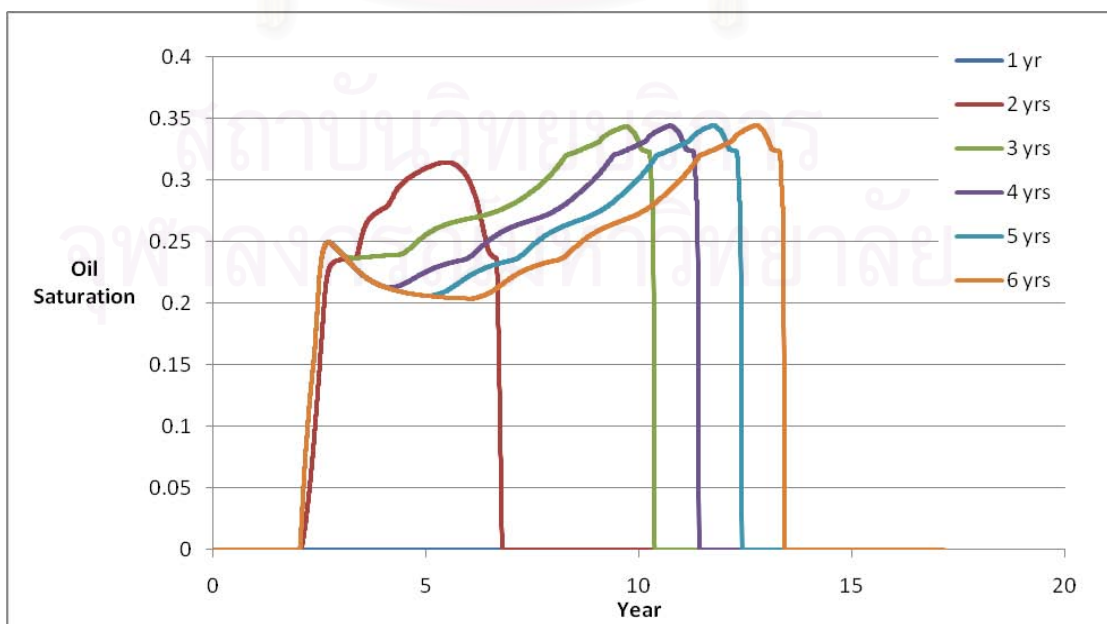


Figure 5.24: Oil Saturation at Grid (4, 4, 2) in the LGR for maximum gas production rate of 4,000 MSCF/D with different times prior to injection.

From the Figures 5.17 to 5.24, we can categorize the time prior to injection to 3 periods which are (1) before the bottomhole pressure of the producer drop below the dew point pressure, (2) after the bottomhole pressure of the producer drops below the dew point pressure but before reaching the BHP limit of 1,800 psia, (3) after the bottomhole pressure of the producer reaches the BHP limit of 1,800 psia. The effect of changing timing to injection to mechanism of CO₂ injection can be summarized as follows:

(1) Injection Starts before the Bottomhole Pressure Drops below the Dew point Pressure

- a) Starting CO₂ injection before the bottomhole pressure drops the below dew point pressure has a similar behavior compared to starting the injection at the beginning. Gas and oil production rates remain constant and start to decline after CO₂ breakthrough. Then, the simulation stops because the oil production rate reaches the oil economic limit.
- b) The bottomhole pressure drops and remains nearly constant after the injection starts. The earlier the injection, the higher the bottomhole pressure is. Thus, early injection will keep the reservoir pressure to be high as well.
- c) CO₂ breakthrough time is slightly delayed when the time prior to injection delays. There is only 0.28 year difference in breakthrough time between starting injection at 1 and 2 years for the production rate limit of 2,000 MSCF/D.

(2) Injection Starts after the Bottomhole Pressure Drops below the Dew point Pressure but Before Reaching the BHP Limit of 1,800 psia

- a) At early times, the oil production rate is constant, then declines after the bottomhole pressure drops below the dew point pressure. When the injection starts, the oil production rate increases. After CO₂ breakthrough,

the hydrocarbon gas production rate decreases due to the increase in CO₂ concentration but the oil production rate increases because the liquid drop out around the wellbore is revaporized by CO₂. These gases will condense as oil at surface conditions. After the liquid dropout around the well bore is completely recovered, the oil production rate starts to decline again. The simulation stops because the oil production rate reaches the economic limit.

- b) CO₂ breakthrough time is slightly delayed when the start of injection delays, similar to the case of injection before the bottomhole pressure drops below the dew point pressure.

(3) Injection Starts After the Bottomhole Pressure Reaches the BHP Limit of 1,800 psia

- a) In this case, the oil and gas production rates decline before the injection starts. After the injection starts, the oil and gas production rates increase. After CO₂ breakthrough, the gas production rate decreases due to the increase in CO₂ concentration but the oil production rate increases because the liquid drop out around the wellbore is revaporized by CO₂. After the liquid drop out around the well bore is completely recovered, the oil production rate starts to decline again. The simulation stops because the oil production rate reaches the economic limit.
- b) Delaying the injection time will delay CO₂ breakthrough time. The times delayed are almost equal for all the cases. In example, there is nearly 1 year delay in breakthrough time between CO₂ injection starts at 7, 8 and 9 years for the production rate limit of 2,000 MSCF/D.

Total Gas Production

The total gas production for maximum gas production rate of 2,000 and 4,000 MSCF/D are shown in Figures 5.25 and 5.26, respectively.

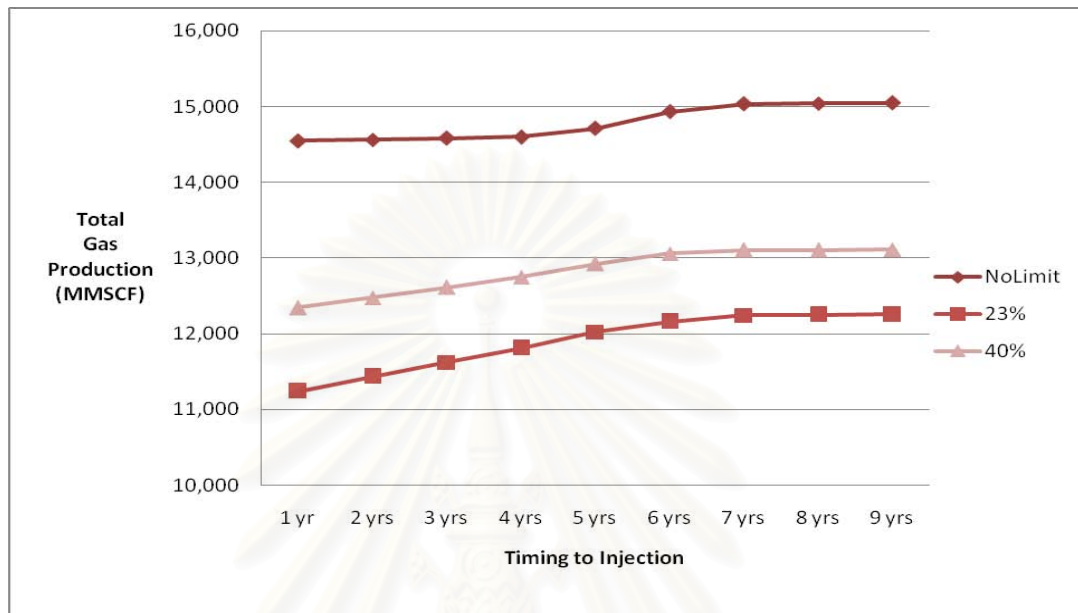


Figure 5.25: Total gas production with maximum gas production rate of 2,000 MSCF/D and varying times prior to injection between 1 – 9 yrs.

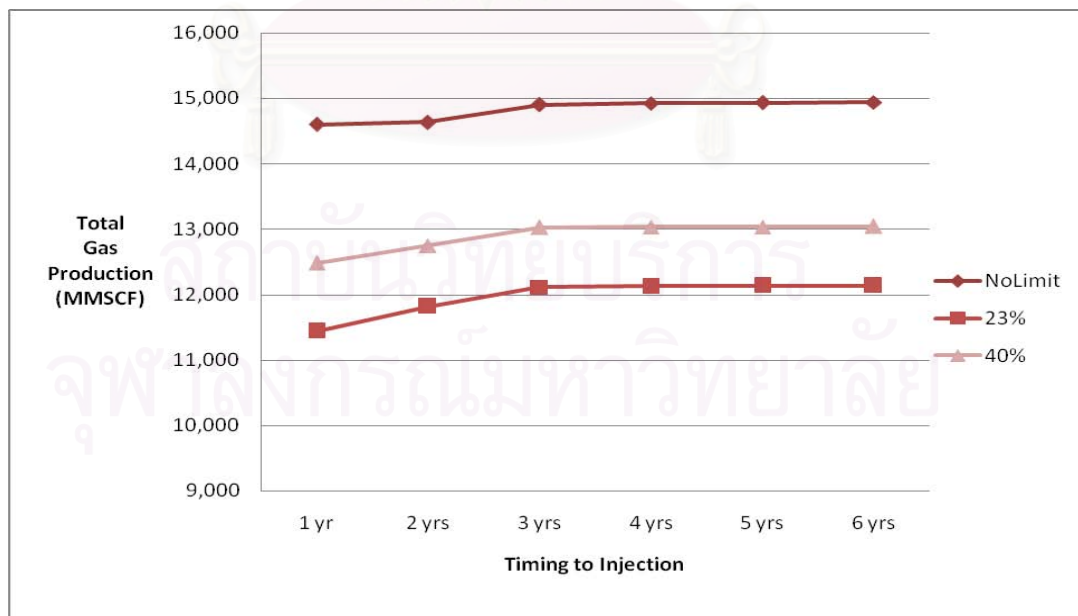


Figure 5.26: Total gas production with maximum gas production rate of 4,000 MSCF/D and varying times prior to injection between 1 – 6 yrs.

Total Oil Production

The total oil production for maximum gas production rate of 2,000 and 4,000 MSCF/D are shown in Figures 5.27 and 5.28, respectively.

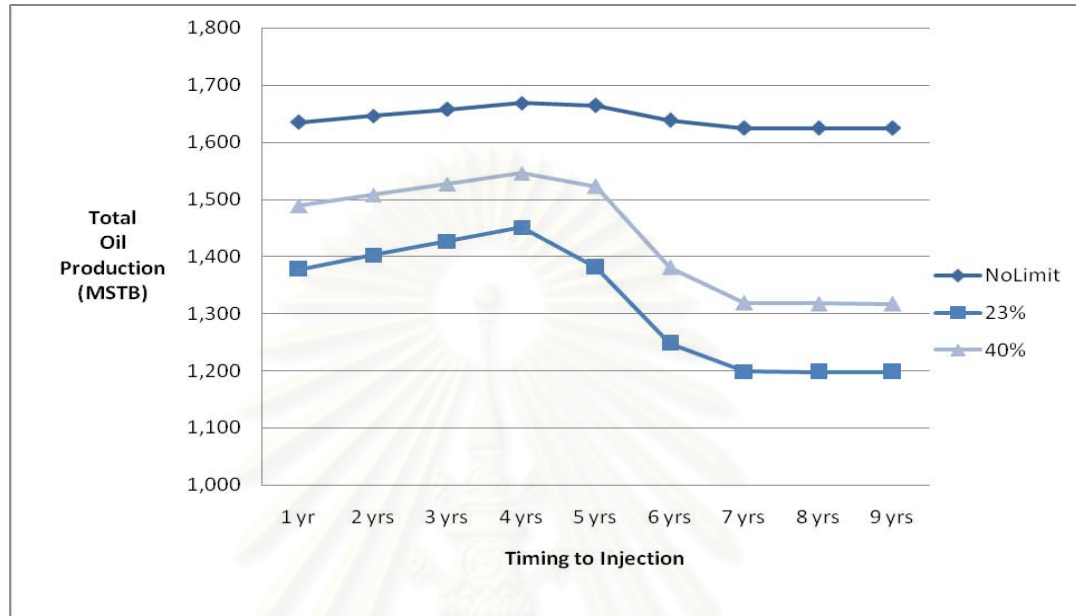


Figure 5.27: Total oil production with maximum gas production rate of 2,000 MSCF/D and varying times prior to injection between 1 – 9 yrs.

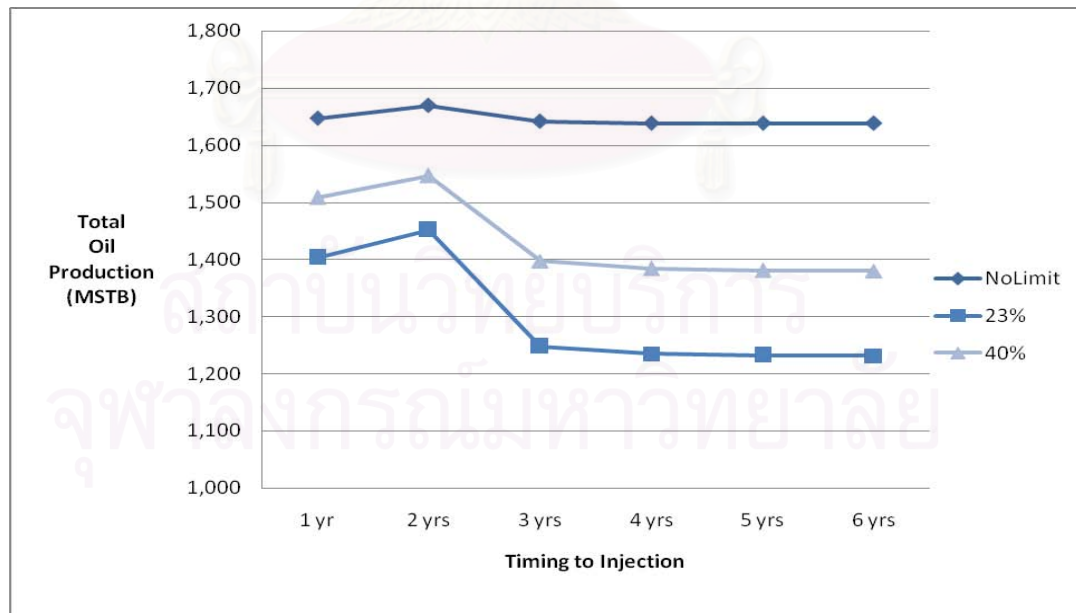


Figure 5.28: Total oil production with maximum gas production rate of 4,000 MSCF/D and varying times prior to injection between 1 – 6 yrs.

Production Life

The production life as a for maximum gas production rate of 2,000 and 4,000 MSCF/D are shown in Figures 5.29 and 5.30, respectively.

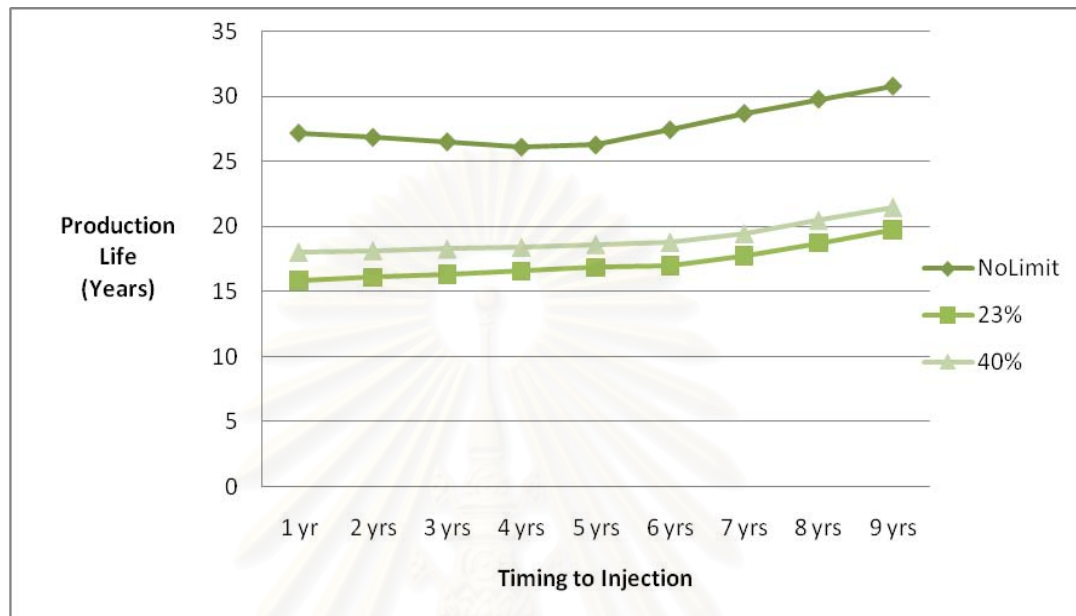


Figure 5.29: Production life with maximum gas production rate of 2,000 MSCF/D and varying times prior to injection between 1 – 9 yrs.

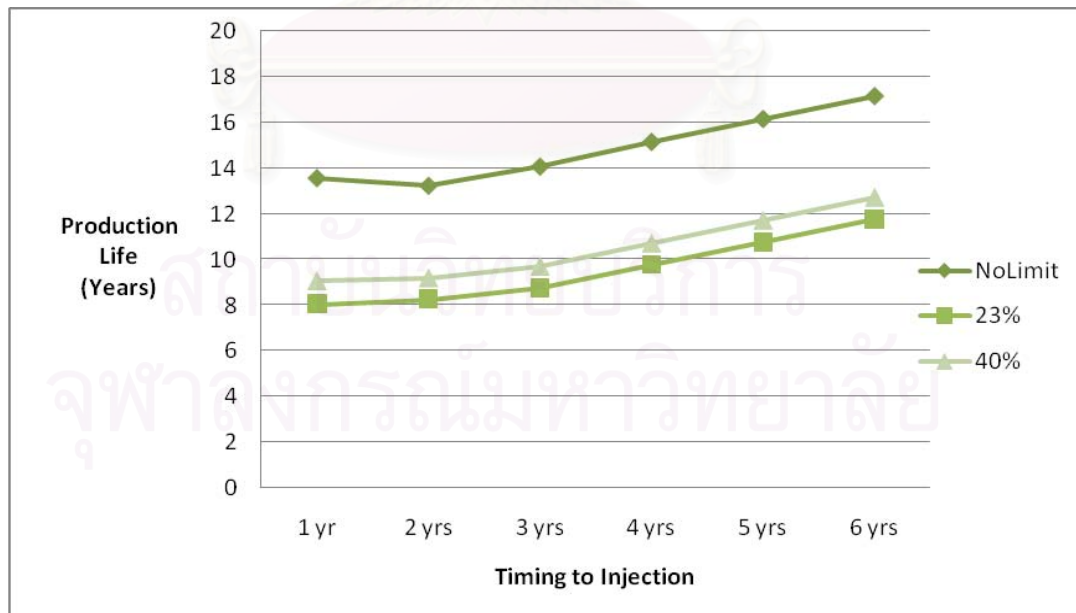


Figure 5.30: Production life with maximum gas production rate of 4,000 MSCF/D and varying times prior to injection between 1 – 6 yrs.

Table 5.8 illustrates the gas and oil recovery, and Table 5.9 illustrates production life with maximum gas production rate of 2,000 MSCF/D and varying times prior to injection between 1 – 9 yrs.

Table 5.8: Total oil and gas production with maximum gas production rate of 2,000 MSCF/D and varying times prior to injection between 1 – 9 yrs.

Case	Gas Recovery (MMSCF)			Oil Recovery (MSTB)		
	No Limit	23% CO ₂ limit	40% CO ₂ limit	No Limit	23% CO ₂ limit	40% CO ₂ limit
1 yr	14,546	11,243	12,345	1,635	1,378	1,489
2 yrs	14,563	11,434	12,479	1,646	1,402	1,508
3 yrs	14,580	11,622	12,612	1,657	1,427	1,527
4 yrs	14,598	11,812	12,747	1,669	1,451	1,546
5 yrs	14,710	12,022	12,926	1,664	1,381	1,523
6 yrs	14,933	12,160	13,060	1,638	1,247	1,381
7 yrs	15,035	12,245	13,104	1,625	1,199	1,319
8 yrs	15,042	12,250	13,108	1,624	1,198	1,317
9 yrs	15,046	12,255	13,112	1,625	1,197	1,317

Table 5.9: Production life for production with maximum gas production rate of 2,000 MSCF/D and varying times prior to injection between 1 – 9 yrs.

Case	Production Life (Years)		
	No Limit	23% CO ₂ limit	40% CO ₂ limit
1 yr	27.18	15.84	18.00
2 yrs	26.85	16.08	18.13
3 yrs	26.51	16.32	18.26
4 yrs	26.10	16.56	18.39
5 yrs	26.26	16.83	18.60
6 yrs	27.43	17.00	18.76
7 yrs	28.69	17.71	19.43
8 yrs	29.77	18.72	20.44
9 yrs	30.77	19.72	21.44

Table 5.10 illustrates the gas and oil recovery, and Table 5.11 illustrates production life with maximum gas production rate of 4,000 MSCF/D and varying times prior to injection between 1 – 6 yrs.

Table 5.10: Total oil and gas production with maximum gas production rate of 4,000 MSCF/D and varying times prior to injection between 1 – 6 yrs.

Case	Gas Recovery (MMSCF)			Oil Recovery (MSTB)		
	No Limit	23% CO ₂ limit	40% CO ₂ limit	No Limit	23% CO ₂ limit	40% CO ₂ limit
1 yr	14,602	11,441	12,483	1,647	1,403	1,509
2 yrs	14,634	11,815	12,751	1,669	1,452	1,546
3 yrs	14,901	12,116	13,028	1,642	1,248	1,397
4 yrs	14,925	12,125	13,034	1,639	1,235	1,384
5 yrs	14,935	12,133	13,039	1,638	1,232	1,381
6 yrs	14,940	12,137	13,042	1,638	1,232	1,380

Table 5.11: Production life for production with maximum gas production rate of 4,000 MSCF/D and varying times prior to injection between 1 – 6 yrs.

Case	Production Life (Years)		
	No Limit	23% CO ₂ limit	40% CO ₂ limit
1 yr	13.59	8.04	9.07
2 yrs	13.26	8.28	9.20
3 yrs	14.09	8.75	9.71
4 yrs	15.17	9.76	10.71
5 yrs	16.17	10.76	11.71
6 yrs	17.17	11.76	12.71

From Figures 5.25 to 5.30, the effect of changing the starting time of injection on the performance of CO₂ injection can be summarized as follow:

- a) By starting injection before the bottomhole pressure drops below the dew point pressure, delaying the injection starting time increases gas recovery for the cases with 23% and 40% CO₂ limit but has no effect to gas recovery for the cases with no CO₂ limit as shown in Figures 5.25 and 5.26. From Figures 5.27 and 5.28, delaying the injection time increases the oil recovery in all CO₂ limit cases.
- b) By starting injection before the bottomhole pressure reaches the BHP limit of 1,800 psia, delaying the injection time increases gas recovery but decreases oil recovery for all different CO₂ limit cases. In this case, the production life is longer when the injection starting time is delayed. When compared to starting injection before the bottomhole pressure drops below the dew point pressure, the gas recovery is higher but the oil recovery is lower. In a case of production rate limit of 4,000 MSCF /D with the time prior to injection of 2 years which is shortly after the bottomhole pressure drops below the dew point pressure, the behavior of this case is similar to the case which the injection starts before the bottomhole pressure drops below the dew point pressure and is the case that provides the maximum oil recovery.
- c) By starting injection after the bottomhole pressure reaches the BHP limit of 1,800 psia, delaying the injection starting time has effect on gas and oil recoveries. And, the production life is longer when the injection starting time is delayed.

In this scenario, we can see that when injecting CO₂ after condensate accumulates, CO₂ can re-vaporize liquid drop-out around the wellbore. The starting time for CO₂ injection has important effects on hydrocarbon recovery. To obtain the maximum oil recovery, the injection should start shortly after the bottomhole pressure drops below the dew point pressure. And, starting injection after the bottomhole pressure reaches the BHP limit can provide the maximum gas recovery.

5.5 Stopping Injection before CO₂ Concentration in Produced Gas Reaches Limit

In this scenario, CO₂ injection is selectively stopped before CO₂ concentration in produced gas reaches the 40% limit. The stopping time are varied from 5% to 35% CO₂ concentration in the produced gas in step of 5% increment. Two scenarios are selected which are the cases with starting CO₂ injection at the beginning and starting CO₂ injection after 2 years of production. In both cases, the maximum production rate is 4,000 MSCF/D. The simulation will stop when the oil or gas production rate reaches the economic limit or CO₂ concentration in the produced gas reaches 40 %.

Gas Production Rate

Gas production rate for starting CO₂ injection at the beginning and after 2 years of production are shown in Figures 5.31 and 5.32, respectively.

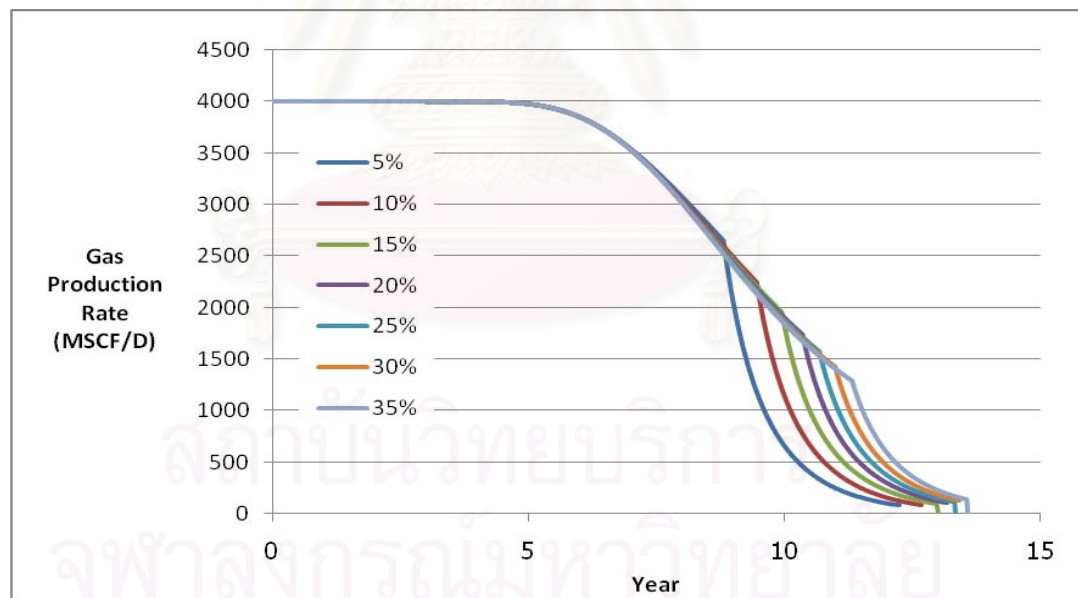


Figure 5.31: Gas production rates for starting CO₂ injection at the beginning and stopping injection when the produced gas has CO₂ concentration of 5%-35%.

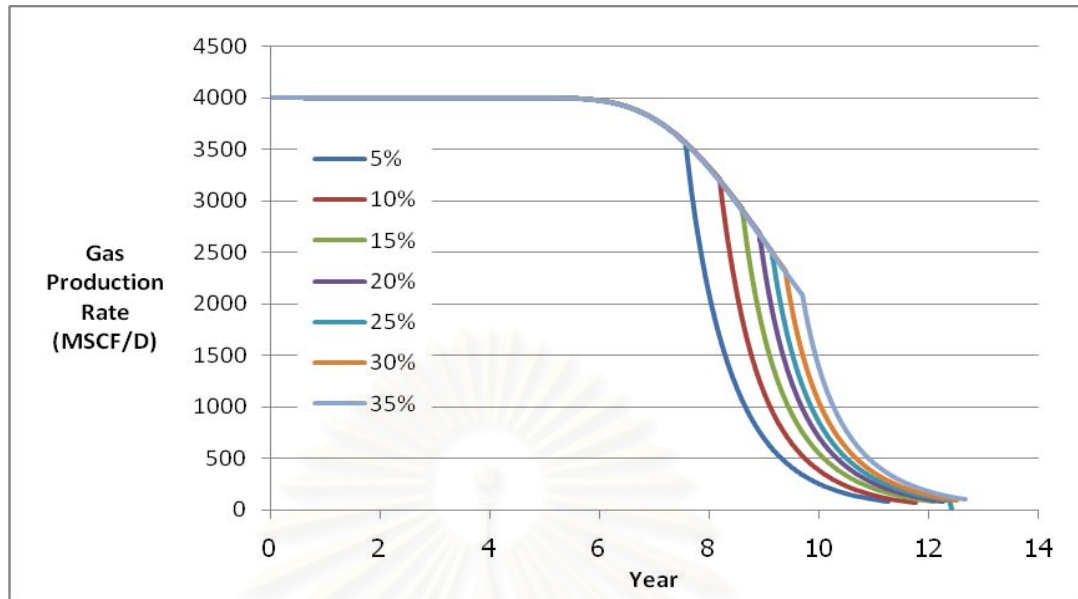


Figure 5.32: Gas production rates for starting CO₂ injection after 2 years of production and stopping injection when the produced gas has CO₂ concentration of 5% - 35%.

Oil Production Rate

Oil production rate for starting CO₂ injection at the beginning and after 2 years of production are shown in Figures 5.33 and 5.34, respectively.

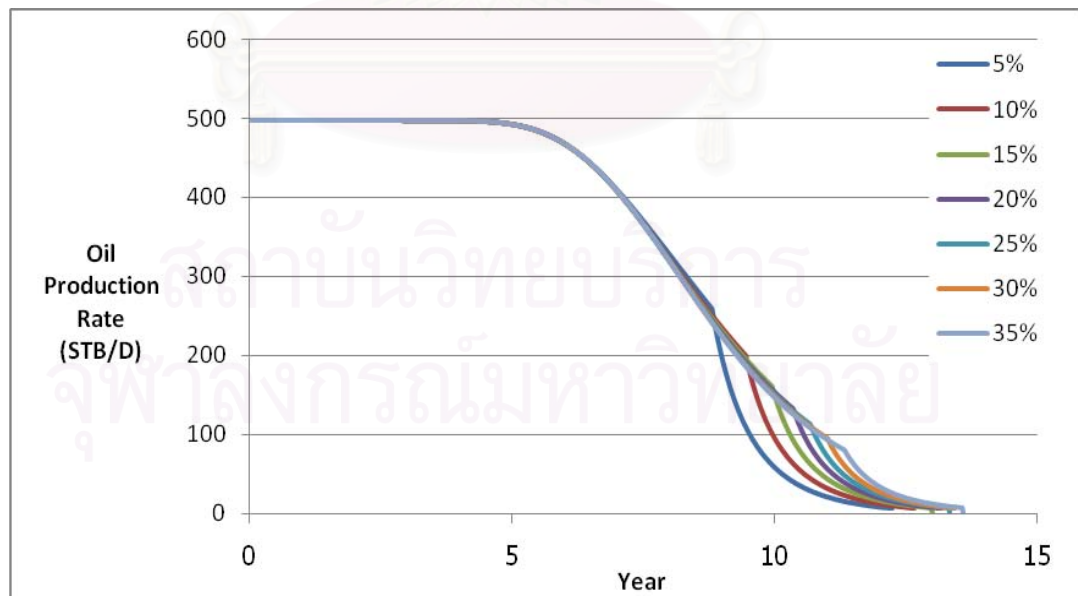


Figure 5.33: Oil production rates for starting CO₂ injection at the beginning and stopping injection when the produced gas has CO₂ concentration of 5% - 35%.

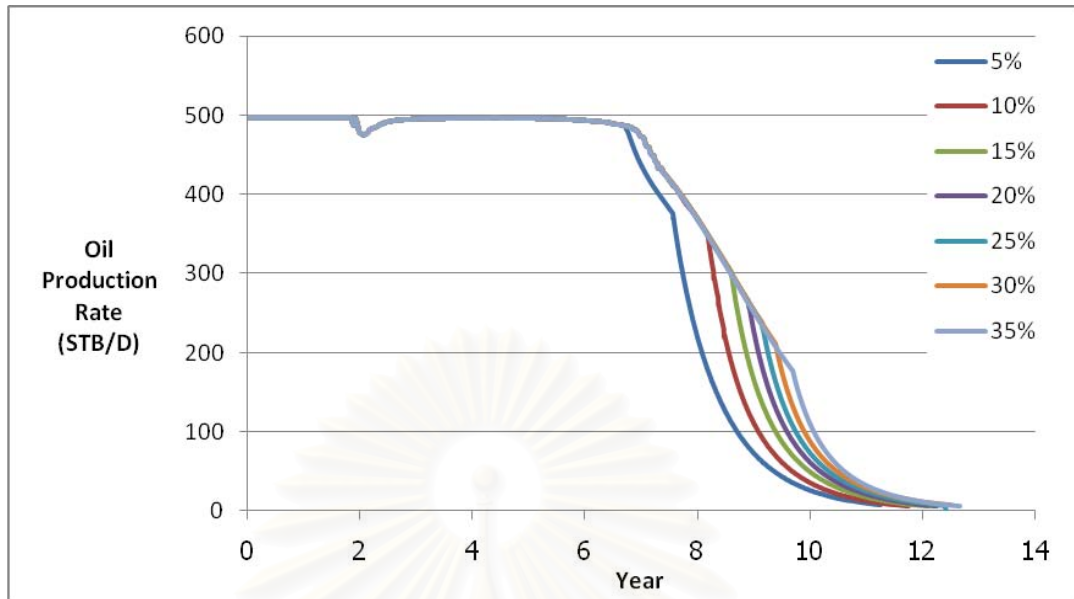


Figure 5.34: Oil production rates for starting CO₂ injection after 2 years of production and stopping injection when the produced gas has CO₂ concentration of 5% - 35%.

Bottomhole Pressure

The bottomhole pressures for starting CO₂ injection at the beginning and after 2 years of production are shown in Figures 5.35 and 5.36, respectively.

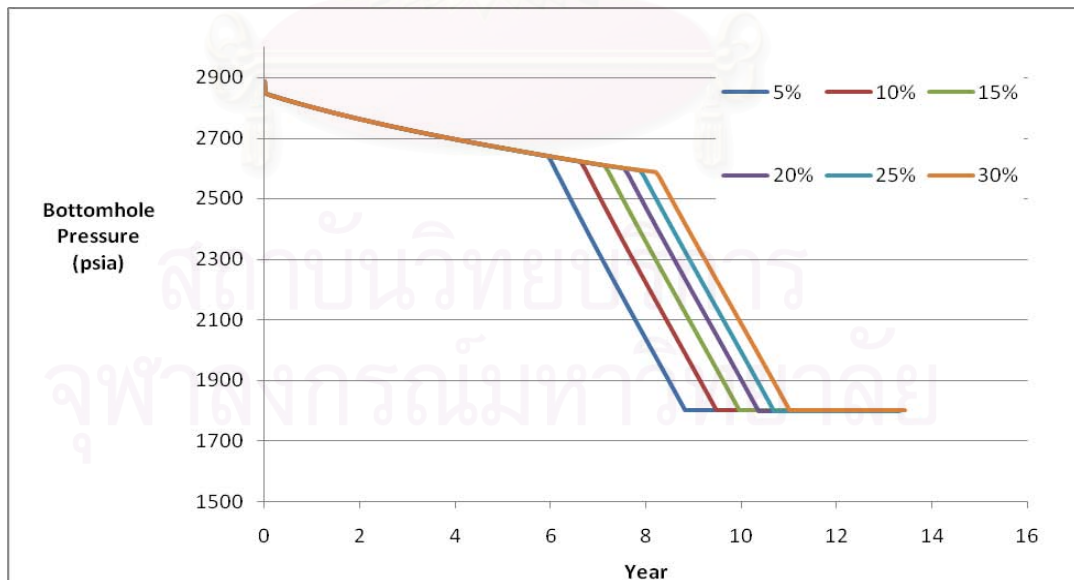


Figure 5.35: The bottomhole pressure for starting CO₂ injection at the beginning and stopping injection when the produced gas has CO₂ concentration of 5% - 35%.

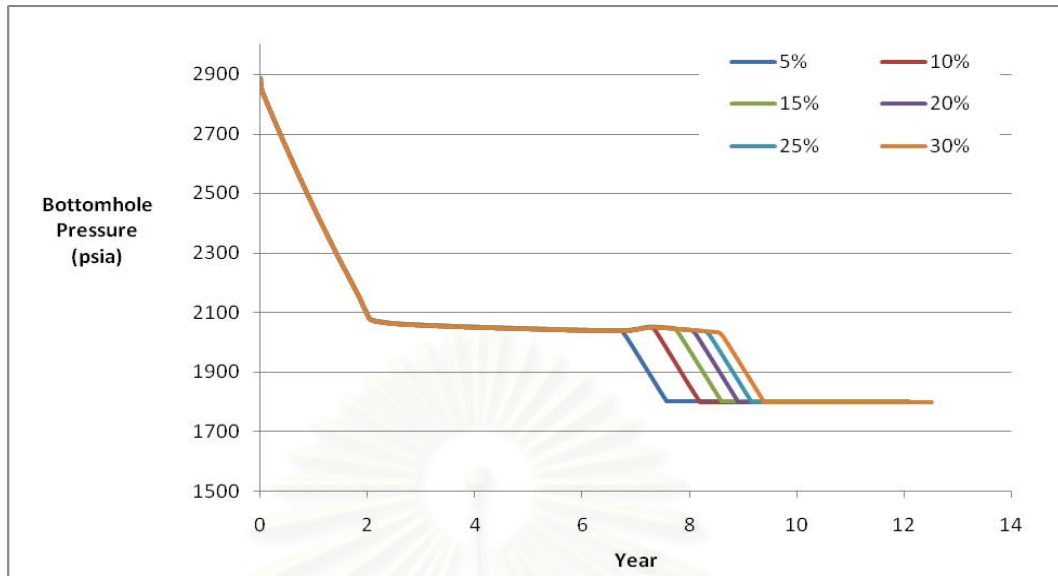


Figure 5.36: The bottomhole pressure for starting CO₂ injection after 2 years of production and stopping injection when the produced gas has CO₂ concentration of 5%- 35%.

CO₂ Mole Fraction in Produced Gas

CO₂ mole fractions in the produced gas for starting CO₂ injection at the beginning and after 2 years of production are shown in Figures 5.37 and 5.38, respectively.

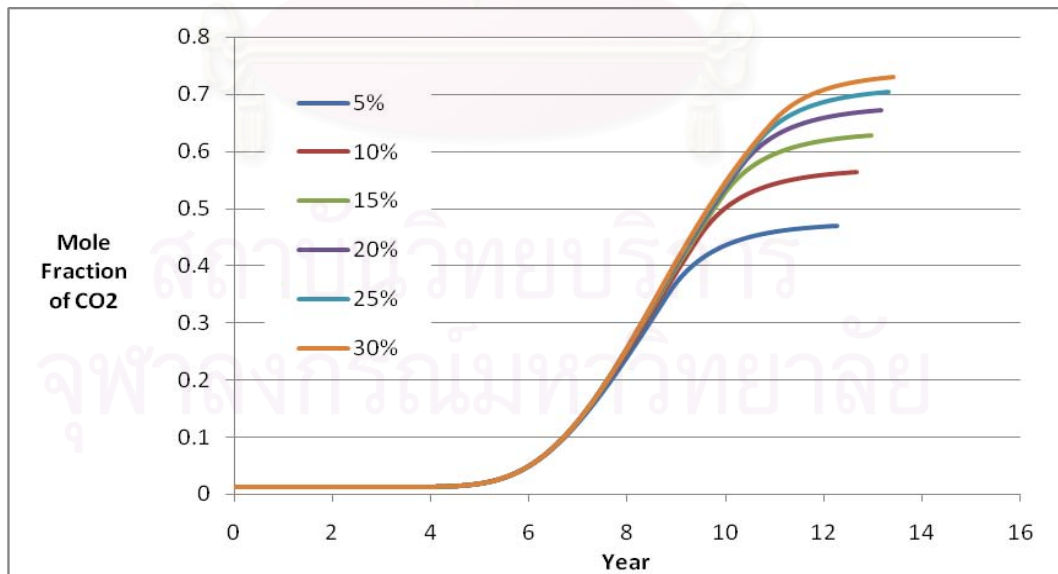


Figure 5.37: CO₂ mole fraction for starting CO₂ injection at the beginning and stopping injection when the produced gas has CO₂ concentration of 5%- 35%.

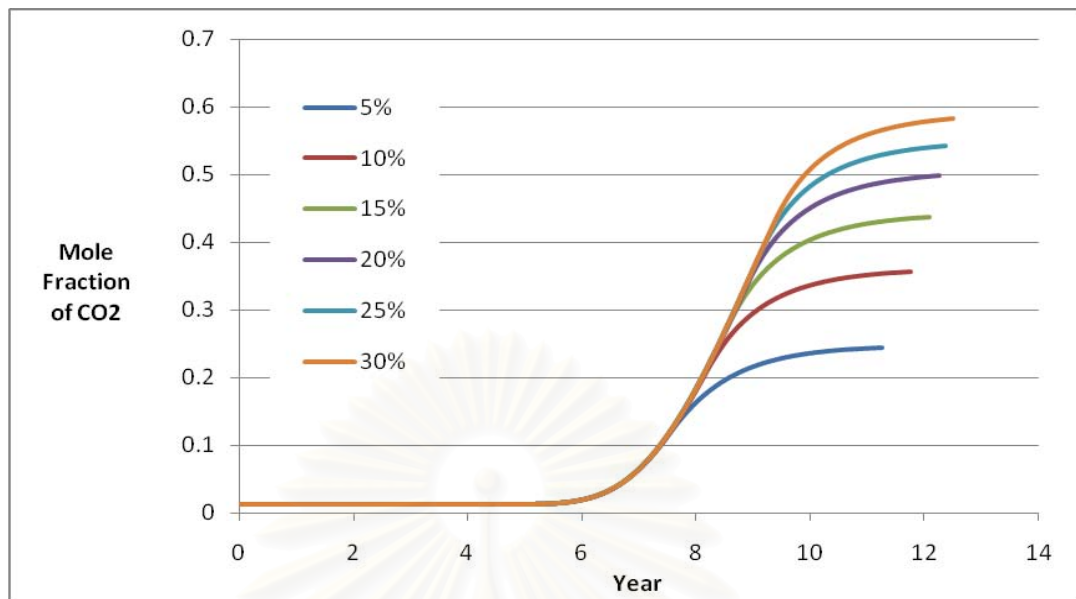


Figure 5.38: CO₂ mole fraction for starting CO₂ injection after 2 years of production and stopping injection when the produced gas has CO₂ concentration of 5% - 35%.

From Figures 5.31 to 5.38, the effect of stopping the injection when the produced gas has a certain CO₂ concentration can be summarized as follows:

- The gas and oil production rates are constant at the beginning and start to decline after CO₂ breakthrough. When the injection stops, CO₂ concentration does not stop increasing immediately. First, the bottomhole pressure drops very quickly after the injection stops until it reaches the BHP limit of 1,800 psia. After that, the gas and oil production rate start to decline and CO₂ concentration stops increasing. The simulation stops because the oil production rate drops below the economic limit.
- When compared between starting injection at the beginning and after 2 years, CO₂ concentration of immediate injection stops increasing at higher CO₂ concentration than that of the delayed injection.
- In the case of starting CO₂ injection after 2 years and stopping at 5% CO₂ concentration, the liquid saturation around the wellbore increases after injection stops because CO₂ concentration around the wellbore is not high enough to prevent liquid drop out in the reservoir.

Starting CO₂ Injection at the Beginning

The total gas and oil production and production life for starting CO₂ injection at the beginning are shown in Figures 5.39, 5.40 and 5.41, respectively.

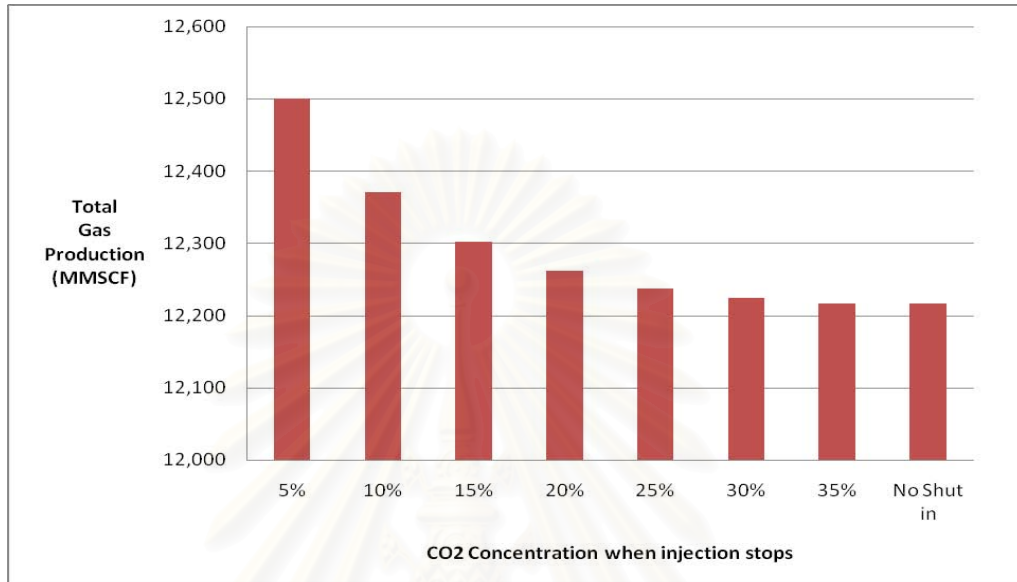


Figure 5.39: Total gas production for starting CO₂ injection at the beginning and stopping the injection when the produced gas has CO₂ concentration of 5%- 35%.

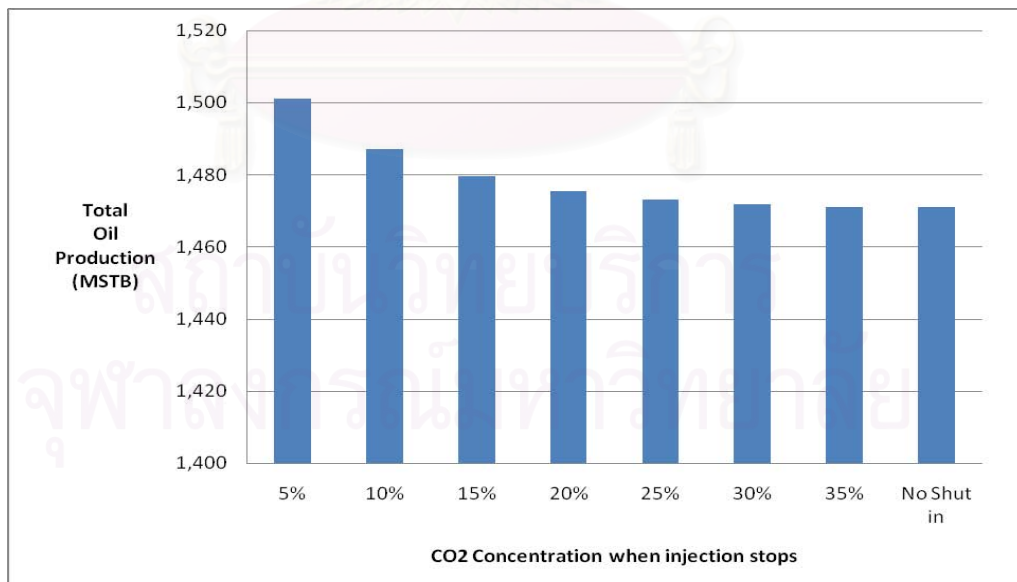


Figure 5.40: Total oil production for starting CO₂ injection at the beginning and stopping the injection when the produced gas has CO₂ concentration of 5%- 35%.

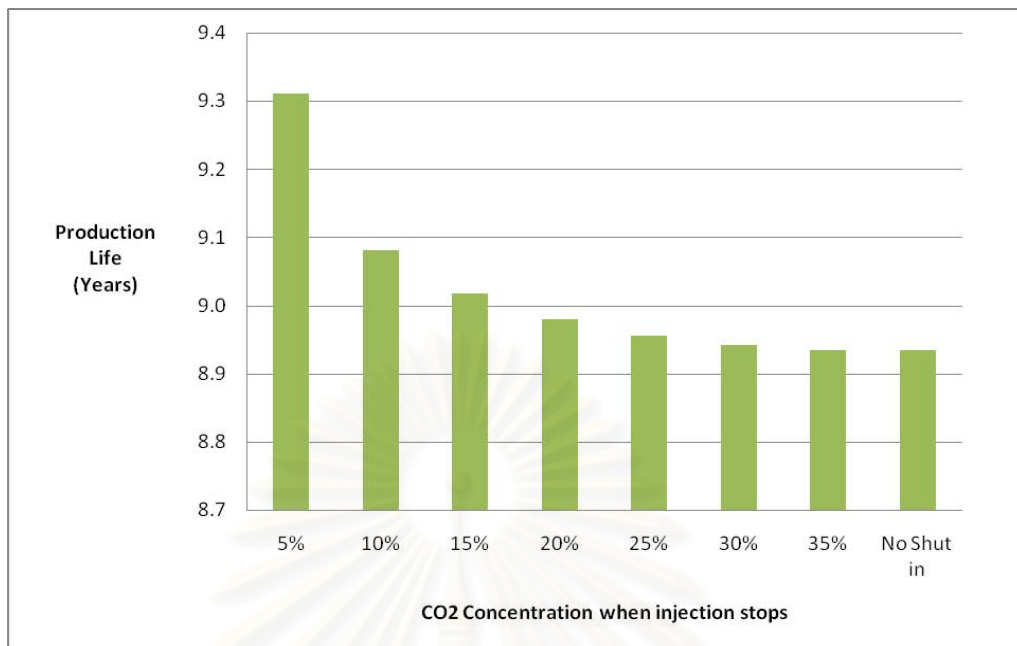


Figure 5.41: Production life for starting CO₂ injection at the beginning and stopping the injection when the produced gas has CO₂ concentration of 5%- 35%.

Tables 5.12 illustrates gas and oil recovery and production life for starting CO₂ injection at the beginning .

Table 5.12: Total oil and gas production and production life for starting CO₂ injection at the beginning and stopping the injection when the produced gas has CO₂ concentration of 5%- 35%.

Case	Gas Recovery (MMSCF)	Oil Recovery (MSTB)	Production Life (Years)
5%	12,500	1,501	9.31
10%	12,371	1,487	9.08
15%	12,302	1,480	9.02
20%	12,262	1,476	8.98
25%	12,237	1,473	8.96
30%	12,225	1,472	8.94
35%	12,217	1,471	8.93
No Shut in	12,216	1,471	8.93

From Figures 5.39 to 5.41, the effect of stopping the injection when the produced gas has a certain CO₂ concentration can be summarized as follows:

- a) As CO₂ concentration in the produced gas at the stopping time increases from 5% to 35%, the total gas production decreases from 12,500 MMSCF to 12,217 MMSCF, and the total oil production decreases from 1,501 MSTB to 1,471 MSTB in the case of immediate injection as shown in Table 5.13. This means that if we stop the injection early, we will recover more gas and oil. For the production life, increase CO₂ concentration in the produced gas at the stopping time shortens the production life.
- b) When compared to CO₂ injection without stopping the injection, stopping injection before CO₂ concentration in the produced gas reaches the limit has more oil and gas recovery for all CO₂ concentration in the produced gas at the stopping time.

Start CO₂ Injection after 2 years

The total gas and oil production and production life for starting CO₂ injection at the beginning and 2 years afterward are shown in Figures 5.42, 5.43, and 5.44, respectively.

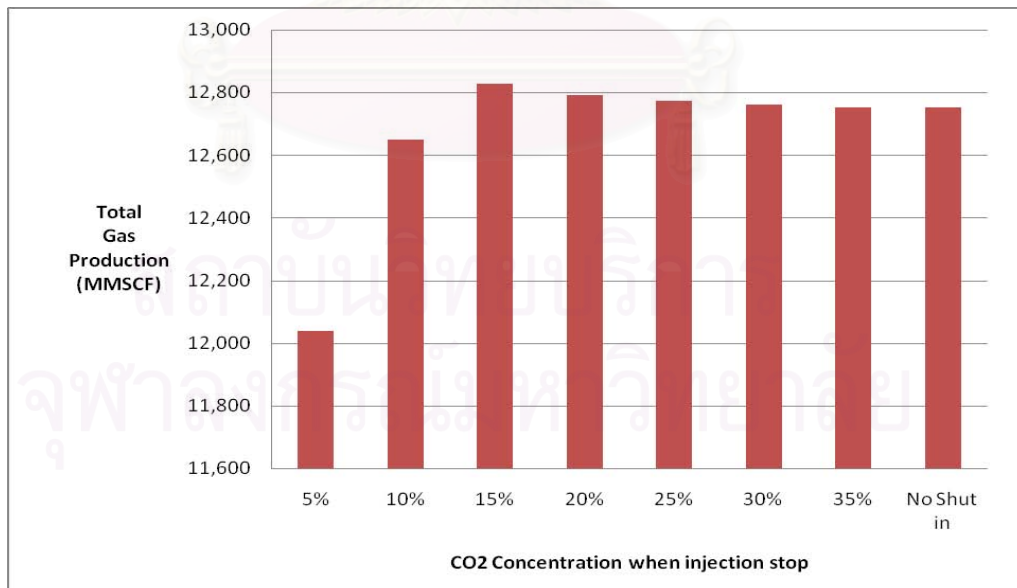


Figure 5.42: Total gas production for starting CO₂ injection 2 years afterward and stopping the injection when the produced gas has CO₂ concentration of 5%- 35%.

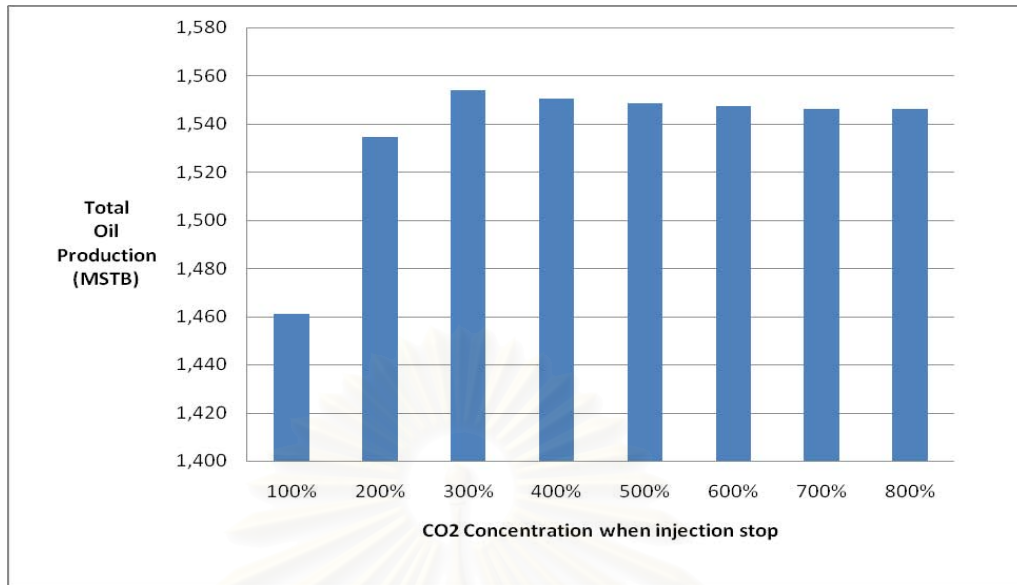


Figure 5.43: Total oil production for starting CO₂ injection 2 years afterward and stopping the injection when the produced gas has CO₂ concentration of 5% - 35%.

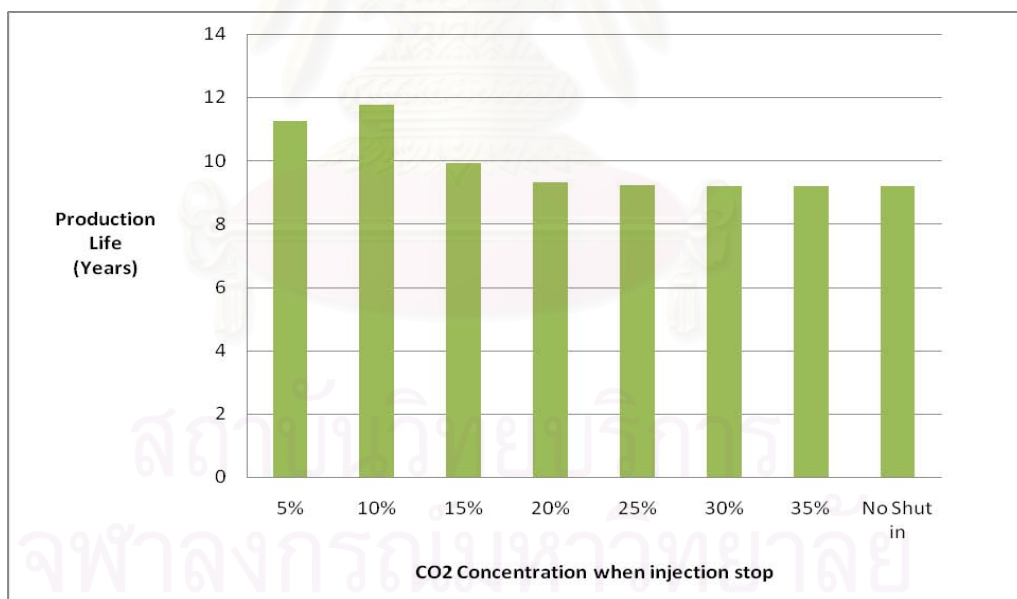


Figure 5.44: Production life for starting CO₂ injection 2 years afterward and stopping the injection when the produced gas has CO₂ concentration of 5% - 35%.

Tables 5.13 illustrate gas and oil recovery and production life for starting CO₂ injection at the beginning.

Table 5.13: Total oil and gas production and production life for starting CO₂ injection 2 years afterward and stopping the injection when the produced gas has CO₂ concentration of 5%- 35%.

Case	Gas Recovery (MMSCF)	Oil Recovery (MSTB)	Production Life (Years)
5%	12,039	1,461	11.26
10%	12,648	1,535	11.76
15%	12,828	1,554	9.91
20%	12,792	1,550	9.33
25%	12,772	1,548	9.22
30%	12,760	1,547	9.21
35%	12,751	1,546	9.20
No Shut in	12,751	1,546	9.20

From Figures 5.42 to 5.44, the effect of stopping the injection when the produced gas has a certain CO₂ concentration can be summarized as follows:

- a) As CO₂ concentration in the produced gas at the stopping time increases from 5% to 15%, the hydrocarbon gas production increases from 12,365 to 12,828 MMSCF, and the total oil production increases from 1,461 to 1,554 MSTB. But when CO₂ concentration at the stopping time increases from 15% to 35%, the hydrocarbon gas production decreases from 12,828 to 12,751 MMSCF, and the total oil production decreases from 1,554 to 1,546 MSTB. The opposite trend is observed because in the case of CO₂ concentration at the stopping time at 5% and 10%, the CO₂ concentration in the produced gas stops increasing before reaching the economic limit.

In this scenario, we can see that stopping injection before CO₂ concentration in the produce gas reaches the limit can improve oil and gas recovery and stopping injection earlier provides more gas and oil recovery in the case of CO₂ injection starting at the beginning. But when the injection starting time is delayed, stopping injection earlier may have lower oil and gas recovery if the oil and gas production rate reach the economic limit before CO₂ concentration reaches the limit.

5.6 Production with Gas-Recycling

In this scenario, the gas obtained from the separator is injected back into the reservoir. The gas injection starts at the same time as the production. Composition of the injected gas is shown in Table 5.14:

Table 5.14: Injected gas composition used in gas recycling scenario.

Component	Mole fraction
C ₁	0.67018
C ₂	0.09385
C ₃	0.07031
i-C ₄	0.03648
n-C ₄	0.04082
i-C ₅	0.01354
n-C ₅	0.01256
C ₆	0.04387
C ₇₊	0.00469
CO ₂	0.0137

In this simulation model, the production well is placed at coordinate (1,1) in LGR grid representing the producer (located at coordinate (1,1) in the global grid), and injection well is placed at coordinate (5,5) in LGR grid representing the injector (located at coordinate (15,15) in the global grid) in order to simulate a quarter five-spot pattern. At the production well, the gas production is controlled at 4,000 MSCF/D. At early times, the separator gas is injected back into the reservoir. When the oil production via gas recycling reaches the economic limit, gas injection is stopped. Then, the production well continues to produce gas and the injection well is switched to production until abandonment. In this scenario, we also compare between producing with gas recycling, producing with CO₂ injection at the beginning, producing with CO₂ injection at 2 years afterward, and producing with natural depletion. We use the 23% CO₂ limit as the economic limit for the CO₂ injection scenario.

The gas and oil production rates for different production strategies are shown in Figures 5.45 and 5.46, respectively.

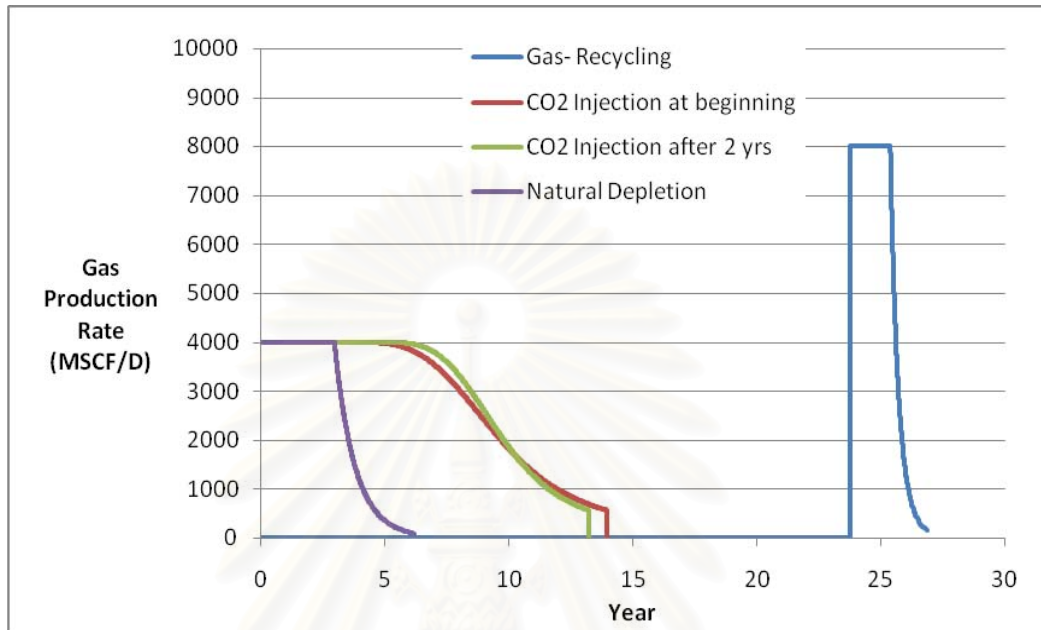


Figure 5.45: Gas production rate for producing with gas recycling in comparison to production with CO₂ injection.

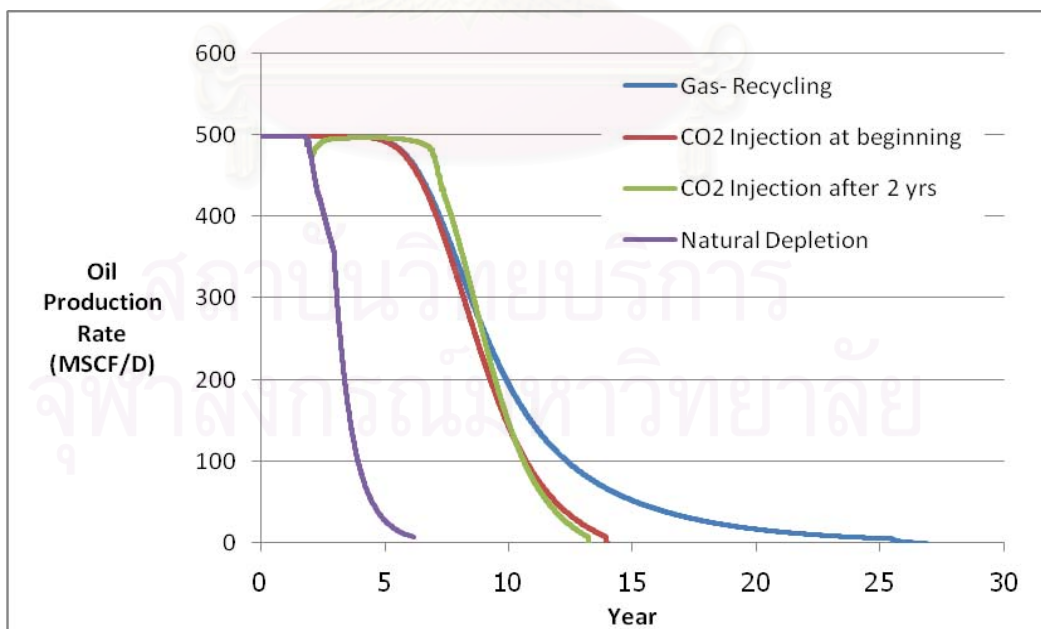


Figure 5.46: Oil production rate for producing with gas recycling in comparison to production with CO₂ injection.

The bottomhole pressure of the production well for different production strategies is shown in Figure 5.47.

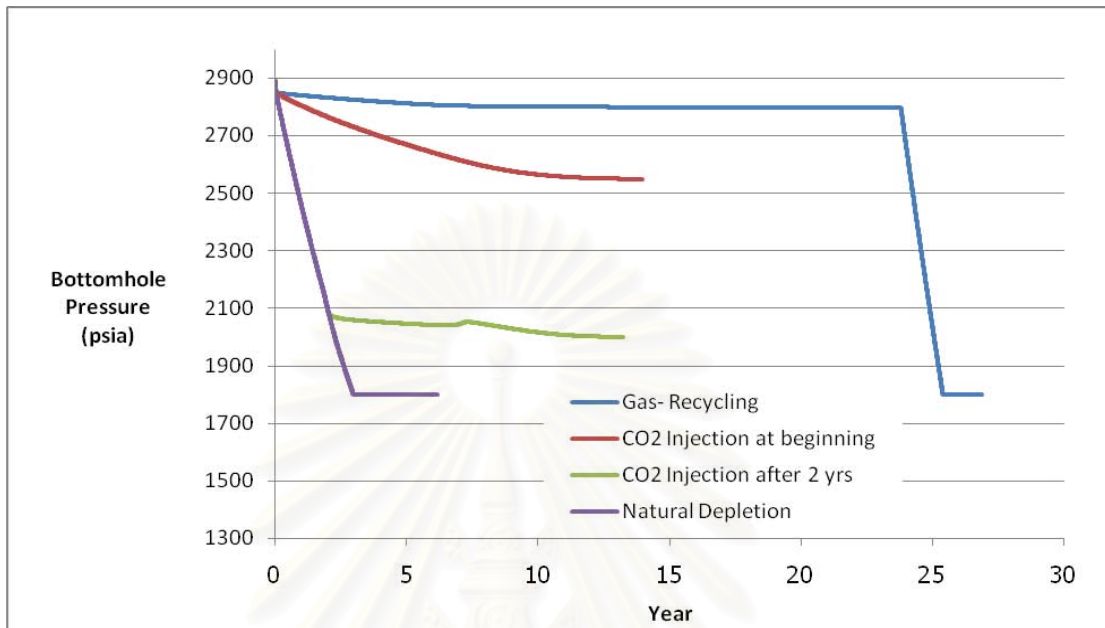


Figure 5.47: Bottomhole pressure for producing with gas recycling in comparison to production with CO₂ injection.

From Figures 5.45 to 5.47, comparison between gas recycling, CO₂ injection at the beginning, CO₂ injection after 2 years, and natural depletion can be summarized as follows:

- In gas recycling, all the gas production for the first 24 years is injected back into the reservoir. After switching injector to producer, the gas production rate increases to a constant value of 8,000 MSCF/D for 3 years before declining and reaching abandonment.
- The oil production rate remains constant at 498 STB/D for the first 6 years before starting to decline. The oil production rate of gas recycling case and CO₂ injection at the beginning drops at the same time because the injected gas breakthrough times are the same. The oil production rate in CO₂ injection case drops faster than that in the gas recycling case for immediate and delayed CO₂ injection.
- The bottomhole pressure in gas recycling case remains nearly constant until the injection stops.

The total oil and gas production and production life for different production strategies are shown in Figures 5.48, 5.49, and 5.50, respectively.

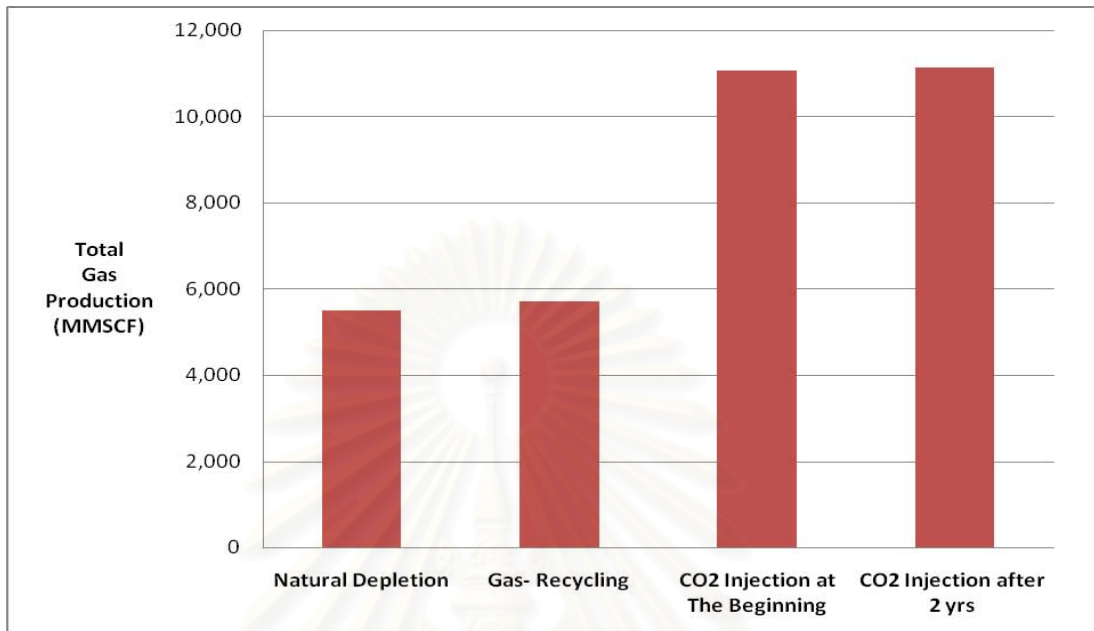


Figure 5.48: Total gas production for producing with gas recycling in comparison to production with CO₂ injection.

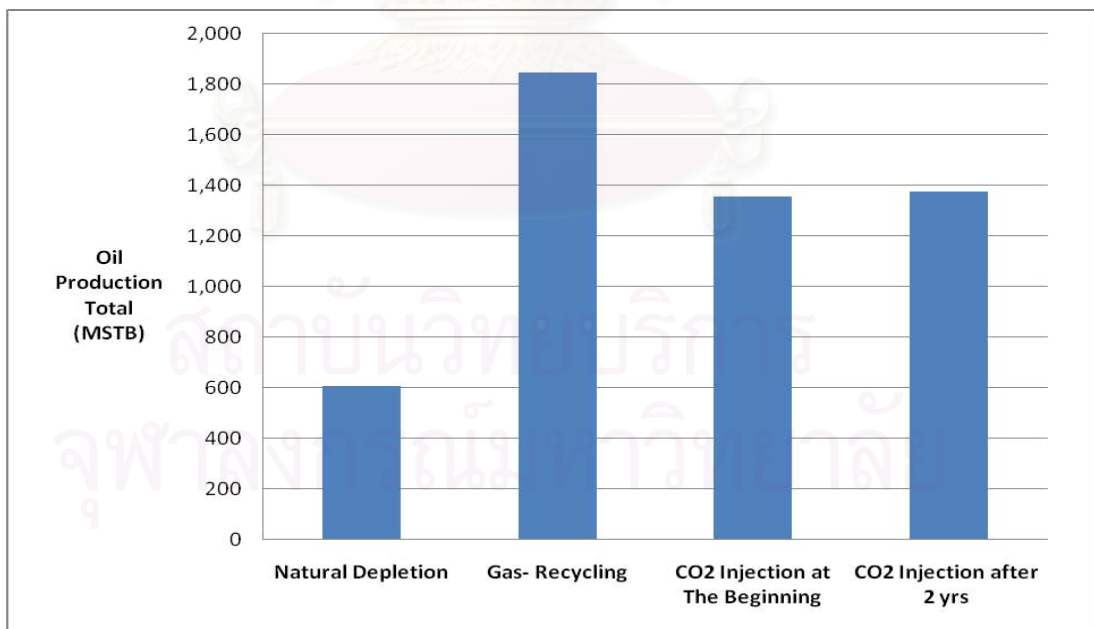


Figure 5.49: Total oil production for producing with gas recycling in comparison to production with CO₂ injection.

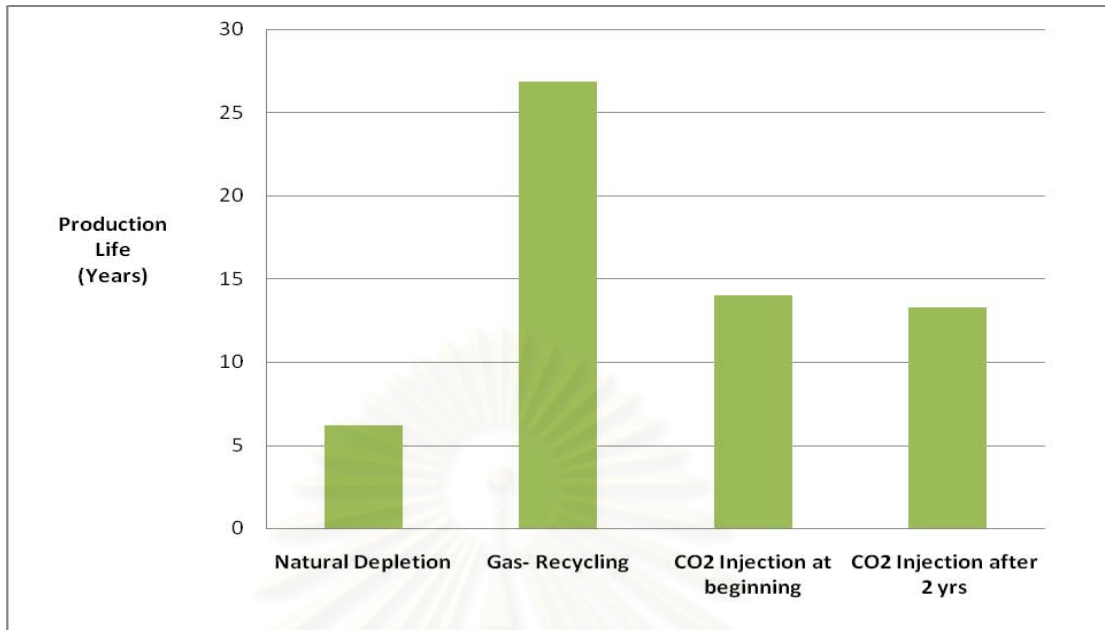


Figure 5.50: Production life for producing with gas recycling in comparison to production with CO₂ injection.

From Figures 5.48 to 5.50, comparison between gas recycling, CO₂ injection at the beginning, CO₂ injection after 2 years, and natural depletion can be summarized as follows:

- a) Gas recycling has around 200 MSTB more oil recovery than CO₂ injection. This is because gas recycling has no limitation of injected gas breakthrough. Gas recycling does enhance oil recovery when compare to natural depletion.
- b) Production life of gas recycling is around 14 years more than CO₂ injection case. Because gas recycling has no limitation of injected gas breakthrough, gas can be reinjected until all condensate is recovered.

When compared between CO₂ injection and gas recycling scenario, we can see that gas recycling is better in maintaining the reservoir pressure and has benefit on no injected gas breakthrough issue. However, the disadvantage of gas recycling is that it cannot sell any gas at the beginning and we can see that the gas recovery of the gas recycling scenario is much lower than that of the CO₂ injection scenario.

5.7 Economic Analysis

The financial aspect of selected production profile of condensate reservoir is evaluated using net present value (NPV). The capital cost is invested since starting the project. The assumptions for this economic evaluation are:

- a) Oil price equal to 62.5 US\$/bbl
- b) Gas price equal to 3.5 US\$/MMBTU
- c) Constant discount rate at 10 %
- d) Total fixed cost/investment cost of production well and injection well equal to 1,800,000 US\$.
- e) Total cost of compressor is 2,725,000 US\$. (The calculation detail n is shown in Appendix B-1)
- f) Total cost of CO₂ removal unit is 2,000,000 US\$ (Cost of CO₂ removal unit is the partial cost of full field CO₂ removal unit).
- g) Apply linear depreciation for salvage cost of compressor, and compressor life time is defined at 5 years.
- h) Operating cost varies only on electricity consumption. (The calculation detail n is shown in Appendix B-2)
- i) The gas processing cost is not accounted in the economic evaluation.
- j) The composition of injection gas is constant throughout the entire production period.

We select the maximum oil recovery case, which is the case with the maximum production rate of 4,000 MSCF/D and CO₂ injection start at 2 years, to perform economic evaluations. Economics analysis will be used to compare among the cases of 23% CO₂ limit, 40% CO₂ limit, producing with natural depletion and producing with gas recycling. NPV and annual cash flow of these selected cases are illustrated in Figure 5.50 and 5.51, respectively. The cash flow table of each case is shown in Appendix C.

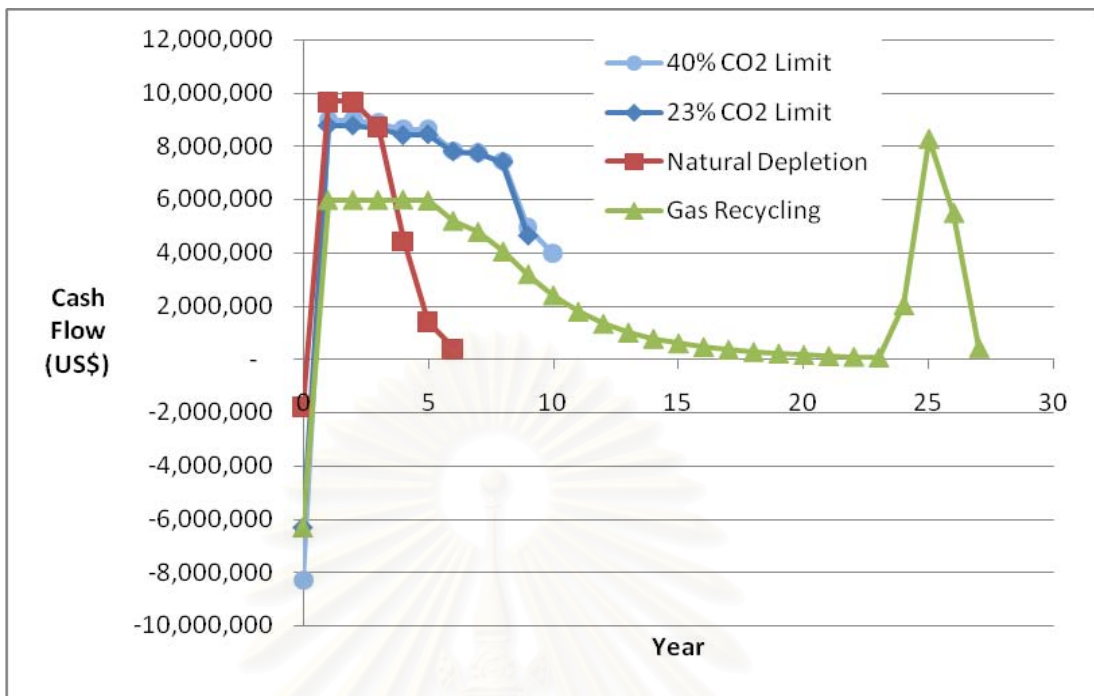


Figure 5.51: Cash flow for selected cases.

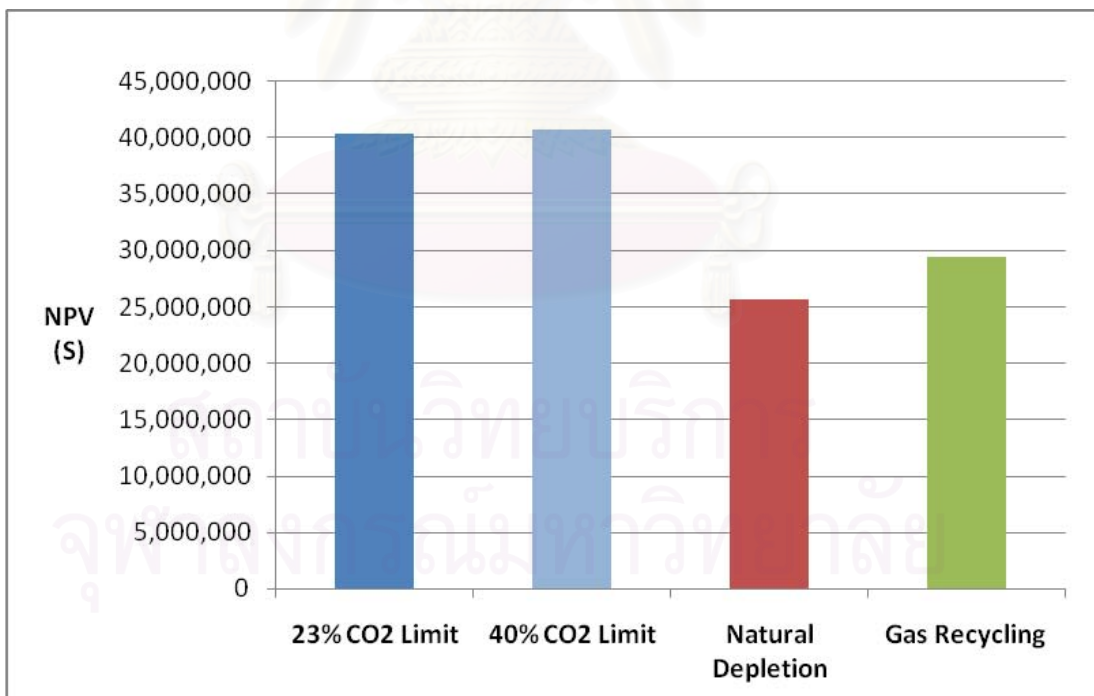


Figure 5.52: Net present value (NPV) for selected cases.

From the economic analysis, the results can be summarized as follows:

- a) From Figure 5.51, we can see that the case with 40% CO₂ concentration limit has the highest investment cost and the natural depletion scenario has the lowest investment cost in year 0. From year 1 to 3, the natural depletion scenario has the highest income because of the lowest operating cost and the gas recycling scenario has the lowest income because this scenario cannot sell any gas at early times. Then from year 4 to 6, the income of the natural depletion case is lowest due to the gas and oil production rate decline at this point.
- b) The income of the case with 23% and 40% CO₂ limit are equal until year 9. At this year, the simulation of the case with 23% CO₂ limit is stop. By installing CO₂ removal unit, we can gain 296,852 US\$ in year 9 and 3,972,476 US\$ in year 10.
- c) All the cases simulated give positive net present values. CO₂ injection cases have higher NPV than the natural depletion case. NPV are 49.4% and 46.5% higher than natural depletion case for 23% and 40% CO₂ concentration limit, respectively. When compared to gas recycling scenario, CO₂ injection have higher NPV. NPV are 33.5% and 30.9% higher than gas recycling case for 23% and 40% CO₂ concentration limit, respectively.
- d) Installing CO₂ removal unit does not significantly increase the NPV as we can see in Figure 5.52 because the operating cost and the investment cost of CO₂ removal unit is high and the gains in year 9 and 10 are low.

CHAPTER VI

CONCLUSIONS AND RECOMMENDATIONS

In this chapter, the conclusions of CO₂ injection into gas condensate reservoir are illustrated in term of the injection mechanism, hydrocarbon recovery enhancements, and economic analysis. In this study, a simple reservoir model and a quarter 5-spot flooding pattern was used. The case with maximum oil recovery was selected to perform economic analysis to compare between producing by natural depletion, producing with CO₂ injection, and gas recycling. The economic analysis is also used to study the feasibility of installing CO₂ removal unit.

6.1 Conclusions

Based on a specific set of input data, simulation results obtained from ECLIPSE 300 simulator, and economic analysis, injection mechanism, hydrocarbon recovery enhancements, and economic analysis of CO₂ injection can be concluded as follows:

6.1.1 Mechanism of CO₂ Injection

- a) In the case of starting CO₂ injection at the beginning and before the bottomhole pressure of the producer drop below the dew point pressure, CO₂ injection does effectively maintain the reservoir pressure above the dew point pressure, preventing condensate dropout in the reservoir.
- b) By starting injection before the bottomhole pressure of the producer reaches the BHP limit, the reservoir pressure and the oil production rate are maintained. The oil production rate is increased when CO₂ reaches the producer because the liquid drop out around the wellbore is effectively recovered by CO₂. The results show that oil saturation around the wellbore can be completely revaporized.

- c) By starting injection after the bottomhole pressure of the producer reaches the BHP limit, the oil and gas production rates decline before the injection starts. After the injection starts, the oil and gas production rates increase. After CO₂ breakthrough, the gas production rate decreases due to the increase in CO₂ concentration but the oil production rate increases because the liquid drop out around the wellbore is revaporized by CO₂. In this case, the results also show that oil round the wellbore can be completely revaporized.
- d) By stopping injection before CO₂ concentration in the produced gas reaches the limit, CO₂ concentration does not stop increasing immediately. First, the bottomhole pressure drops very quickly after the injection stops until it reaches the BHP limit. After that, gas and oil production rates start to decline and CO₂ concentration stops increasing.

6.1.2 Hydrocarbon Recovery Enhancement by CO₂ Injection

- a) Changing the production rate limit has no significant effect on the gas and oil recovery.
- b) By varying times prior to injection, the effects on hydrocarbon recovery depend on the bottomhole pressure when the injection starts. Starting injection shortly after the bottomhole pressure drops below the dew point pressure is the case that provides the maximum oil recovery. When starting injection after the bottomhole pressure reaches the BHP limit, delaying the injection time increases gas recovery but decreases oil recovery. And starting injection after the bottomhole pressure reaches the BHP limit, changing time prior to injection has no effect on oil and gas recovery.
- c) By stopping injection before CO₂ concentration in the produced gas reaches the limit, oil and gas recoveries are increased. If we stop the injection earlier, we will recover more gas and oil. The opposite trend is observed, if the CO₂ concentration in the produced gas stops increasing before reaching the economic limit.

- d) Gas recycling has more oil recovery but less gas recovery compared to CO₂ injection.

6.1.3 Economic analysis of CO₂ Injection

- a) All the cases simulated give positive net present values, and the CO₂ injection scenario has the highest NPV when compared to the natural depletion and gas recycling scenario.
- b) Installing CO₂ removal unit does not significantly increase the NPV. Because the operating cost and the investment cost of CO₂ removal unit is high, and the gains are low.

6.2 Recommendations

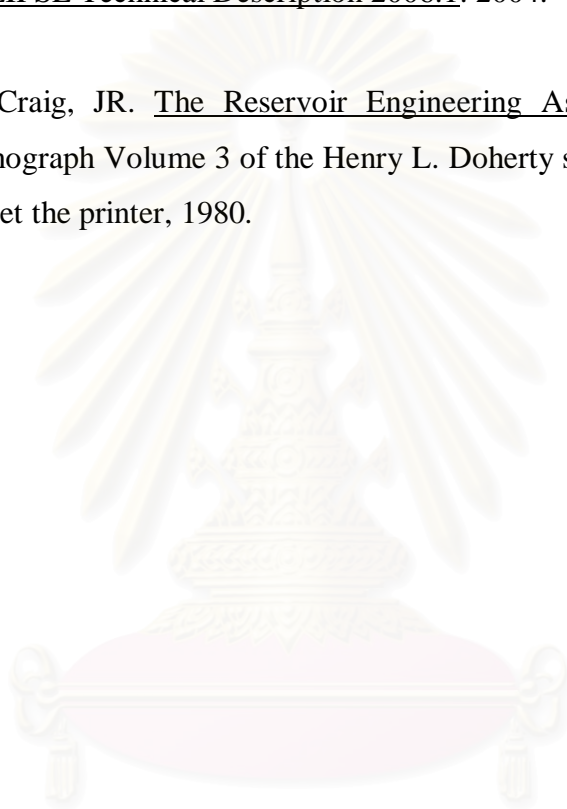
In this study, we studied the mechanism and performance of CO₂ injection with different production and injection scenarios. The effects of production and injection rate, time prior to injection and stopping injection before CO₂ concentration in produced gas reaches limit were studied. We also compared the mechanism and performance of CO₂ injection with production with gas recycling.

However, the conclusions are made from simulation results which come from a hypothetical model which has one specific reservoir composition, homogeneous reservoir properties, no dip angle, and immobile reservoir water. The field results may be different due to the effect of the parameters mentioned above. Future works should study the influence of these parameters for more understanding on mechanism and performance of CO₂ injection into a gas condensate reservoir.

References

- [1] E. Shtepani. CO₂ Sequestration in Depleted Gas/Condensate Reservoirs. Paper SPE 102284 presented at the 2006 SPE Annual Technical Conference and Exhibition held in San Antonio, Texas, U.S.A. September 2006.
- [2] J.J. Chaback and M.L. Willium. p-x behavior of a rich-gas-condensate reservoir fluid in admixture of CO₂ and (N₂ + CO₂). Paper SPE 24132 Presented at the 1992 SPE/DOE Symposium on Enhanced Oil Recovery held Tulsa April 1992.
- [3] A. Al-Hashami, S.R. Ren, and B. Tohidi. CO₂ Injection for Enhanced Gas Recovery and Geo-Storage Reservoir Simulation and Economics. presentation at the SPE Europec/EAGE Annual Conference held in Madrid, Spain June 2005.
- [4] Chang, Yih-Bor, Coats, B.K. and Nolen, J.S. A Compositional Model for CO₂ Floods Including CO₂ Solubility in Water. SPE Reservoir Evaluation & Engineering, 155-160. April 1998.
- [5] Sinisha A. Jikich, H. Smith, W. Neal Sams, S. Bromhal. Enhanced Gas Recovery (EGR) with Carbon Dioxide Sequestration, A Simulation Study of Effects of Injection Strategy and Operational Parameters. Paper SPE 84813 presented at the SPE Eastern Regional/AAPG Eastern Section Joint Meeting held in Pittsburgh, Pennsylvania, U.S.A 6-10 September 2003.
- [6] Curtis M. Oldenburg and Sally M. Benson. CO₂ Injection for Enhanced Gas Production and Carbon Sequestration. Paper SPE 74367 presented at the SPE International Petroleum Conference and Exhibition in Mexico held in Villahermosa, Mexico February 2002.

- [7] M. Sengul. CO₂ Sequestration—A Safe Transition Technology. Paper SPE 98617 presented at the SPE International Conference on Health, Safety, and Environment in Oil and Gas Exploration and Production held in Abu Dhabi, U.A.E. April 2006.
- [8] Schlumberger Informatin Solutions. ECLIPSE Reference Manual 2006.1 and ECLIPSE Technical Description 2006.1. 2004.
- [9] Forrest F. Craig, JR. The Reservoir Engineering Aspects of Waterflooding. Monograph Volume 3 of the Henry L. Doherty series. New York, U.S.A : Millet the printer, 1980.



สถาบันวิทยบริการ
จุฬาลงกรณ์มหาวิทยาลัย



APPENDICES

สถาบันวิทยบริการ
จุฬาลงกรณ์มหาวิทยาลัย

APPENDIX A

A-1) Reservoir model

The reservoir model is generated by input the required data in Eclipse simulator. The geological model composes of number of cells or blocks in X, Y and Z directions and in this study, the number of block is 15 x 15 x 3.

A-1) Case Definition

Simulator:	Compositional		
Model Dimensions:	Number of cells in the x direction		15
	Number of cells in the y direction		15
	Number of cells in the z direction		3
Grid type:	Cartesian		
Geometry type:	Block Centered		
Oil-Gas-Water Options:	Water, Gas Condensate (ISGAS)		
Number of Components:	10		
Pressure Saturation Options (Solution Type):	AIM		

A-2) Reservoir properties

Grid

Properties:	Active grid blocks	X (15) =	1
		Y (15) =	1
		Z (8) =	1
	Porosity	=	0.165
Permeability		k-x =	10.85 mD
		k-y =	10.85 mD
		k-z =	1.27 mD
	X Grid block sizes	=	150 ft
	Y Grid block sizes	=	150 ft
	Z Grid block sizes	=	40 ft
	Depth of Top face (Top layer)	=	8,000 ft

Cartesian Local Grid Refinement

LGR Name	LGR Coordinate			Number of refined cells		
	I	J	K	X	Y	Z
Producer	1	1	1-3	5	5	3
Injector	15	15	1-3	5	5	3

PVT Table

Fluid Densities at Surface Conditions	Oil density	49.99914	Lb/ft ³
	Water density	62.42797	Lb/ft ³
	Gas density	0.04947417	Lb/ft ³
Rock Properties	Reference Pressure	3000	Psia
	Rock Compressibility	2.403571E-6	/psi

A-3) Miscellaneous

Specify properties of water-CO2 system *(SOLUBILLI)

Press (psia)	VisCmp (Scf/stb)	FVF (rb /stb)	Viscos (cp)	Cmprss (/psi)
14.7	0.2069819	1.085391	0.187655	4.1271E-06
200	3.2210995	1.086144	0.187661	4.11422E-06
400	6.4743294	1.086956	0.187681	4.10031E-06
600	9.7275593	1.087767	0.187714	4.08641E-06
800	12.980789	1.088577	0.187761	4.0725E-06
1000	16.234019	1.089387	0.187821	4.05859E-06
1200	19.487249	1.090197	0.187894	4.04469E-06
1400	22.740479	1.091006	0.18798	4.03078E-06
1600	25.993709	1.091815	0.18808	4.01688E-06
1800	29.246939	1.092623	0.188193	4.00297E-06
2000	32.500169	1.09343	0.188319	3.98906E-06
2200	35.753399	1.094237	0.188459	3.97516E-06
2400	39.006629	1.095043	0.188612	3.96125E-06
2600	42.259859	1.095849	0.188778	3.94734E-06
2800	45.513089	1.096654	0.188957	3.93344E-06
3000	48.766319	1.097459	0.18915	3.91953E-06
3200	52.019549	1.098264	0.189356	3.90563E-06
3400	55.272779	1.099067	0.189575	3.89172E-06
3600	58.526009	1.099871	0.189808	3.87781E-06
3800	61.779238	1.100673	0.190054	3.86391E-06

Number of Component	Number of Component	10	
Standard Condition	Standard Temperature	60	F
	Standard Pressure	14.7	Psia
Component Names	Component 1	C ₁	
	Component 2	C ₂	
	Component 3	C ₃	
	Component 4	i-C ₄	
	Component 5	n-C ₄	
	Component 6	i-C ₅	
	Component 7	n-C ₅	
	Component 8	C ₆	
	Component 9	C ₇₊	
	Component 10	CO ₂	
PROPS Reporting Options	Oil PVT Tables	No output	
	Gas PVT Tables	No output	
	Water PVT Tables	No output	

EoS Res Tables

Pure Component Boiling Points (Reservoir EoS)	Component C ₁	200.94	R
	Component C ₂	332.18	R
	Component C ₃	415.92	R
	Component IC ₄	470.45	R
	Component NC ₄	490.75	R
	Component IC ₅	521.79	R
	Component NC ₅	556.59	R
	Component C ₆	615.39	R
	Component C ₇₊	734.08	R
	Component CO ₂	350.413	R
Critical Temperature (Reservoir EoS)	Component C ₁	343	R
	Component C ₂	549.59	R
	Component C ₃	665.73	R
	Component IC ₄	734.13	R
	Component NC ₄	765.29	R
	Component IC ₅	828.77	R
	Component NC ₅	845.47	R
	Component C ₆	913.27	R
	Component C ₇₊	1061.29	R
	Component CO ₂	547.58	R
Constant Reservoir Temperature	Initial Reservoir Temperature	293	F
Critical Volume (Reservoir EoS)	Component C ₁	0.0988	ft ³ /lb-mole
	Component C ₂	0.0783	ft ³ /lb-mole
	Component C ₃	0.0727	ft ³ /lb-mole
	Component IC ₄	0.0714	ft ³ /lb-mole
	Component NC ₄	0.0703	ft ³ /lb-mole
	Component IC ₅	0.0679	ft ³ /lb-mole
	Component NC ₅	0.0675	ft ³ /lb-mole
	Component C ₆	0.0688	ft ³ /lb-mole
	Component C ₇₊	7.509	ft ³ /lb-mole
	Component CO ₂	0.0344	ft ³ /lb-mole

Overall Composition	Component C ₁	59.991	%
	Component C ₂	8.4326	%
	Component C ₃	6.3988	%
	Component IC ₄	3.4127	%
	Component NC ₄	3.8989	%
	Component IC ₅	1.4286	%
	Component NC ₅	1.3988	%
	Component C ₆	7.2718	%
	Component C ₇₊	6.5366	%
	Component CO ₂	1.2302	%
Critical Pressure (Reservoir EoS)	Component C ₁	666.4	Psia
	Component C ₂	706.5	Psia
	Component C ₃	616	Psia
	Component IC ₄	527.9	Psia
	Component NC ₄	550.6	Psia
	Component IC ₅	490.4	Psia
	Component NC ₅	488.6	Psia
	Component C ₆	436.9	Psia
	Component C ₇₊	403.29	Psia
	Component CO ₂	1071	Psia
Equation of State (Reservoir EoS)	Equation of State Method	PR (Peng-Robinson)	
Molecular Weights (Reservoir EoS)	Component C ₁	16.043	
	Component C ₂	30.07	
	Component C ₃	44.097	
	Component IC ₄	58.123	
	Component NC ₄	58.123	
	Component IC ₅	72.15	
	Component NC ₅	72.15	
	Component C ₆	86.177	
	Component C ₇₊	115	
	Component CO ₂	44.01	
Acentric Factor (Reservoir EoS)	Component C ₁	0.0104	
	Component C ₂	0.0979	
	Component C ₃	0.1522	
	Component IC ₄	0.1852	
	Component NC ₄	0.1995	
	Component IC ₅	0.228	
	Component NC ₅	0.2514	
	Component C ₆	0.2994	
	Component C ₇₊	0.38056	
	Component CO ₂	0.2667	

A-4) SCAL
Saturation Function

Oil Saturation Functions	Row	So	Krow	Krowg
	1	0	0	0
	2	0.2	0	0
	3	0.32	0.00463	0.015625
	4	0.44	0.037037	0.125
	5	0.56	0.125	0.421875
	6	0.68	0.296296	1
7	0.95	1	1	
Water Saturation Function	Row	Sw	Krw	Pc (psia)
	1	0.11	0	250
	2	0.157	0	53
	3	0.216	0	13
	4	0.313	0.02	1
	5	0.44	0.06	0
	6	0.56	0.10	0
	7	0.68	0.15	0
	8	0.80	0.30	0
	9	0.90	0.65	0
Gas Saturation Function	Row	Sg	Krg	Pc (psia)
	1	0	0	
	2	0.1	0	
	3	0.2	0	
	4	0.3	0.2	
	5	0.4	0.4	
	6	0.6	0.85	
	7	0.7	0.90	
	8	0.8	0.92	
	9	0.9	0.95	
10	0.95	0.95		

A-5) Initialization Equilibration

Equilibration Region	Keywords	NEI (Non-Equilibrium Initialisation)	
EquilReg 1	Non-Equilibrium Initialisation	Row	Fractions
		1	0.59991
		2	0.084326
		3	0.063988
		4	0.034127
		5	0.038989
		6	0.014286
		7	0.013988
		8	0.072718
		9	0.065366
10	0.012302		

Region/Array

Initial Water Saturation (SWAT)	:	0.11
Initial Gas Saturation (SGAS)	:	0.89
Initial Pressure	:	3000 psia
Dew Point Pressure	:	2250 psia

A-6) Region N/A

A-7) Schedule

Production

LGR Well Specification (Prod1) [WELSPECL]

Well	Prod1
Group	1
LGR	Producer
I Location	1
J Location	1
Datum depth	8,000 ft
Preferred Phase	Gas
Inflow Equation	STD
Automatic Shut-In instruction	Shut
Cross Flow	Yes
Density calculation	SEG
Type of Well Model	STD

Amalgamated LGR Well Comp Data (Prod1) [COMPDATL]

Well	Prod1
LGR	Producer
K Upper	1
K Lower	3
Open/Shut Flag	Open
Well bore ID	0.448 ft.
Direction	Z

Production Well Control (Prod1) [WCONPROD]

Well	Prod1
Open/Shut Flag	Open
Control	GRAT
Gas rate	1000 MSCF/D
THP target	500 psia

Economic Limit Data On Component Mole Fraction (WECONCMF)

Well	Prod1
Component Index	10
Maximum Mole Fration	0.25
Workover procedure	Well
End run	YES

Production Well Economics Limit [WECON]

Well	Prod1
Minimum oil rate	5 STB/D
Minimum gas rate	100 MSCF/D
Workover procedure	None
End run	YES

Injection*Well Specification (Inj1) [WELSPECS]*

Well	Inj1
Group	-
LGR	Injector
I Location	5
J Location	5
Preferred Phase	Gas
Inflow Equation	STD
Automatic Shut-In instruction	Shut
Cross Flow	Yes
Density calculation	SEG
Type of Well Model	STD

Well Connection Data (Inj1) [COMPDAT]

Well	Inj1
K Upper	1
K Lower	3
Open/Shut Flag	Open
Well bore ID	0.625 ft
Direction	Z

Injection Well Control (Inj1) [WCONINJE]

Well	Inj1
Injector type	Gas
Open/Shut Flag	Open
Control Mode	Rate
Gas Surface Rate	1000 MSCF/D

Nature of Injection Gas (Inj1) [WINJGAS]

Well	Inj1
Injection fluid	Gas
Well stream	1

Injection Gas Composition [WELLSTRE]

Well Stream	1
Comp10	1

APPENDIX B

B-1) Compressor specification and Cost

Compressor Spec

Make	:	
Type	:	Reciprocating
Design capacity	:	14.0 MMSCFD
Operating capacity	:	12.5 MMSCFD
Operating suction pressure	:	275 psig
Operating discharge pressure	:	1,350 psig ($\Delta p = 1,075$ psig)
Operating temperature	:	50 C
Estimated required power	:	1,400 HP
Driver	:	

Table B-1 Cost estimation of compressor

Items	Cost ¹ (1000 US\$)
PDS Tariff	
- Detailed design	25.0
- Construction	30.0
- Project management	25.0
Materials	1,760
- Compressor package	
- Compressor frame and cylinders	
- F&G lube system	
- Pulsation dampener and separator	
- Air cooler	
- Gas engine driver	
- Skid	
- Water cooling system	
- PLC control unit	
- Drawings	
- Transportation and insurance for major equipment	137.5
- Foundation and grouting work	100.0
- Mechanical modification	50.0
- Instrumentation (replace the aging facility)	25.0
- Electrical modification (hook-up to power supply from the existing facility) ²	112.5
- Soft starter panel, 110 kW, IP55 for fan motor	
- Cables	
- RCU	
- Small distribution board	
- Lightings	
- Splice box	
- Accessories	

- Modification of fire and gas detection system - New sensor units (5 sets) - Modification of existing fire and gas alarm panel - Software	30.0
- Commissioning spare parts ³	0.0
- Other bulks	25.0
Construction and Commissioning Cost	
- Civil work	20.0
- Mechanical work	37.5
- Electrical work ⁴	20.0
- Instrument work	5.0
- Third party inspection of K-3850 at the factory	15.0
- Installation, commissioning, and training (vendor)	60.0
- Contingency (10%)	247.75
Total	2,725.25

The above costs form part of BI 5DXX

Notes: Cost for electrical facility has been based on the estimated electrical consumption (by the air cooler fan) of 90-110 kW.

B-2) Electrical/Power consumption calculation

Pumping power is defined as the time-rate of pumping work. It is related to pumping rate and pressure by

$$power = \frac{work}{time} = q\Delta p$$

The customary unit of power for combustion engines is horsepower (HP) and for electrical motors is the kilowatt (kw). The power units are related by

$$1 \text{ HP} = 0.746 \text{ kw.}$$

The approximate compressor power

$$P = 0.23q_g \left[\left(\frac{p_2}{p_1} \right)^{0.2} - 1 \right]$$

where

- q_g is gas compression rate, mscf/D
- p_1 is compressor suction pressure, psia
- p_2 is compressor discharge pressure, psia
- P is compression power, HP

Injection Rate ; q (Mscf/D)	Power (HP)	Power (kw)	Consumption Total Power Cost(USD/Year) EGAT Power
1000	83.58	59.84	23,538.66
2000	167.16	119.68	47,077.32
3000	250.73	179.53	70,619.91
4000	334.31	239.37	94,158.97
5000	417.89	299.21	117,697.23
6000	501.47	359.05	141,235.89
7000	585.05	418.89	164,774.55
8000	668.62	478.73	188,313.21
9000	752.20	538.58	211,855.80
10000	835.78	598.42	235,394.46

B-3) Calculation of Btu for produced gas

Component	Mole Fraction y_j	Gross Heating value, (Btu/scf) L_{cj}	$y_j * L_{cj}$	Compressibility Factor at Standard Conditions	
				z_j	$y_j(1-z_j)^{0.5}$
C1	0.67018	1010.0	676.8818	0.9980	0.0299714
C2	0.09385	1769.6	166.077	0.9919	0.0084465
C3	0.07031	2516.1	176.907	0.9825	0.0093011
i-C4	0.03648	3251.9	118.6293	0.9711	0.0062016
n-C4	0.04082	3262.3	133.1671	0.9667	0.007449
i-C5	0.01354	4000.9	54.17219	0.9480	0.0030876
n-C5	0.01256	4008.9	50.35178	0.9420	0.0030248
C6	0.04387	4755.9	208.6413	0.9100	0.013161
C7+	0.00469	5502.5	25.80673	0.8520	0.0018043
CO2	0.0137	0.0	0	0.9943	0.0010343
	1.0000		1610.634		0.0834816

$$Z = 1 - (\sum y_j (1-z_j)^{0.5})^2$$

$$Z = 1 - (0.0834816)^2$$

$$= 0.993031$$

$$L_c = L_{c \text{ ideal}} / Z$$

$$L_c = (1610.634 \text{ Btu/scf}) / 0.993031$$

$$\text{Btu / scf} = \mathbf{1621.938}$$

Appendix C

C-1) Cash flow of CO₂ injection scenario with 23% CO₂ limit

Year	Gross Revenue (US\$)		5% Royalties (US\$)	Power Consum. (US\$)	Capex (US\$)	Depletion (US\$)	Taxes (US\$)	Net Income (US\$)	Present Value (US\$)
	Gas	Oil							
0	-	-	-	-	6,325,250	-	-	- 6,325,250	-6,325,250
1	8,288,067	8,513,882	425,694	70,620		1,265,050	7,520,293	8,785,343	7,986,675
2	8,287,975	8,513,796	425,690	70,620		1,265,050	7,520,205	8,785,255	7,260,542
3	8,287,825	8,345,913	417,296	70,620		1,265,050	7,440,386	8,705,436	6,540,523
4	8,291,213	7,746,523	387,326	70,620		1,265,050	7,157,370	8,422,420	5,752,626
5	8,287,965	7,822,614	391,131	70,620		1,265,050	7,191,889	8,456,939	5,251,094
6	8,270,226	7,822,089	391,104	70,620		-	7,815,296	7,815,296	4,411,531
7	8,082,908	7,879,805	393,990	70,620		-	7,749,051	7,749,051	3,976,489
8	7,412,267	7,902,573	395,129	70,620			7,424,545	7,424,545	3,463,605
9	1,864,071	7,902,635	395,132	70,621			4,650,477	4,650,477	1,972,256

C-2) Cash flow of CO₂ injection scenario with 40% CO₂ limit

Year	Gross Revenue (US\$)		5% Royalties (US\$)	Power Consum. (US\$)	Remove CO ₂ (US\$)	Capex (US\$)	Depletion (US\$)	Taxes (US\$)	Net Income (US\$)	Present Value (US\$)
	Gas	Oil								
0	-	-	-	-	-	8,325,250	-	-	- 8,325,250	-8,325,250
1	8,288,067	8,513,882	425,694	70,620	-	-	1,665,050	7,320,293	8,985,343	8,168,493
2	8,287,975	8,513,796	425,690	70,620	-	-	1,665,050	7,320,205	8,985,255	7,425,831
3	8,287,825	8,345,913	417,296	70,620	-	-	1,665,050	7,240,386	8,905,436	6,690,786
4	8,291,213	7,746,523	387,326	70,620	-	-	1,665,050	6,957,370	8,622,420	5,889,229
5	8,287,965	7,822,614	391,131	70,620	-	-	1,665,050	6,991,889	8,656,939	5,375,278
6	8,270,226	7,822,089	391,104	70,620	-	-	-	7,815,296	7,815,296	4,411,531
7	8,082,908	7,879,805	393,990	70,620	-	-	-	7,749,051	7,749,051	3,976,489
8	7,412,267	7,902,573	395,129	70,620	-	-	-	7,424,545	7,424,545	3,463,605
9	6,150,861	7,989,619	399,481	70,620	3,775,721	-	-	4,947,329	4,947,329	2,098,150
10	1,024,695	8,308,850	415,443	70,620	902,531	-	-	3,972,476	3,972,476	1,531,561

C-3) Cash flow of production with gas recycling

Year	Gross Revenue (US\$)		5% Royalties (US\$)	Power Consum. (US\$)	Capex (US\$)	Depletion (US\$)	Taxes (US\$)	Net Income (US\$)	Present Value (US\$)
	Gas	Oil							
0	-	-	-	-	6,325,250	-	-	- 6,325,250	-6,325,250
1	-	11,351,898	567,595	70,620	-	1,265,050	4,724,316	5,989,366	5,444,879
2	-	11,351,901	567,595	70,620	-	1,265,050	4,724,318	5,989,368	4,949,891
3	-	11,351,889	567,594	70,620	-	1,265,050	4,724,312	5,989,362	4,499,896
4	-	11,381,352	569,068	70,620	-	1,265,050	4,738,307	6,003,357	4,100,374
5	-	11,312,301	565,615	70,620	-	1,265,050	4,705,508	5,970,558	3,707,247
6	-	11,037,910	551,896	70,620	-	-	5,207,697	5,207,697	2,939,609
7	-	10,163,413	508,171	70,620	-	-	4,792,311	4,792,311	2,459,213
8	-	8,618,487	430,924	70,620	-	-	4,058,472	4,058,472	1,893,307
9	-	6,810,906	340,545	70,620	-	-	3,199,871	3,199,871	1,357,057
10	-	5,152,381	257,619	70,620	-	-	2,412,071	2,412,071	929,958
11	-	3,843,550	192,178	70,620	-	-	1,790,376	1,790,376	627,516
12	-	2,884,756	144,238	70,620	-	-	1,334,949	1,334,949	425,356
13	-	2,202,263	110,113	70,620	-	-	1,010,765	1,010,765	292,783
14	-	1,702,888	85,144	70,620	-	-	773,562	773,562	203,703
15	-	1,334,350	66,717	70,620	-	-	598,506	598,506	143,278
16	-	1,052,500	52,625	70,620	-	-	464,628	464,628	101,116
17	-	836,400	41,820	70,620	-	-	361,980	361,980	71,616
18	-	665,375	33,269	70,620	-	-	280,743	280,743	50,494
19	-	531,438	26,572	70,620	-	-	217,123	217,123	35,501

C-3) Cash flow of production with gas recycling (con't)

Year	Gross Revenue (US\$)		5% Royalties (US\$)	Power Consum. (US\$)	Capex (US\$)	Depletion (US\$)	Taxes (US\$)	Net Income (US\$)	Present Value (US\$)
	Gas	Oil							
20	-	424,281	21,214	70,620	-	-	166,224	166,224	24,708
21	-	339,769	16,988	70,620	-	-	126,080	126,080	17,037
22	-	272,469	13,623	70,620	-	-	94,113	94,113	11,561
23	-	218,569	10,928	70,620	-	-	68,510	68,510	7,651
24	3,970,932	175,288	8,764	70,620	-	-	2,033,418	2,033,418	206,444
25	16,529,362	141,706	7,085	70,620	-	-	8,296,681	8,296,681	765,750
26	10,998,903	83,525	4,176	70,620	-	-	5,503,816	5,503,816	461,800
27	921,138	6,750	338	70,620	-	-	428,465	428,465	32,682

C-4) Cash flow of production with natural depletion

Year	Gross Revenue (US\$)		5% Royalties (US\$)	Power Consum. (US\$)	Capex (US\$)	Depletion (US\$)	Taxes (US\$)	Net Income (US\$)	Present Value (US\$)
	Gas	Oil							
0	-	-	-	-	1,800,000	-	-	- 1,800,000	-1,800,000
1	8,288,103	11,351,821	567,591	70,620	-	360,000	9,320,856	9,680,856	8,800,779
2	8,288,103	11,318,478	565,924	70,620	-	360,000	9,305,019	9,665,019	7,987,619
3	8,276,792	9,344,859	467,243	70,620	-	360,000	8,361,894	8,721,894	6,552,888
4	4,538,015	4,242,959	212,148	70,620	-	360,000	4,069,103	4,429,103	3,025,137
5	1,362,448	1,199,391	59,970	70,620	-	360,000	1,035,624	1,395,624	866,573
6	459,709	397,648	19,882	70,620	-	-	383,427	383,427	216,435

Vitae

Phakphum Tangkprasert was born on November 3rd, 1982 in Sukhothai, Thailand. He received his Bachelor of Engineering in Chemical Engineering from the Faculty of Engineering, Kasetsart University in 2004. He has been a graduate student in the Master's Degree Program in Petroleum Engineering of the Department of Mining and Petroleum Engineering, Chulalongkorn University since 2006.



สถาบันวิทยบริการ
จุฬาลงกรณ์มหาวิทยาลัย